Complexation and Photochemical Properties of Azobenzocrown Ethers

Ruriko TAHARA

Division of Material Science,
Graduate School of Environmental Earth Science,
Hokkaido University

Complexation and Photochemical Properties of Azobenzocrown Ethers

Ruriko TAHARA

Division of Material Science,
Graduate School of Environmental Earth Science,
Hokkaido University

Contents

CHAPTER 1
General Introduction

Since prehistoric time, man have utilized numerous metals as tools for their daily activities. Most of these metal elements exist as salts, *e.g.* silicate, carbonate, oxide, sulfide in nature. Since metal elements are usually highly electropositive, they exist as positive ions rather than free metal in nature. In the terrestrial ecosystem they are found in the soil, plants, water and most importantly the organism. Similarly, they are also found in the marine ecosystem. Seawater act as a large reservoir of metal ions. In conjunction with this, most of metal elements are in the form of metal ions, and they play important roles in biological materials which involves enzyme, chlorophyll, and other vital compounds. Therefore, it is obvious and apparent that metal ions are a important part of our lives.

Therefore, due to its importants, many methods to analyze metal ions have been developed. Samples that are to be analyzed are usually in the form of solution which is the most convenient form for handling purpose. One of the simplest methods to analyze the solution is colorimetry. This instrumentation is readily available and generally fairly easy to operate.[1] In the case of colorimetric analysis for metal ions, transition metal ions which have *d orbital* electrons turn various color, and their colors change to different one by the coordination by ligands.[2] Hence, it is also easy to analyze transition metal ions by colorimetry. On the other hand, metal ions, which belong to first or second group element or do not have *d orbital* electrons, in its original form, does not exhibit color themselves. Ligands with chromophore are utilized to color them. Azo dyes and triphenylmethane dyes, (*e.g.* eriochrome black T, xylenol orange, and so on) are used to colorate the ions of these colorless metal ions. However, these ligands can not color alkali metal ions. These ligands color the metal ions by complexation. However, these can not form any complexes with alkali

metal ions.

Coloration of alkali metal ions became possible by using of crown ethers. Crown ethers, which were found by C. J. Pedersen in 1967,[3] are one of macrocyclic compounds with hetero atoms *e.g.* oxygen, nitrogen and so on. When these hetero atoms face to the inside of crown ether ring, polar cavity appears. Crown ethers form stable complexes with a metal ion by taking it in this cavity. The most important property is selective complexation with metal ions, whose size is suitable for the size of the cavity. And the complex is possible to dissolve in organic solvents.[4] Therefore, application of crown ethers have been extended widely.[5] The first compound called crown ether is dibenzo-18-crown-6.[3] It was reported that dibenzo-18-crown-6 formed complex with K^+ selectively,[3] and its absorption spectra was slightly changed by complexation.[6] Takagi et al. synthesized the first crown ether dyes, 4'-picrylamino-15-crown-5 derivatives.[7] They carried out selective solvent extraction of K^+ and Rb^+ using these compounds. It was confirmed that metal ion exists in organic phase and are due to the changes of absorption spectrum of organic phase. Many crown ether dyes have been reported since then. The many chromophores (*e.g.* azophenol,[8] nitirophenol,[9] resocyanin,[10] and so on) have been introduced to crown ethers. Many crown ethers with fluorophore instead of chromophore have been reported by Valeur.[11]

On the other hand, dyes have been manufactured since thousand B. C. Natural dyes such as indigo or alyzarin, were being used for very long time. In 1856, the first artificial dye, mauveine, was found by W. H. Perkin.[12] Since then, many dyes, thioindigo, azo dye, phthalocyanine, and so on have been developed, and they have replaced natural dyes. There are functional dyes among many dyes. One of the most famous functional dyes is litmus. Litmus turns red in acidic solution and blue in basic solution. Photosynthesis is carried out by dyes mainly, such as chlorophyll in plants.

One of functions that was attracted attention is its photo response.

Photo response is the reversible change in physical and/or chemical properties (*e.g.* polarity of the medium, absorption spectra, and so on) rupon being excited by light. Photo response is usually based on photoisomerization behavior the of dye molecule. The most important molecule showing photoisomerization behavior is a retinal. Eye of animals is sensitive to light by photoisomerization of retinal. Other compounds showing photoisomerization are azobenzene, spiropyran, thioindigo, fulgide, and so on. Azobenzene compounds change to *cis* isomers by irradiation of UV light, and return to *trans* isomers by irradiation of visible light. *Cis* isomer has 5.5 Å of molecular size, a non-planar structure, and high polarity as shown in Fig. 1.1. On the other hand, *trans* isomer has 9.0 Å of molecular size, a plane structure, and low polarity.[13] Many functional macromolecules including azobenzene derivatives have been reported.[14,15]

The most familiar method to vary function of the organic compounds is by introducing and/or varying functional group as substituents. This means synthesis of a new compound, and both varying the function of new compound further and getting back to an original function are impossible. If a complexation unit exists within a molecule, the function could be expected to vary easily and reversibly by the changing complexed metal ion.

In this study, an azobenzene and crown ether was chosen as a photofunctional unit and a complexation unit, respectively, and the *trans*-*cis* photoisomerization of azobenzocrown ethers shown in Fig. 1.2, azobenzo-13-crown-4 (AB13C4), azobenzo-16-crown-5 (AB16C5), azobenzo-19-crown-6 (AB19C6), and their metal complexes was investigated. Although initial expectation was that the complexation would suppress those photoisomerization due to steric effect of complexed metal ions, in some cases the unexpected promotion of the photoisomerization by the metal ions was observed. In addition, these azobenzocrown ethers and their analogue compound, 2,2'-dimethoxy

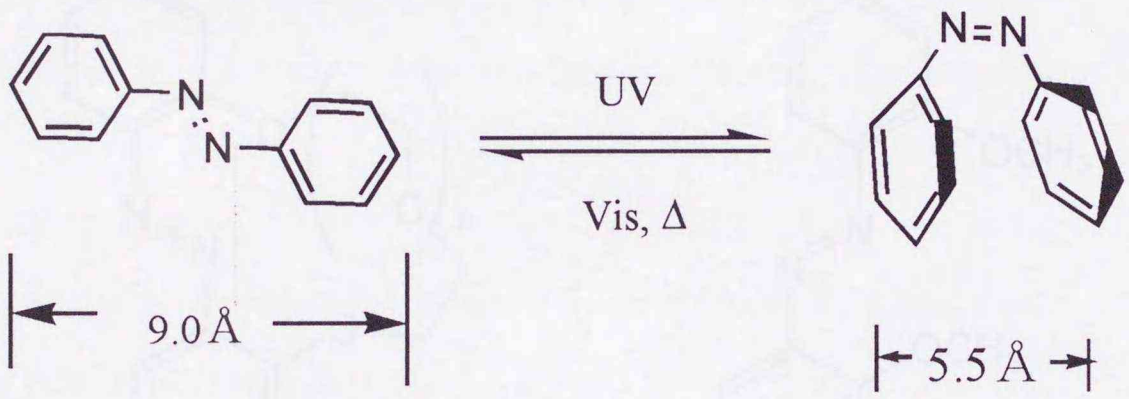

trans isomer

cis isomer

Fig. 1.1 Isomerization of azobenzene.

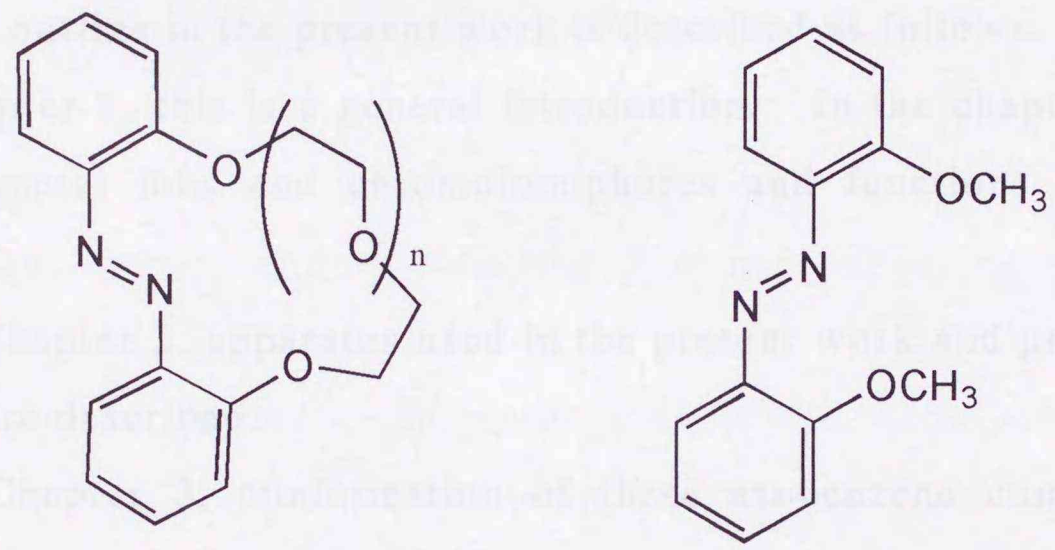

n = 1: *trans* AB13C4
2: *trans* AB16C5
3: *trans* AB19C6

DMAB

Fig. 1.2 Structural formulae of azobenzocrown ethers.

azobenzene (DMAB), themselves showed unique photoisomerization behavior.

In order to clarify these unexpected photoisomerization of these azobenzocrown ethers, the investigations on 1) absorption spectrum of these azobenzenes, 2) complexation behavior of these azobenzenes with metal ions based on crown ether moiety, and 3) photoisomerization based on azobenzene moiety of AB13C4, AB16C5, AB19C6, and DMAB were carried out.

The outline in the present work is described as follows.

Chapter 1, this is a general introduction. In the chapter, relations between metal ions and chromoionophores and functions of dyes are described.

In Chapter 2, apparatus used in the present work and preparation of samples are described.

In Chapter 3, conformation of these azobenzene compounds and interaction between complexed metal ion and azo group are discussed in accordance with their absorption spectra.

In Chapter 4, complexation behavior of azobenzocrown ethers is described. In this chapter, factors for complexation abilities and selectivity of these azobenzenes are discussed.

In Chapter 5, photoisomerization behavior of azobenzenes used in the previous chapter is discussed. In this chapter, effects of complexed metal ion on photoisomerization of azobenzene moiety are discussed in terms of ionic size and surface charge of metal ions.

In Chapter 6, the conclusion of this work is described.

CHAPTER 2

Materials and Apparatus

2.1 Materials.

2.1.1 Azobenzocrown Ethers.

AB16C5, AB19C6, and DMAB, which were synthesized by Shiga who was graduated from Department of Organic Synthesis, Faculty of Engineering, Kyushu University[16] were used. AB13C4 was synthesized according to the method reported in the literature 16.

2.1.2 Metal Perchlorate.

In this study, metal perchlorates were used as the source of metal ions.

Alkali and alkaline earth metal perchlorates were purchased from Kishida Chem. Co., and were used without further purification.

Rare earth metal perchlorates were prepared from the corresponding chloride salts by passing the chloride-salt solution through an anion exchanger (Amberlite IRA-400) of perchlorate form.

2.1.3 Other materials.

Anion exchange resin (Amberlite IRA-400) was purchased from Organo. Co. as a chloride form. The perchlorate form was prepared by the following method; the resin was washed by dilute hydrochloric acid. After rinsed by pure water, it was soaked in 0.1 M aqueous sodium perchlorate solution and shaken hard for several hours. This procedure was repeated several times by exchanging the aqueous solution. During this procedure, the existence of chloride anion in the aqueous phase was monitered by the treatment with aqueous solution of silver nitrate. Finally, it was rinsed by pure water until perchlorate anion was not detected in the washed water.

Acetonitrile used for solvent was purified by distillations, twice on

phosphorus pentoxide and once on calcium hydride.

2.1.4 Apparatus.

Absorption spectra were recorded by a SHIMADZU UV2200 spectrophotometer. ^{1}H NMR spectra were obtained by a JOEL EX-400 ^{1}H NMR spectrometer. Photoirradiations were carried out by an USHIO 500 W Xenon short arc lamp after passing through a Jovin Ybon UV-10 monochrometer (band width: 16 nm). The light intensity was monitored by photocurrent of a photo diode (Hamamatsu S1336 BQ).

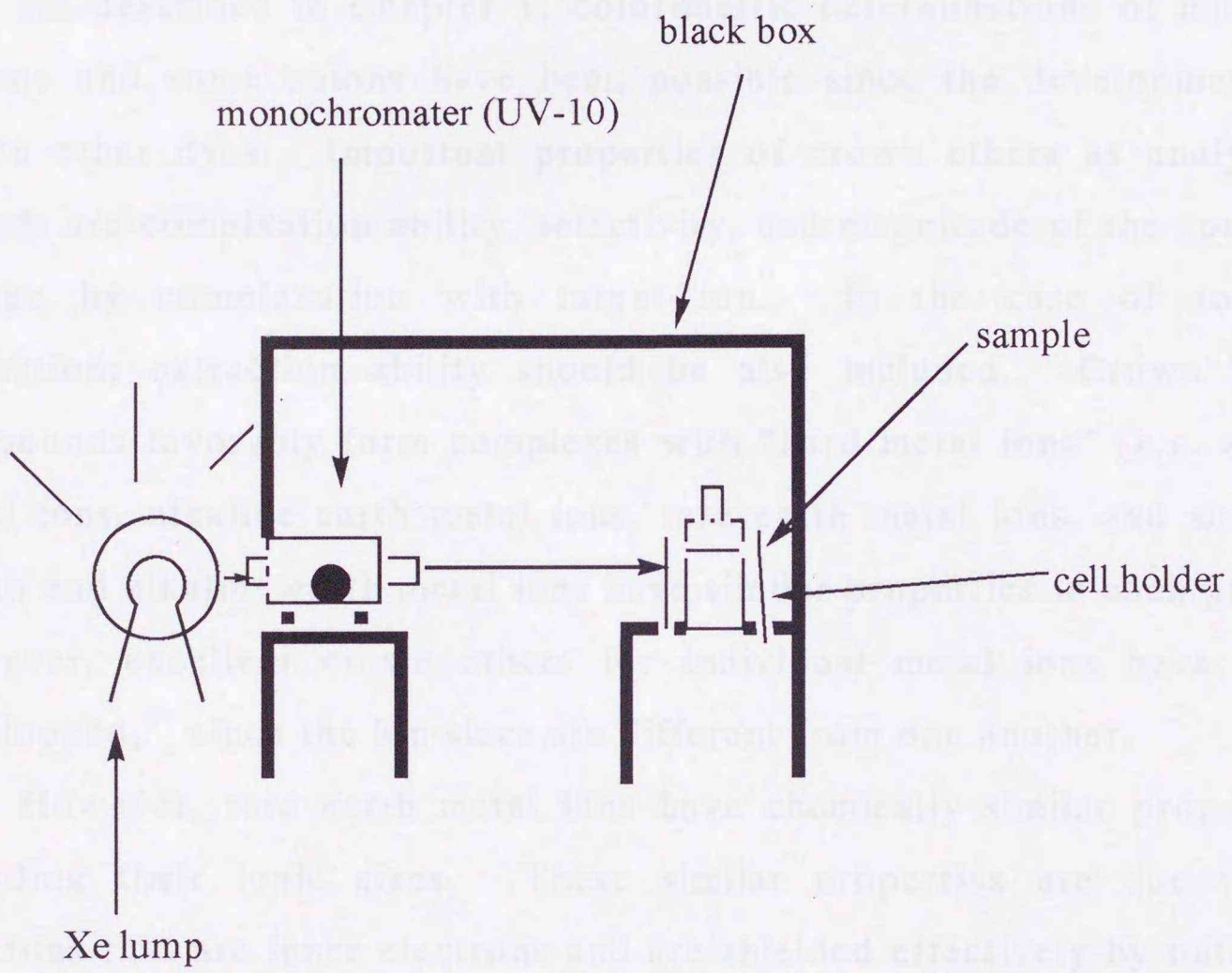

Fig. 2.1 Arrangement of apparatus.

CHAPTER 3

Complexation behavior of Azobenzocrown ethers for several metal ions.

3.1 Introduction.

As described in Chapter 1, colorimetric determinations of most of cations and some anions have been possible since the development of crown ether dyes. Important properties of crown ethers as analytical ligands are complxation ability, selectivity, and magnitude of the spectral change by complexation with target ion. In the case of solvent extraction, extraction ability should be also included. Crown ether compounds favorably form complexes with "hard metal ions" (*e.g.* alkali metal ions, alkaline earth metal ions, rare earth metal ions, and so on). Alkali and alkaline earth metal ions have similar properties in each group. However, excellent crown ethers for individual metal ions have been developped,[17] since the ion sizes are different from one another.

However, rare earth metal ions have chemically similar properties including their ionic sizes. These similar properties are due to *4f* electrons that are inner electrons and are shielded effectively by outer 5s and 5p shells. Therefore, separation of these metal ions has been difficult. The methods used for separation of rare earth metal ions are ion chromatography,[18,19] solvent extraction and so on.[20] Many chelating ligands were synthesized, and have been applied for these methods.[21,22] In these investigations, macrocyclic ionophores have been generally used as an extractant.[23-26]

In this chapter, the complexation behavior of *trans* isomers of AB13C4, AB16C5, and AB19C6 for hard metal ions is discussed.

3.2 Experimental Section.

3.2.1 Measurement of Complex Formation Constants.

Various amounts of several metal perchlorate ($[M^{n+}] = 1.0 \times 10^{-6}$ to 1.0×10^{-5} M) were added to a certain concentration of acetonitrile solution of azobenzocrown ether compounds (AB13C4, AB16C5 or AB19C6), and the resulting spectral changes were measured by using a standard 1 cm quartz cell. Absorbances at a certain wavelength which gave the largest absorbance difference were treated by a non-linear least square method (Marquardt method),[27] and complex formation constants were evaluated. To prevent the effects of photo isomerization, these experiments were carried out in the dark.

3.2.2 Evaluation of complex formation constants.

The formation constants (K) defined by eq. 3.1 for 1:1 complex (ligand : metal ion) were calculated according to the following method.

$$K = [ML] / ([M^{n+}][L]) \qquad (3.1)$$

Here, M^{n+} and L represent the metal ion and the ligand (i.e., azobenzocrown ethers), respectively. And optical absorbance of the solution of this system can be expressed by eq. 3.2,

$$Abs = \varepsilon_{ML}[ML] + \varepsilon_{L}[L] \qquad (3.2)$$

where, Abs, ε_{ML}, and ε_{L} represent an absorbance at a certain wavelength, a molar absorption coefficient of complex, and that of ligand, respectively. The total concentrations of metal ions and ligand are defined as follows:

$$[L]_t = [L] + [ML] \qquad (3.3)$$

$$[M]_t = [ML] + [M^{n+}] \qquad (3.4)$$

By combining eqs. 3.1-4, the Abs is derived as in eq. 3.5.

$$\begin{aligned} Abs = (\varepsilon_{ML} - \varepsilon_L)[\{1 + K([L]_t + [M]_t)\} \\ - [\{K([M]_t - [L]_t) + 1\}^2 + 4K[L]_t]^{1/2} / 2K] + \varepsilon_L[L]_t \end{aligned} \qquad (3.5)$$

Since the solution of these *trans* isomers became mixtures of *trans* and *cis* isomers under the room light (the ratio were *ca.* 1:1) and *cis* isomers have very weak complexation ability, the actual concentration of these *trans* isomers was used for this calculation. Some constants ($K < 10^3\ M^{-1}$) could not be evaluated due to too low accuracy.

3.3 Results.

The absorption spectra of *trans* AB13C4, AB16C5, and AB19C6 changed gradually when metal perchlorates were added into these acetonitrile solutions as shown in Fig. 3.1. In any case, the absorption spectra revealed isosbestic point, indicating the formation of a 1:1 complex of a ligand and respective metal ion. Complex formation constants ($\log_{10} K$) of *trans* azobenzene compounds with several metal ions were evaluated from these electronic spectra as in the previous section, and they are listed in Table 3.1. Several complex formation constants of AB16C5 and AB19C6 with alkali metal ions were already determined by Shiga et al.[16] Those values for alkali metal complex except for Li^+ complex of *trans* AB13C4 or Mg^{2+} complex of *trans* AB19C6 can not be determined accurately due to a weak complexing ability.

All of *cis* isomers of these azobenzocrown ethers and DMAB had so weak complexation abilities for these metal ions, that their formation constants could not be evaluated.

3.3.1 Complexation Behavior of trans *AB13C4 with Alkaline Earth Metal Ions.*

Trans AB13C4 formed complexes with all alkaline earth metal ions, and it did with only Li^+ in alkali metal ions. It complexed with Ca^{2+} most strongly among alkaline earth metal ions. The complex formation constants of *trans* AB13C4 for alklaine earth metal ions were in the order of $Ca^{2+} > Mg^{2+} \cong Sr^{2+} \cong Ba^{2+}$.

3.3.2 Complexation Behavior of trans *AB16C5 with Alkaline Earth Metal Ions.*

Trans AB16C5 formed complexes with all alkaline earth metal ions and Li^+, Na^+, and K^+. *Trans* AB16C5 complexed with Ca^{2+} most

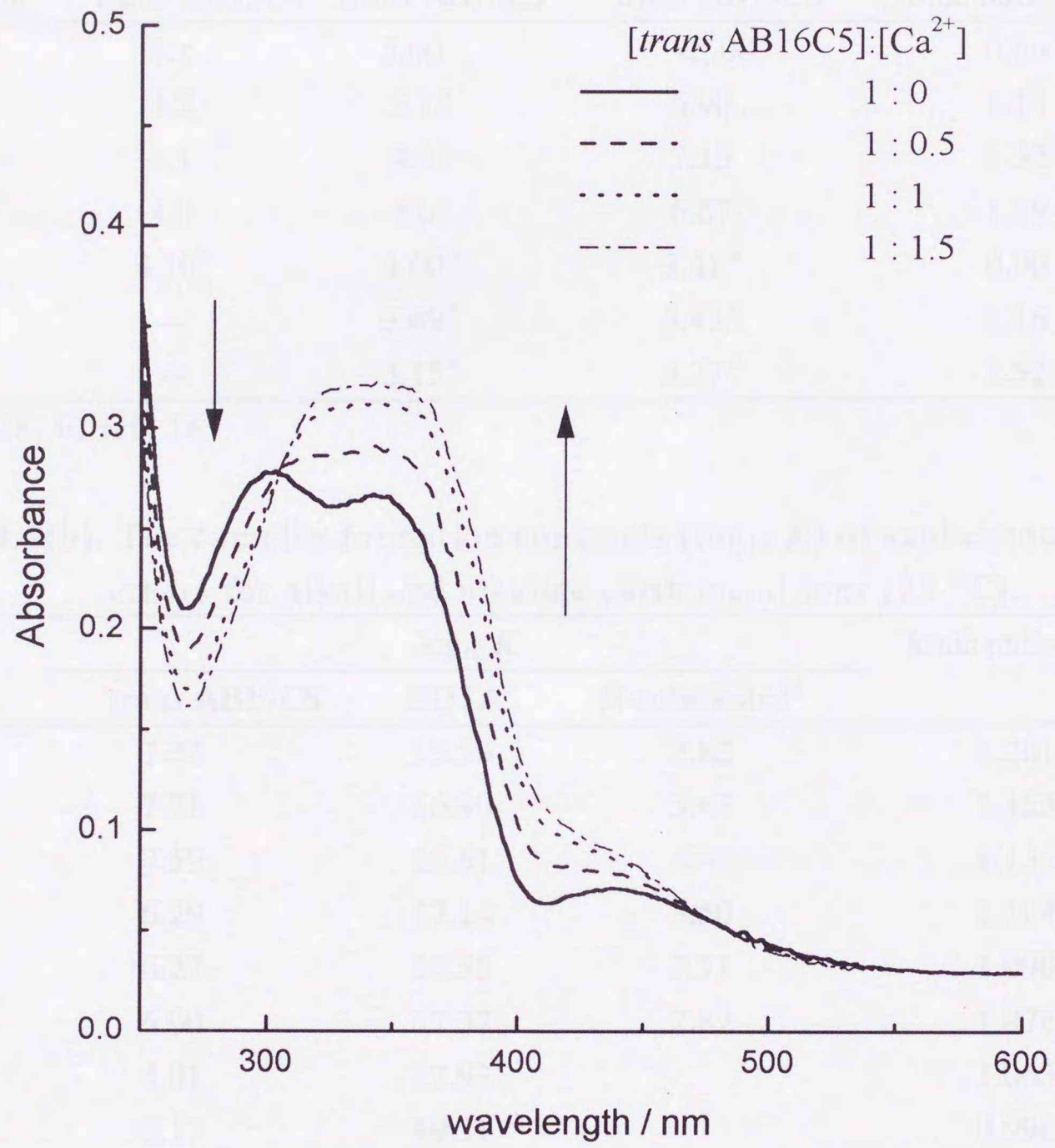

Fig. 3.1 Spectral change of *trans* AB16C5 by complexation with Ca^{2+}.

[*trans* AB16C5] = 1.0×10^{-5} M in acetonitrile at 25 °C.

Table 3.1(a). The complex formation constants ($\log_{10} K$) of azobenzocrown ethers for metal ions (25 °C).

Metal ion	*trans* AB13C4	*trans* AB16C5	*trans* AB19C6	Ionic radius[a]/Å
Mg^{2+}	4.1	5.00	<3.00	0.86
Ca^{2+}	4.5	5.15	6.90	1.14
Sr^{2+}	4.1	4.91	7.13	1.32
Ba^{2+}	4.0	4.61	6.67	1.49
Li^{+}	4.10[b]	4.00[b]	3.41[b]	0.90
Na^{+}	--	3.69[b]	3.43[b]	1.16
K^{+}	--	3.15[b]	3.37[b]	1.52

a: ref. 28, b: ref. 16

Table 3.1(b). The complex formation constants ($\log_{10} K$) of azobenzocrown ethers for alkali and alkaline earth metal ions (25 °C).

Metal ion	$\log_{10} K$			ionic radius[a]/Å
	trans AB19C6	EDTA[c]	N-substituted[d]	
La^{3+}	7.34	15.50	2.82	1.201
Pr^{3+}	7.71	16.40	3.47	1.153
Nd^{3+}	7.59	16.61	4.41	1.135
Sm^{3+}	6.29	17.14	3.50	1.104
Eu^{3+}	6.27	17.35	2.71	1.090
Gd^{3+}	6.00	17.37	2.82	1.078
Tb^{3+}	4.01	17.93		1.063
Yb^{3+}	3.17	19.51		0.998

a: ref.28, b: ref. 16, c: ref. 29, d: ref. 22

strongly among in these metal ions. The complex formation constants of *trans* AB16C5 for alkaline earth metal ions was in the order of Ca^{2+} > Mg^{2+} > Sr^{2+} > Ba^{2+} as in the case of *trans* AB13C4. That for alkali metal ions was in the order of Li^{+} > Na^{+} > K^{+}. While *trans* AB13C4 complexed with Li^{+} as strong as with alkaline earth metal ions, the complexation ability of *trans* AB16C5 for alkali metal ions was smaller than that for alkaline earth metal ions.

3.3.3 Complexation Behavior of trans *AB19C6 with Alkaline Earth Metal Ions.*

Trans AB19C6 formed complexes with Ca^{2+}, Sr^{2+}, and Ba^{2+} among alkaline earth metal ions, and Na^{+} and K^{+}. However, it did not form a stable complex with Mg^{2+}. The complex formation constants were in the order of Sr^{2+} > Ca^{2+} > Ba^{2+} for alkaline earth metal ions. The difference of complex formation constants between Sr^{2+} and Ba^{2+} complex was so small, that a selective complexation for alkaline earth metal ions was not observed.

3.3.4 Complexation Behavior of trans *AB19C6 with Rare Earth Metal Ions.*

Trans AB19C6 was found to have complexation ability with some rare earth metal ions, while AB13C4 and AB16C5 do not have complexation ability with them. The ability of *trans* AB19C6 to form complexes with some rare earth metal ions was found, while those of *trans* AB13C4 and AB16C5 were not observed. *Trans* AB19C6 formed the most stable complex with Pr^{3+} among the rare earth metal ions. The complex formation constants were in the order of Pr^{3+} > Nd^{3+} > La^{3+} > Sm^{3+} = Eu^{3+} > Gd^{3+} >> Tb^{3+} > Yb^{3+}. While that value for Sr^{2+} was only ca. 2.5 times larger than that for Ba^{2+}, that for Pr^{3+} was 10^4 larger than that for Yb^{3+} and 1.3 times larger than that of Nd^{3+}. The complex

formation constant for Sr^{2+} was smaller than that for La^{3+} and larger than that for Sm^{3+}.

3.4 Discussion.

Complexation behavior of these azobenzocrown ethers with alkali metal ions (Li^+, Na^+, and K^+) have been studied by Shiga and et.al.[16] They concluded on complexation behavior of azobenzocrown ethers for alkali metal ions as follows. Complexation with alkali metal ions did not agree with the generally accepted ion-cavity size fitting concept, and it was suggested that the energy of metal ion-crown ether interaction is primary governed by a simple ion-dipole interaction rather than a macrocyclic encapsulating interaction. Here, complexation of these azobenzocrown ethers for alkaline earth and rare earth metal ions is discussed.

3.4.1 Complexation behavior of trans *Azobenzocrown ethers for Alkaline Earth Metal Ions.*

AB13C4: *Trans* AB13C4 has the largest complexation ability for Ca^{2+} as shown in Table 3.1. The strength of complexation ability with other alkaline earth metal ions was almost the same as each other. CPK model consideration suggests that *trans* AB13C4 can not take a conformation in which all oxygene atoms of polyoxyethylene moiety can face to inside of crown ether ring. CPK model also clarifies that the cavity radius of *trans* AB13C4 is ca. 0.50 Å. The quite small cavity of crown ether ring gives the suppressed motion of crown ether ring and less ability to take metal ion in it. Therefore, metal ions can not enter inside of crown ether ring of *trans* AB13C4. From this result, the forms of their complexes are expected to be "*perching*" type.

On the other hand, *trans* AB13C4 did not form complex with Na^+ and K^+ [16] even if the ionic sizes of Na^+ are almost the same as that of Ca^{2+}. These results also suggested that complexation behavior of *trans* AB13C4 is dominated by ionic charge rather than by ionic size.

AB16C5: As shown in Table 3.1, *trans* AB16C5 formed a complex with

Ca^{2+} most strongly. Effects of metal ion size on complexation with alkaline earth metal ions were observed. CPK model consideration gave the hole radius of *trans* AB16C5 to be 0.85-0.90 Å. This hole size seems to be the most suitable for complexation with Mg^{2+} whose ionic radius is 0.86 Å.[28] The value of complex formation constant for Ca^{2+} is only ca. 1.6 times larger than that for Mg^{2+}, and the difference between these values is small. The ionic sizes which is larger than Ca^{2+} are too large for the hole size of *trans* AB16C5.

AB19C6: *Trans* AB19C6 formed complexes with several metal ions. In the complexation with alkaline earth metal ions, selectivity was smaller than that in the case of AB13C4, as shown in Table 3.1. However, it had a little ability of ionic size recognition for alkaline earth metal ions as in the case of *trans* AB16C5, compared with the ability of ionic size recognition for alkali metal ions. The hole radius of AB19C6 was found to be 1.25-1.30 Å from CPK model consideration. This size is suitable for Sr^{2+} whose ionic radius is 1.32 Å.[28] On the other hand, Mg^{2+} whose ionic radius of 0.86 Å is too small to be complexed with *trans* AB19C6. *Trans* AB19C6 is a more flexible molecule due to its larger polyoxyethylene ring, and has more oxygen atoms in the polyoxyethylene ring. It is suggested by Shiga et al. that the driving force for complex formation of azobenzocrown ethers with alkali metal ions is an ion-dipole interaction.[16] The number of oxygen atoms within it affects the dipole moment of polyoxyethylene moiety. Therefore, *trans* AB19C6 usually forms more stable complexes with alkaline earth metal ions than *trans* AB13C4 or *trans* AB16C5 except for Mg^{2+} whose ionic size is too small. In the case of complexation with alkali metal ions, *trans* AB19C6 usually formed a less stable complex than *trans* AB16C5.[16] For only K^+, however, *trans* AB19C6 formed a more stable complex than *trans* AB16C5. Since the ionic radius of K^+ is suitable for the cavity size of *trans* AB19C6 as Sr^{2+}, the slight effect of "size-fitting" was observed.

3.4.2 Effects of Polyoxyethylene size for complexation ability with Alkaline Earth Metal Ions.

In order to visualize the complexation abilities of azobenzocrown ether, the profile of the complex formation constants is plotted as a function of ionic radius in Fig. 3.2. The order of strength of interaction of these compounds with alkaline earth metal ions are generally *trans* AB19C6 > *trans* AB16C5 > *trans* AB13C4. The factors of complex formation ability and relative selectivity are relative size of the crown ether's cavity to the radius of metal ion, surface charge density, ligand's structural rigidity, spatial arrangement of the donor atoms, and so on. Total charge on surface of crown ether moiety is carried by a number of oxygene atoms in polyoxyethylene, in other words, by the length of polyoxyethylene. Structural rigidity is carried by smaller polyoxyethylene moiety. Spatial arrangement of the donor atoms is brought by large polyoxyethylene moiety. Since large polyoxyethylene moiety gives structural flexibility, crown ether compounds can be adjusted to a suitable conformation for the metal ion.

In the case of azobenzocrown ethers, what is required for large interaction with alkaline earth metal ions are relative size of the crown ether's cavity of the to the radii of metal ions and the surface charge density. On the other hand, the effects of spatial arrangement of the donor atoms and what is required for selective complexation could not be clear.

3.4.3 Complexation behavior of trans *AB19C6 for rare earth metal ions.*

As mentioned in the previous section, only *trans* AB19C6 had complexation ability for several rare earth metal ions. *Trans* AB19C6 exhibited large complexation abilities for light rare earth metal ions, *e.g.* Pr^{3+} and Nd^{3+}. In order to visualize the complexation ability of *trans*

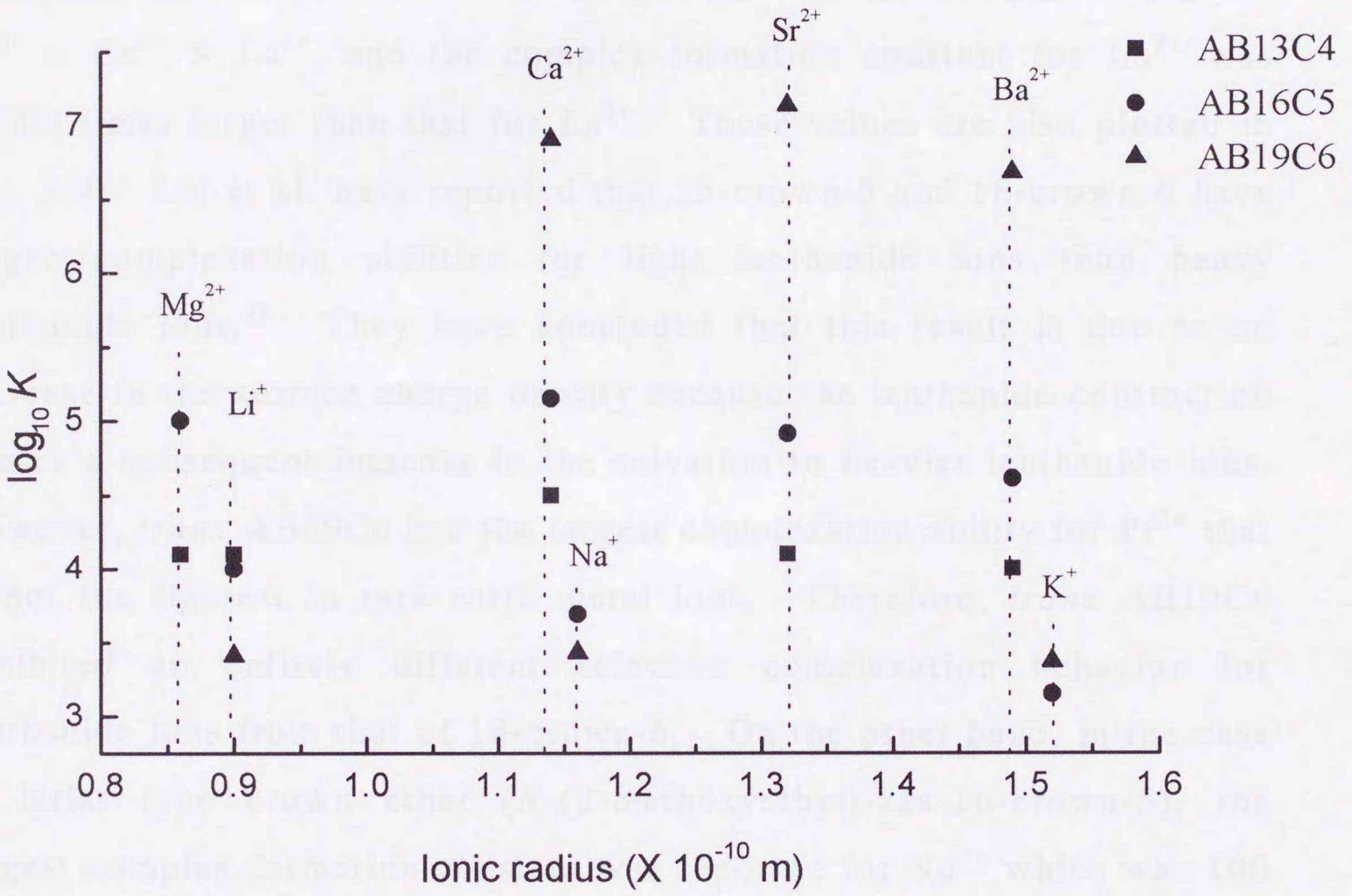

Fig. 3.2 Plots of $\log_{10} K$ of azobenzocrown ethers for alkali and alkaline earth metal ions.

AB19C6, the complex formation constants are plotted as a function of the ionic radius in Fig. 3.3. It is well known that the rare earth metal ion with more *f orbital* electrons usually forms a more stable complex with chelating compounds, e.g. EDTA.[29] In the case of EDTA, the order of complex formation constants is parallel to the number of *f orbital* electrons, $Lu^{3+} > Yb^{3+} > \cdots\cdots > Tb^{3+} > Gd^{3+} >> Eu^{3+} > Sm^{3+} > Nd^{3+} > Pr^{3+} > Ce^{3+} > La^{3+}$, and the complex formation constant for Lu^{3+} was 20000 times larger than that for La^{3+}. These values are also plotted in Fig. 3.3. Liu et al. have reported that 15-crown-5 and 18-crown-6 have larger complexation abilities for light lanthanide ions than heavy lanthanide ions.[30] They have concluded that this result is due to an increase in the surface charge density because the lanthanide contraction causes a subsequent increase in the solvation to heavier lanthanide ions. However, *trans* AB19C6 had the largest complexation ability for Pr^{3+} that is not the lightest in rare earth metal ions. Therefore, *trans* AB19C6 exhibited an entirely different selective complexation behavior for lanthanide ions from that of 18-crown-6. On the other hand, in the case of lariat type crown ether (*N*-(2-methoxyethyl)-aza-16-crown-5), the largest complex formation constant was reported for Nd^{3+} which was 100 times larger than that for Gd^{3+}.[24] The plots of these values are superimposed in Fig 3.3. However, it must be mentioned that the selectivity was smaller than that of *trans* AB19C6.

The observed absorption spectral change of *trans* AB19C6 should be due to the interaction between azobenzene unit and metal ion in the complex. These complexes gave almost the same absorption spectra to each other (Fig. 4.11), which will be discussed in detail in Chapter 4. This result shows that there are almost the same spectral shifts in $\pi \rightarrow \pi^*$ or $n \rightarrow \pi^*$ transitions on the complexation with rare earth metal ions. The excitation seems to cause the same change of interaction between azobenzene unit and metal ion in these rare earth metal complexes. This

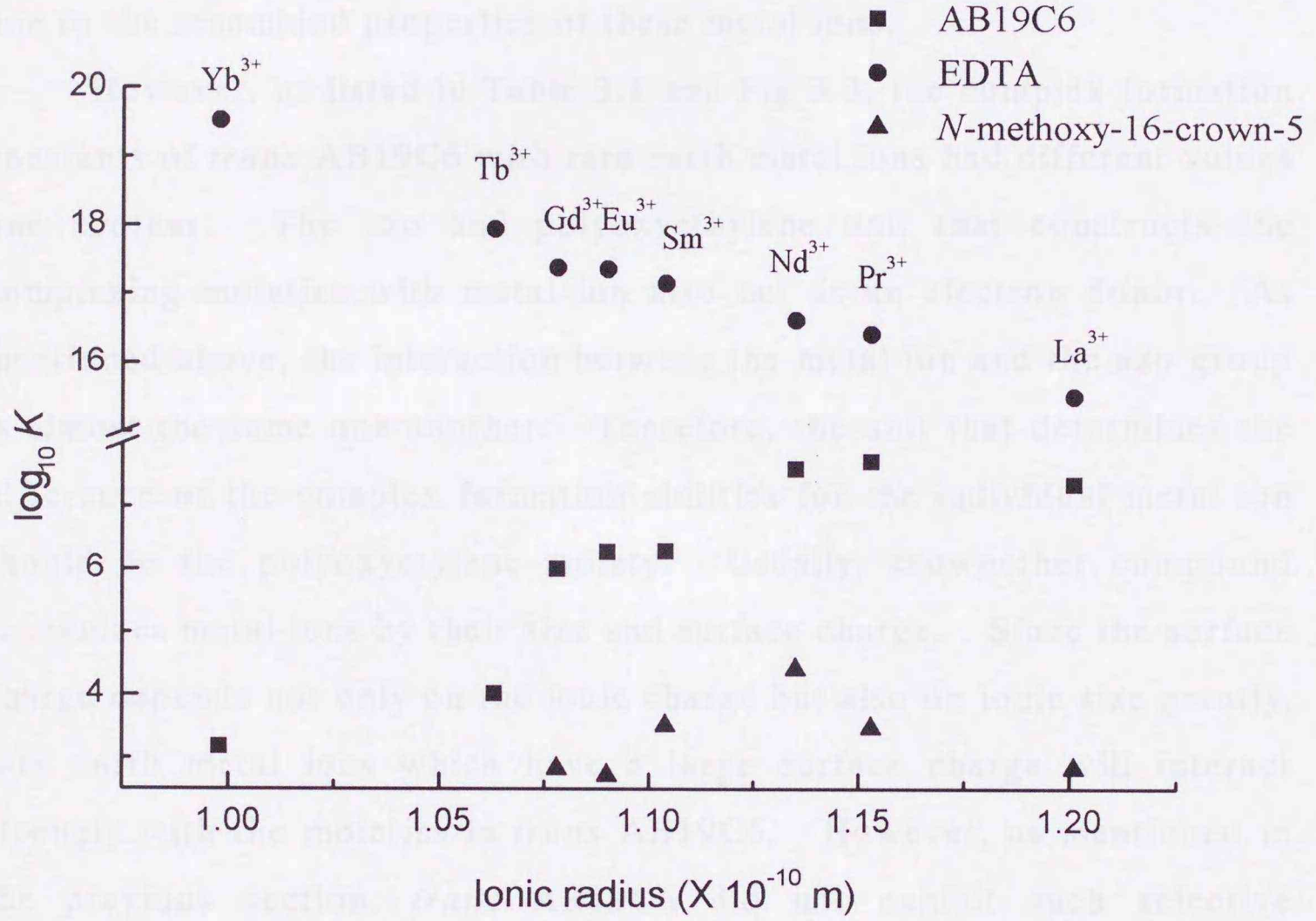

Fig. 3.3 Plots of $\log_{10} K$ for rare earth metal ions.

is not the case for other alkali or alkaline earth metal ion, the spectral changes were different from each other, which will be discussed in detail in Chapter 4, reflecting the differences of the interactions between metal ion and azo moiety of AB19C6 in ground state and $\pi\pi^*$ or $n\pi^*$ excited state. Almost the same change in the rare earth metal complexes will be due to the resembled properties of these metal ions.

However, as listed in Table 3.1 and Fig 3.3, the complex formation constants of *trans* AB19C6 with rare earth metal ions had different values one another. The azo and polyoxyethylene unit that constructs the complexing moieties with metal ion also act as an electron donor. As mentioned above, the interaction between the metal ion and the azo group is almost the same one another. Therefore, the unit that determines the difference of the complex formation abilities for the individual metal ion should be the polyoxyetylene moiety. Usually, crownether compound recognizes metal ions by their size and surface charge. Since the surface charge depends not only on the ionic charge but also on ionic size greatly, rare earth metal ions which have a large surface charge will interact strongly with the moieties in *trans* AB19C6. However, as mentioned in the previous section, *trans* AB19C6 did not exhibit such selective complexation ability for alkaline earth metal ions except for magnesium ion, and did not have a size recognition ability for divalent metal ions. Therefore, in non protic solvent, such as acetonitrile, in which the solvation energy was weaker than that in protic solvent, surface charge of metal ions and sizes of them determine the complexation ability of *trans* AB19C6.

On the other hand, as mentioned above, *trans* AB16C5, which formed complex with alkaline earth metal ions, exhibited a very weak complexation ability for the rare earth metal ions, and did not allow to be determine the complex formation constant accurately. Although Ca^{2+} has ionic radius closer to that of rare earth metal ions than other alkaline

earth metal ions, *trans* AB16C5 exhibited the strongest complexation ability for Ca^{2+} among alkaline earth metal ions. In the case of *trans* AB19C6, it formed complex with Sr^{2+} most strongly, and formed complex with Ca^{2+} more stable than *trans* AB16C5. From "size-fitting" concept, *trans* AB16C5 should form a complex with rare earth metal ions, since it forms complex with Ca^{2+}. And, in terms of charge interaction, *trans* AB16C5 forms a complex with rare earth metal ions which has a larger charge than alkaline earth metal ions, since it forms complex with alkaline earth metal ions. However, *trans* AB16C5 did not make any complex with rare earth metal ions. There may be several ways to explain this result. Either *trans* AB16C5 may not have ability to desolvate rare earth metal ions, or not be flexible enough to orient a good for the formation of the complex with rare earth metal ions. However, further investigation will be required for the detailed discussion.

3.5 Conclusion.

Complexation behaviors of *trans* azobenzene compounds were studied for alkaline earth metal ions, and also for rare earth metal ions. It was found that *trans* AB19C6 has a selective complexation with rare earth metal ions. The factors of complexation for several metal ions of these azobenzene compounds in non-protic solvent, *e.g.* acetonitorile, are (1) a surface charge of metal ion and (2) a ionic size. These azobenzene compounds can complex with metal ions with appropriate charge. In other words, these compounds can not complex strongly with metal ions with small surface charge, *i.e.* alkali metal ions. They can not complex strongly with metal ions with too large surface charge, i.e. rare earth metal ions, for AB13C4 or AB16C5. *Trans* AB19C6 exhibited selective complexation with rare earth metal ions. This selectivity was due to the interaction between the metal ion and the polyoxyethylene unit of *trans* AB19C6.

Chapter 4

Absorption Spectrum of Azobenzocrown ethers

4.1 Introduction.

The electronic transitions that take place in the visible and ultraviolet regions of the spectrum are due to the absorption of radiation by specific type of group, bonds, and functional group within the molecule. The wavelength of absorption is a measure of the energy required by the transition. Its intensity is dependent on the probability of the transition occurring when electronic system and the radiation interact and on the polarity of the excited state.[1] Electron within the molecule which concerns with the absorption in visible and ultraviolet regions are 1) non bonding outer-shell paired electrons (n electrons), and 2) electrons in π orbitals. The transition of these electrons to an excited π^* state take place by photon absorption.

One of reasons why metal complexes have absorption bands in visible and ultraviolet regions is an excitation of the ligand. Complexation with a metal ion is similar to a protonation of the molecule, and will exhibit a little change in the wavelength and intensity of absorption as a result.[1]

Spectroscopic properties of azobenzene were summarized by Rau.[31] *Trans* azobenzene has absorption bands due to $\pi \rightarrow \pi^*$ transition and $n \rightarrow \pi^*$ transition of azo group in ultraviolet and visible region, respectively. Since $n \rightarrow \pi^*$ transition is basically forbidden, the intensity of absorption band is much smaller than that for the $\pi \rightarrow \pi^*$ transition. On the other hand, *cis* azobenzene has an absorption band due to $n \rightarrow \pi^*$ transition. However, there is no absorption band due to $\pi \rightarrow \pi^*$ transition of azo group in the ultraviolet region. Since the $n \rightarrow \pi^*$ transition of *cis* azobenzene is partially allowed, *cis* azobenzene exhibits larger absorption in the visible region than *trans* azobenzene.

It can be expected that absorption spectra of azobenzocrown ethers used in this study are affected by 1) substituents at ortho positions, 2) length of polyoxyethylene giving distortion of azobenzene unit due to crown ether structure, and 3) complexation with metal ions.

In this chapter, these three effects of azobenzocrown ether on absorption spectra are discussed.

4.2 Experimental.

4.2.1 Measurement of absorption spectra.

Absorption spectra of azobenzocrown ethers were obtained in an acetonitrile solution at 25 °C. A solution of the complex was prepared by adding a salt into the acetonitrile solution of azobenzocrown ether. This procedure was carried out in the dark to prevent photoisomerization.

4.2.2 Spectral Resolution.

Obtained absorption spectra were resolved to three transition bands, two $\pi \rightarrow \pi^*$ bands and one $n \rightarrow \pi^*$ band shown in Fig. 4.1. This resolution was conducted by assuming the Gaussian shape with a nonlinear curve-fitting method (Marquardt method).

4.2.3 Energy Levels of Excited State of the Complexes.

The free energies of the excited states of azobenzocrown ethers and their complexes are calculated by the following equation.

$$\begin{aligned} G_{ex} &= G_{gnd} + \Delta E \\ &= G_{gnd} + h\nu \end{aligned} \qquad (4.1)$$

where, ΔE is an excitation energy, and G_{ex} and G_{gnd} are the free energy of the excited and ground states, respectively, in the free or the complexed form, and ν is frequency of the absorbed light. Photon energy of fluorescence light is usually used for calculation of ΔE. However, these azobenzocrown ethers have no fluorescence at all as many azobenzene compounds. A photon energy of absorbed light ($h\nu$) was used for ΔE in this study.

The free energy changes at the complexation of azobenzocrown ethers with metal ions in a ground state are calculated by the following thermodynamical relation.

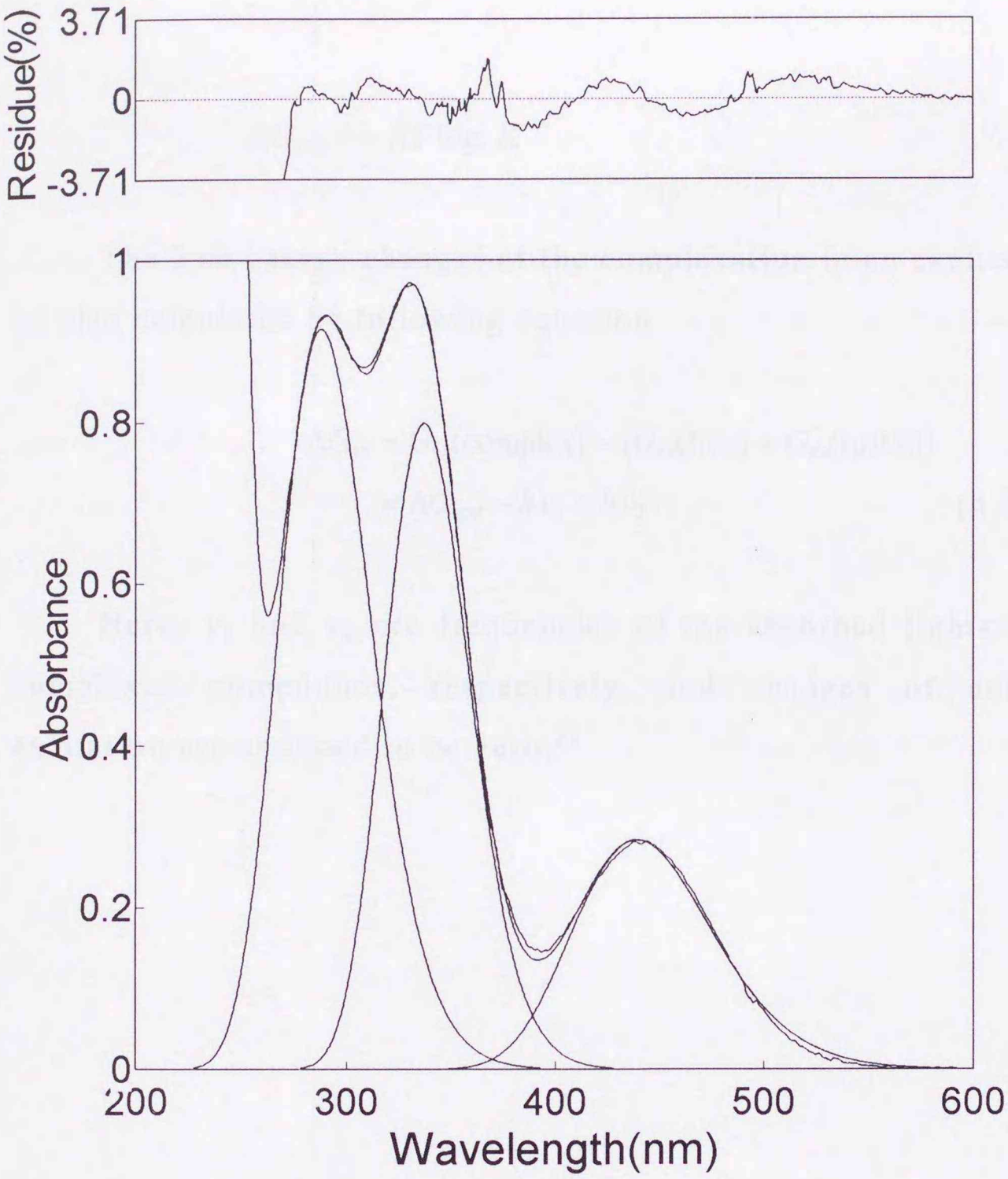

Fig. 4.1 Spectral resolution of *trans* AB19C6
to three transition bands (Gaussian Shape)

$$\Delta G_{gnd} = -RT \log_e K \qquad (4.2)$$

The free energy changes at the complexation in an excited state can be also calculated by following equation.

$$\Delta G_{ex} = G_{ex}(\text{complex}) - (G_{ex}(\text{free}) + G_{ex}(\text{metal}))$$
$$= \Delta G_{gnd} - h\nu_1 + h\nu_2 \qquad (4.3)$$

Here, ν_1 and ν_2 are frequencies of the absorbed lights of free and complexed compounds, respectively, and changes of enthology by excitation are assumed to be zero.[32]

4.3 Results.

Absorption spectra of *cis* and *trans* isomers of AB13C4, AB16C5, AB19C6, and DMAB are shown in Figs. 4.2-5, respectively. These compounds in *trans* forms exhibit absorption peaks at 300-400 and ca. 450 nm due to $\pi \rightarrow \pi^*$ and $n \rightarrow \pi^*$ transitions, respectively. The absorption coefficient of $n \rightarrow \pi^*$ transition peak of *cis* isomers of AB13C4 and AB16C5 are larger than those of these *trans* isomers as in the case of unsubstituted azobenzene. However, those of *cis* isomer of DMAB and AB19C6 are less than those of *trans* isomers differently from usual azobenzene. These *trans* azobenzocrown ethers gave spectral changes by the complexation with metal ions as follows: (1) $n \rightarrow \pi^*$ shifted to shorter wavelength side, and (2) $\pi \rightarrow \pi^*$ shifted to longer wavelength side.

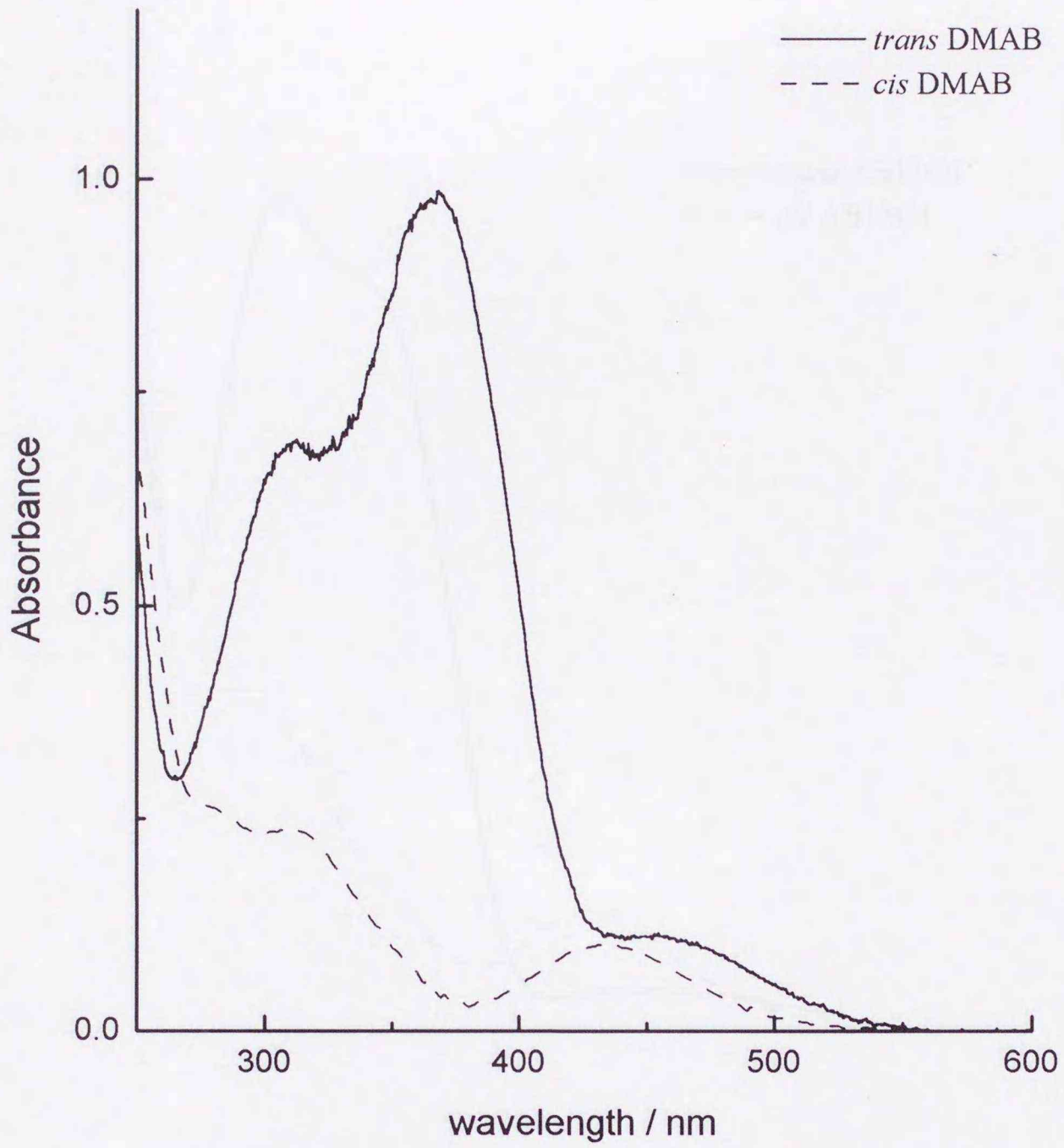

Fig. 4.2 Absorption spectra of *trans* and *cis* DMAB.
[DMAB] = 1.0 $\times 10^{-4}$ M in acetonitrile at 25 °C.

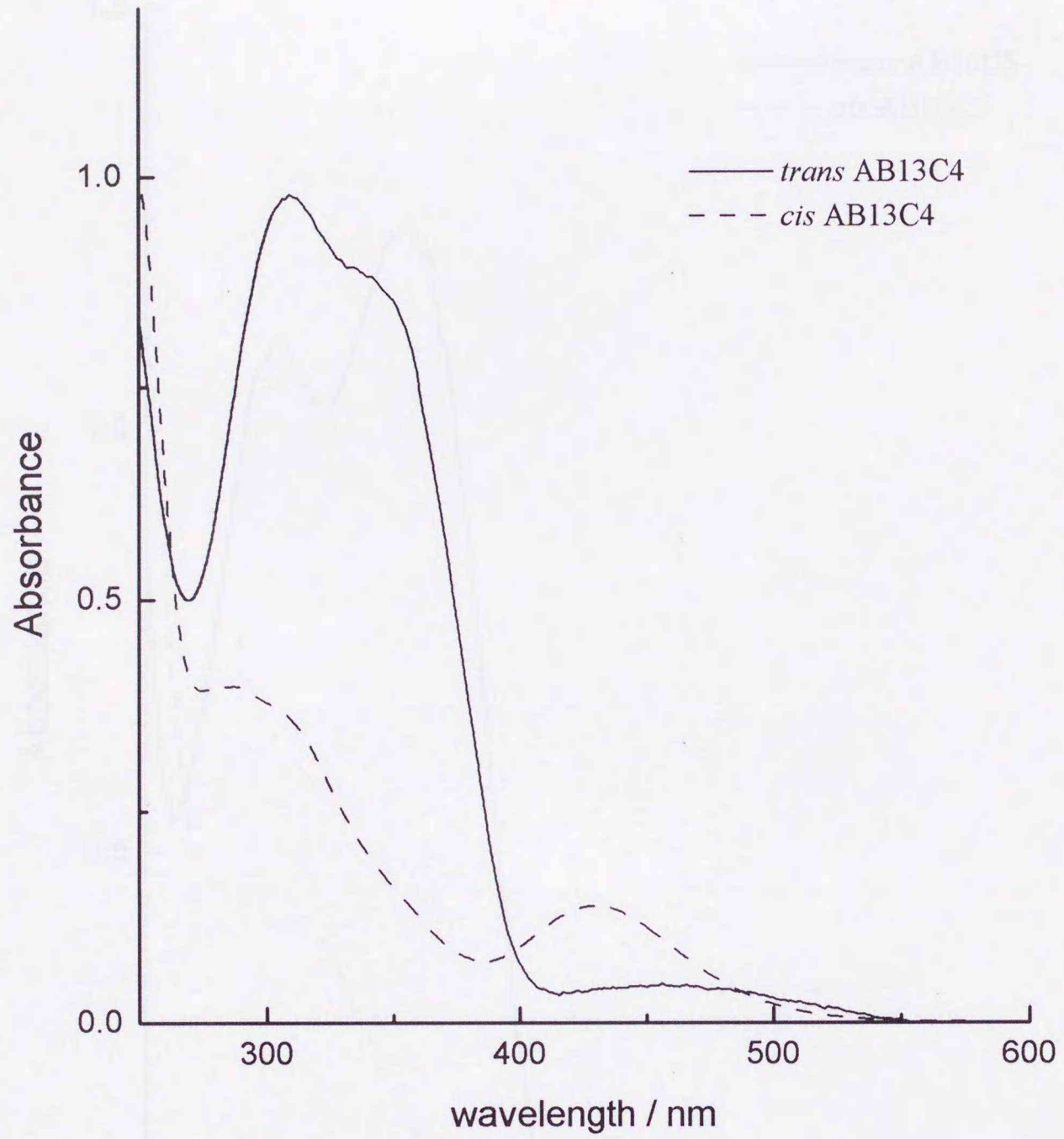

Fig. 4.3 Absorption spectra of *trans* and *cis* AB13C4.
[AB13C4] = 1.0×10^{-4} M in acetonitrile at 25 °C.

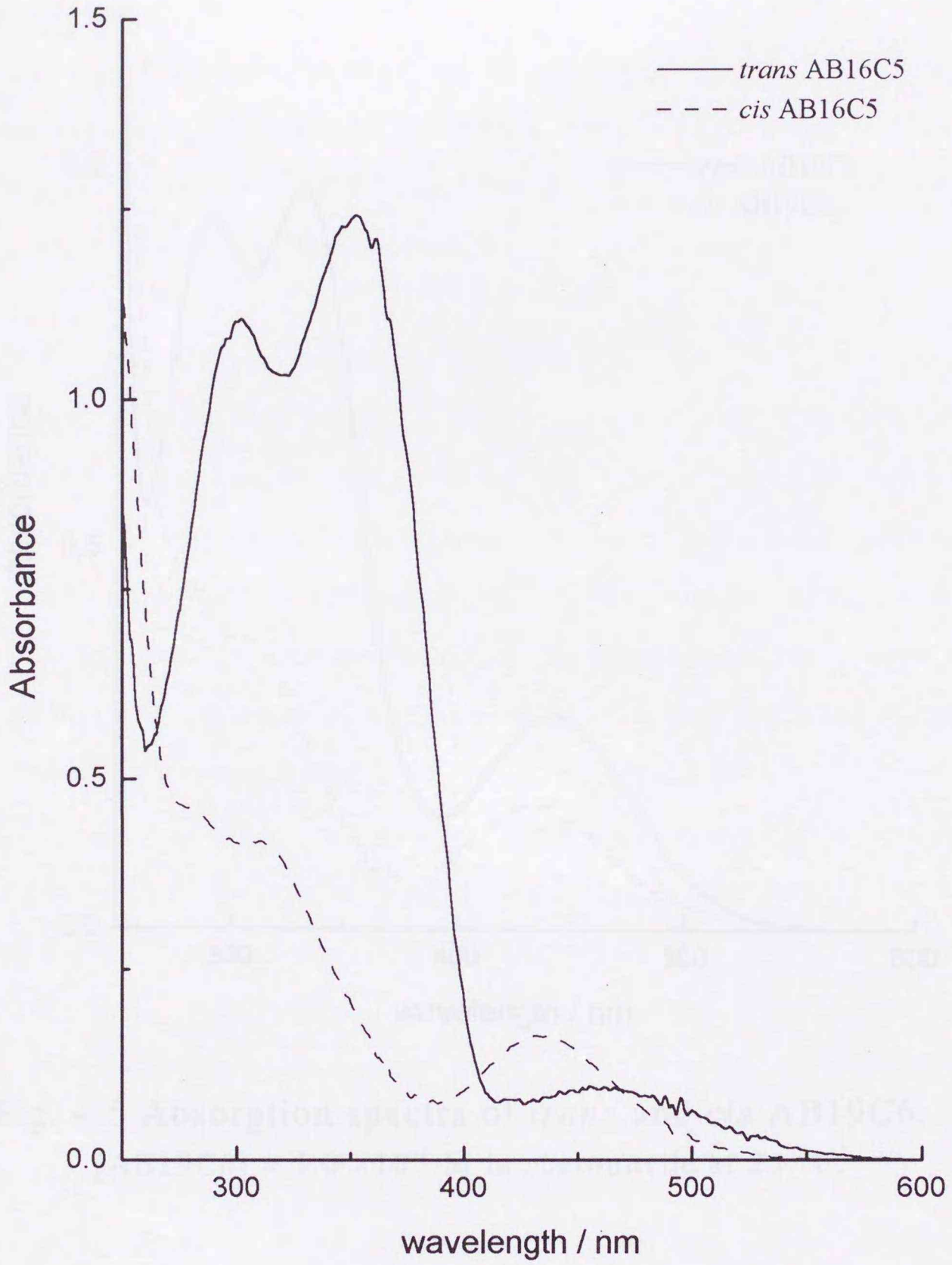

Fig. 4.4 Absorption spectra of *trans* and *cis* AB16C5.
[AB16C5] = 1.0×10^{-4} M in acetonitrile at 25 °C.

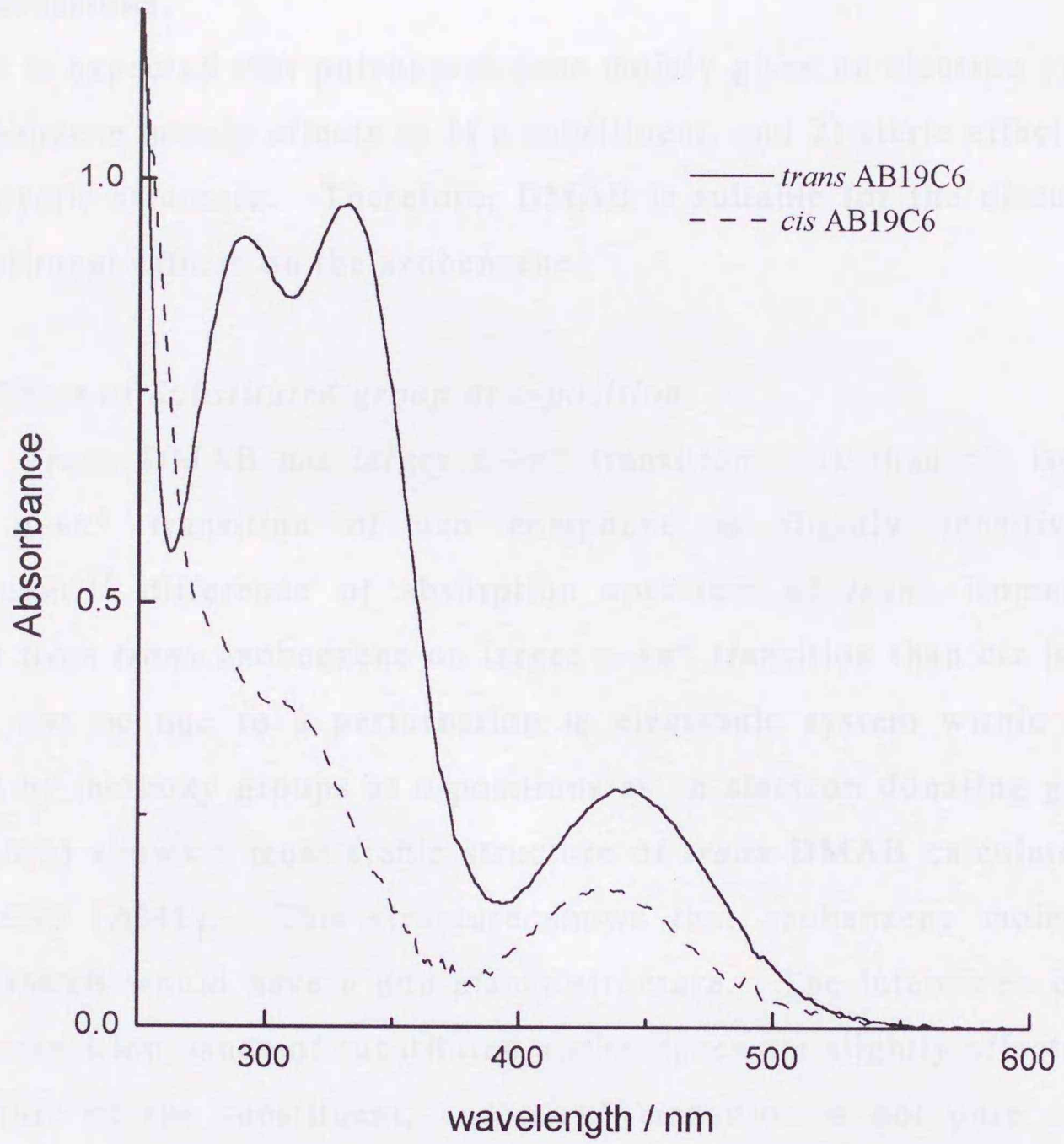

Fig. 4.5 Absorption spectra of *trans* and *cis* AB19C6.
[AB19C6] = 1.0 $\times 10^{-4}$ M in acetonitrile at 25 °C.

4.4 Discussions.

It is expected that polyoxyethylene moiety gives an electron system in azobenzene moiety effects as 1) a substituent, and 2) steric effects due to its cyclic structure. Therefore, DMAB is suitable for the discussion of substituent effects on the azobenzene.

4.4.1 Effect of Substituted group at o*-position.*

Trans DMAB has larger n→π* transition peak than *cis* isomer. Since n→π* transition of azo compound is slightly sensitive to substituent,[17] difference of absorption spectrum of *trans* isomers of DMAB from *trans* azobenzene on larger n→π* transition than *cis* isomer should not be due to a perturbation in electronic system within *trans* DMAB by methoxy groups at *o*-positions as an electron donating group. Fig. 4.6(b) shows a most stable structure of *trans* DMAB calculated by MOPAC93 (AM1). This structure shows that azobenzene moiety of *trans* DMAB would have a non-planar structure. The intensities of the n→π* transition bands of substituted azobenzenes are slightly affected by the nature of the substituent, and n→π* transition is not pure and is coupling with another state. This coupling is out-of-plane deformation vibration. Therefore, this non-planar structure should be mainly due to the repulsion between the methoxy groups at *o*-positions and lone pairs of azo nitrogen atoms in *trans* isomers. This distortion of azobenzene plane may cause partial cancellation of forbidden n→π* transition. Rau described following explanation by MO model; n→π* transition of *trans* azobenzene is result of coupling between nπ* excited state and neighboring allowed ππ* state, and this coupling is possible through an out-of-plane deformation by vibration.[17] *Trans* DMAB probably have larger n→π* transition due to this non-planar structure.

4.4.2 Effects of length of polyoxyethylene.

(a) *trans* azobenzene

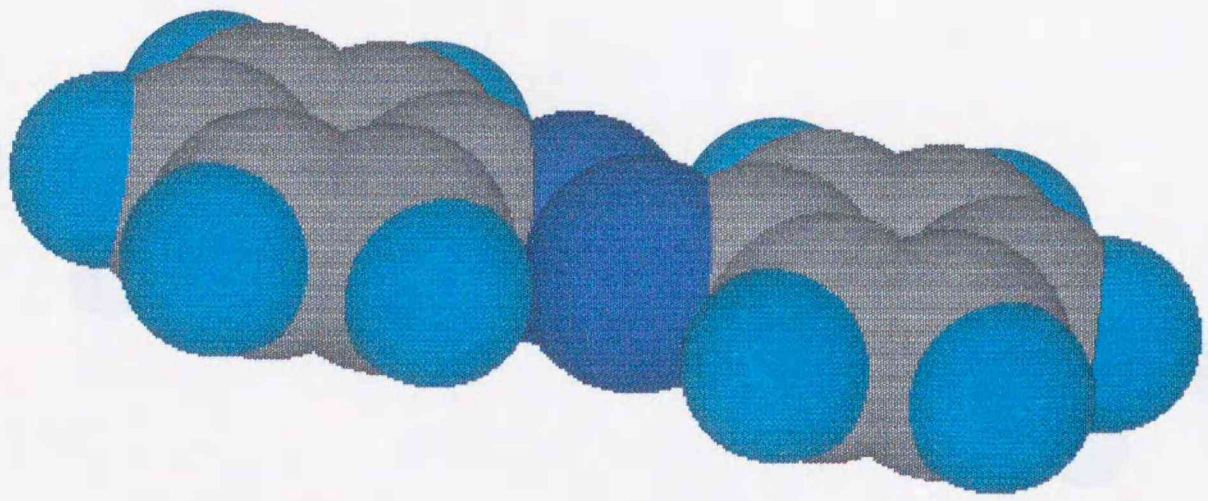

(b) *trans* DMAB

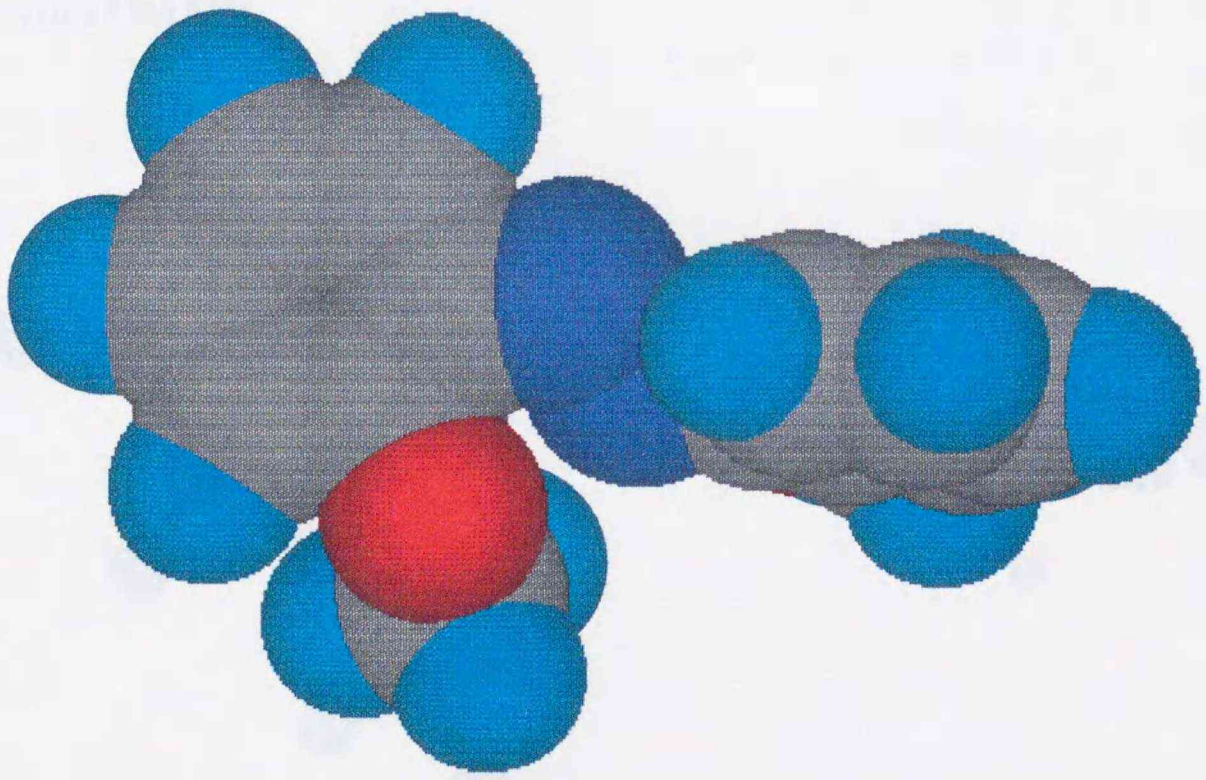

Fig. 4.6 Molecular structures of (a) *trans* azobenzene and (b) *trans* DMAB calculated by MOPAC.

(a) *trans* azobenzene

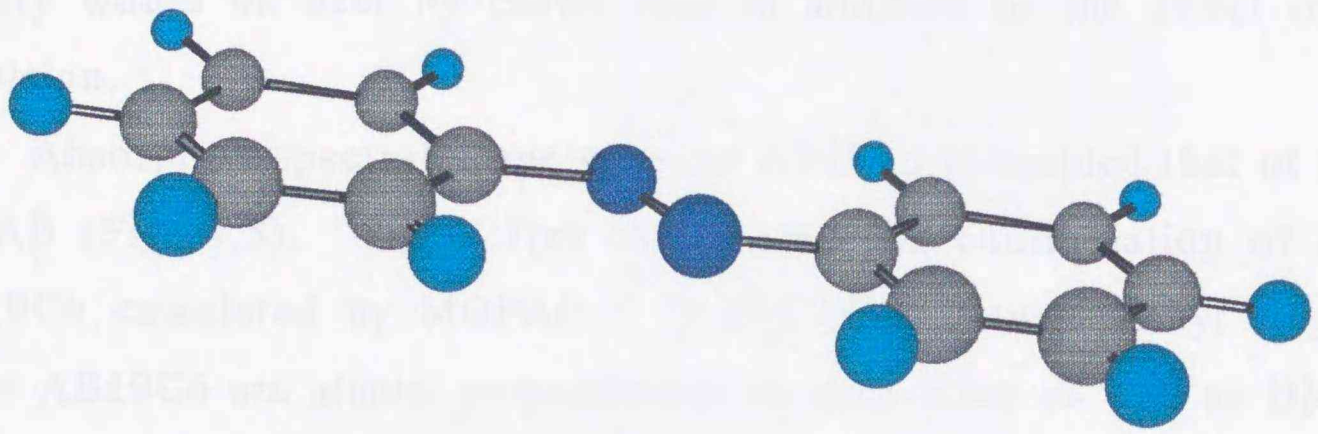

(b) *trans* DMAB

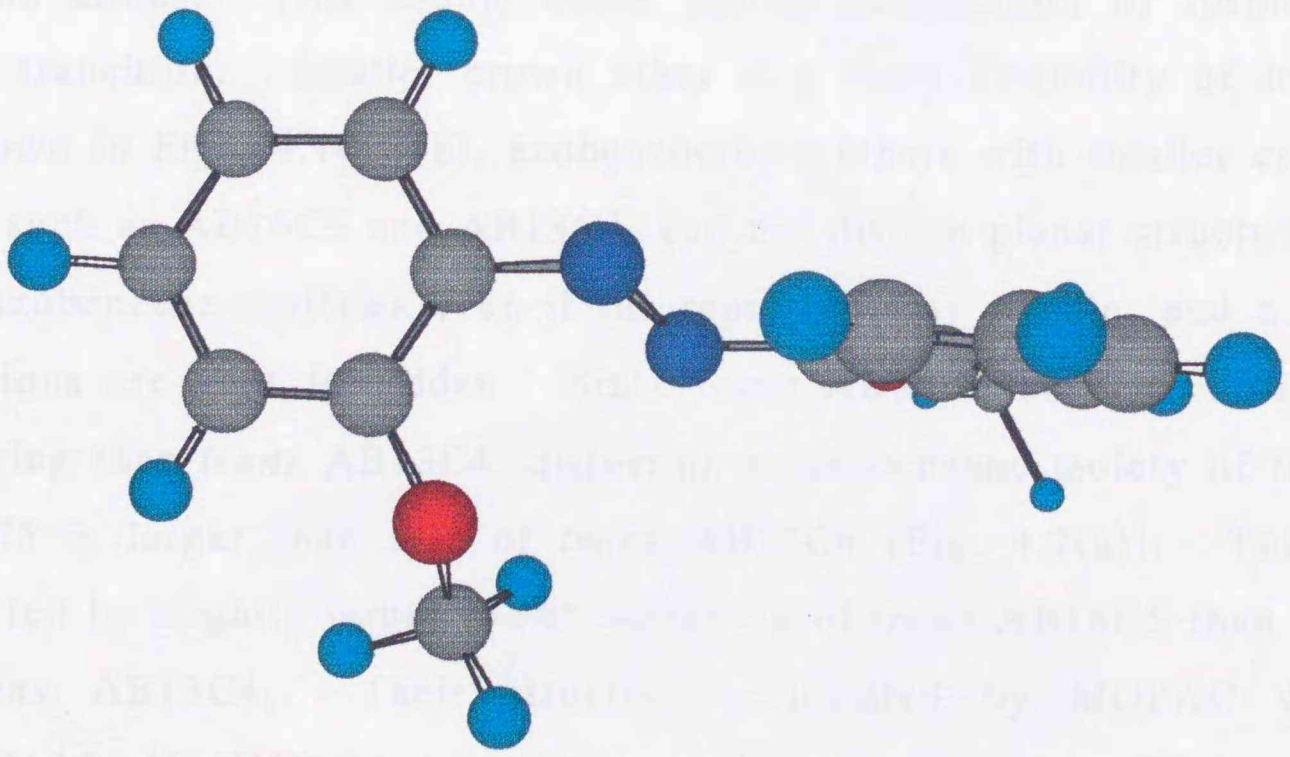

In the case of DMAB, what affects absorption spectra of *trans* isomer is only the repulsion between the substituents at 2,2'-position. In the case of azobenzocrown ethers, polyoxyethylene moiety would prevent conformational change of azobenzene moiety, and azobenzene moiety would be bent by crown ring in addition to the effect of the repulsion.

Absorption spectral shape of *trans* AB19C6 resembled that of *trans* DMAB (Fig. 4.5). Fig. 4.7(c) shows plausible conformation of *trans* AB19C6 calculated by MOPAC. In Fig. 4.7(c), two phenyl rings of *trans* AB19C6 are almost perpendicular to each other as well as DMAB. Since *trans* AB19C6 has large conformational flexibility due to large crown ether moiety, it can take a conformation with the smallest repulsion between the oxgen atoms at *o*-positions and lone pairs of azo nitrogen atoms. This should cause partial cancellation of forbidden $n \rightarrow \pi^*$ transition. Smaller crown ether ring loses flexibility of itself. As shown in Figs. 4.7(a) (b), azobenzocrown ethers with smaller crown ether, such as AB16C5 and AB13C4, can not disturb planar structure of their azobenzene moieties even if the repulsion may remain, and $n \rightarrow \pi^*$ transitions are kept forbidden. Since *trans* AB16C5 has larger crown ether ring than *trans* AB13C4, distortion at azobenzene moiety of *trans* AB16C5 is larger than that of *trans* AB13C4 (Fig. 4.7(a)). This is supported by slightly larger $n \rightarrow \pi^*$ transition of *trans* AB16C5 than that of *trans* AB13C4. Their structures calculated by MOPAC were supported by ^{1}H NMR spectra of these azobenzocrown ethers (Fig. 4.8).

4.4.3 The effects of complexation with metal ions.

Figs. 4.9-4.12 also show absorption spectra of the alkaline earth metal complexes of *trans* azobenzocrown ethers, and rare earth metal complexes of *trans* AB19C6. The resolved wavelength data are listed in Table 4.1.

(a) *trans*AB13C4

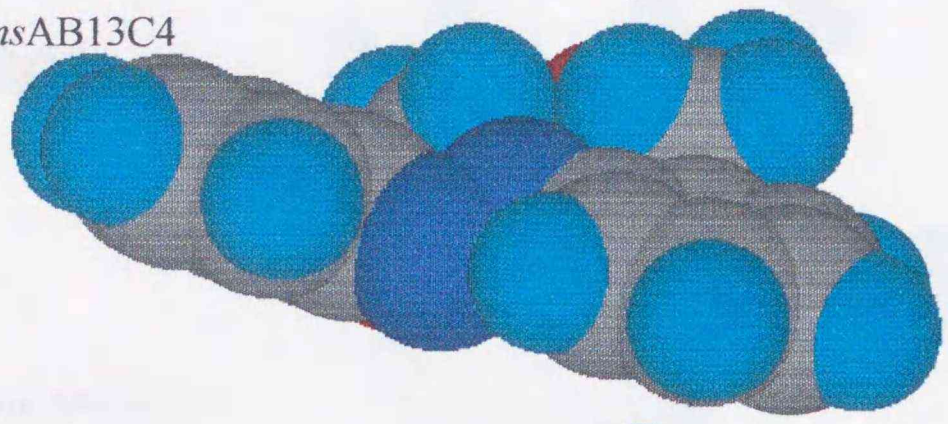

(b) *trans* AB16C5

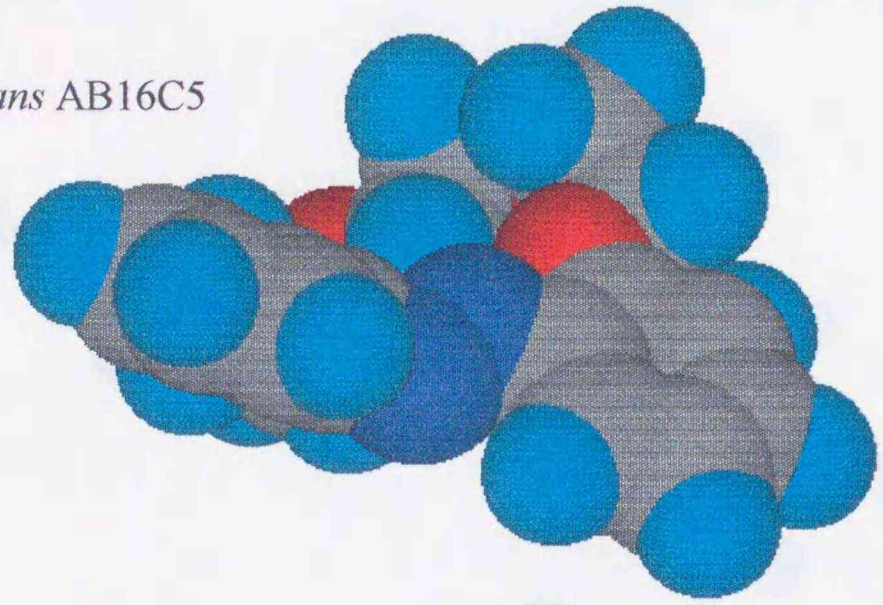

(c) *trans* AB19C6

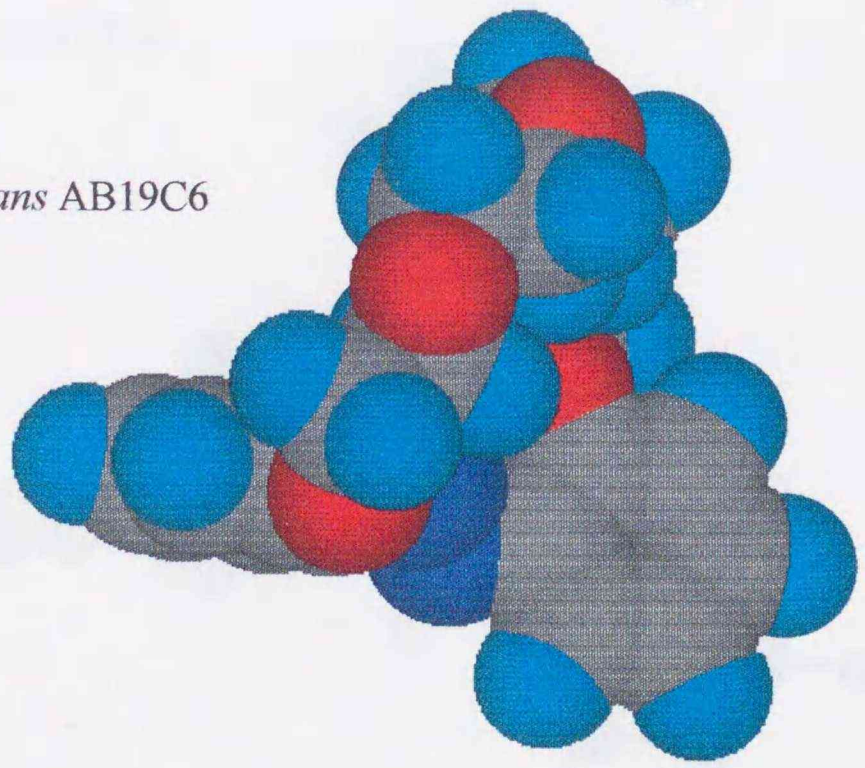

Fig 4.7 Molecular structures of *trans* azobenzocrown ethers (a) AB13C4, (b) AB16C5, (c) AB19C6 calculated by MOPAC.

*trans*AB13C4

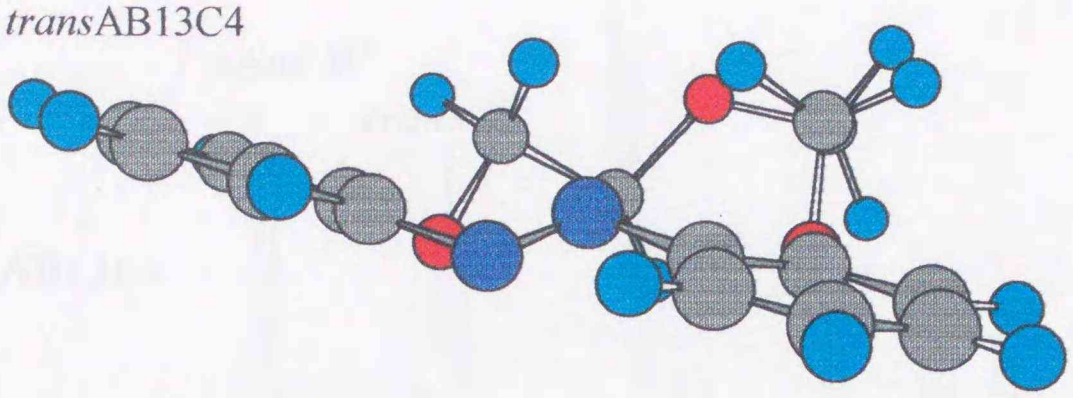

trans AB16C5

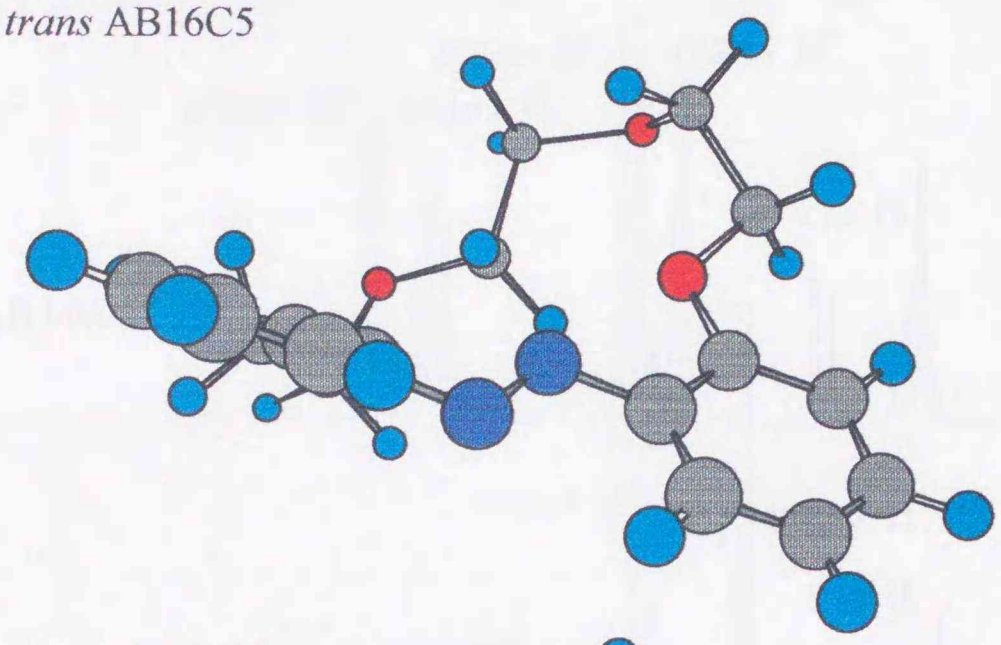

trans AB19C6

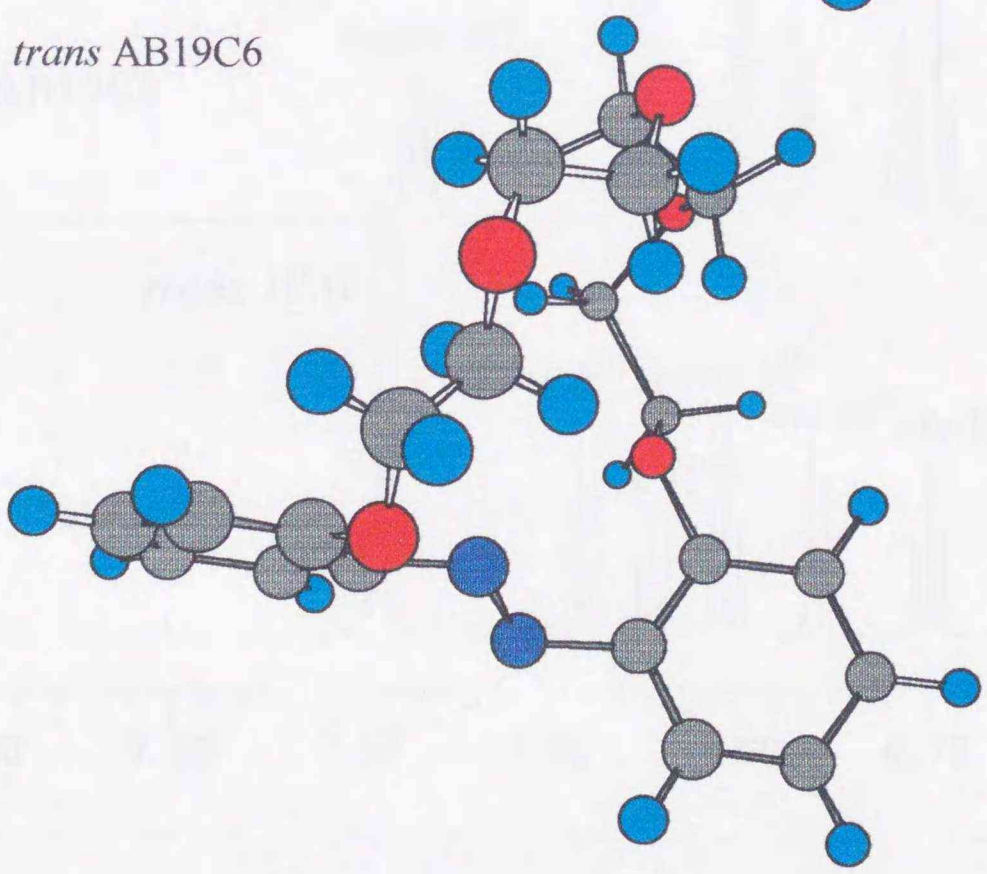

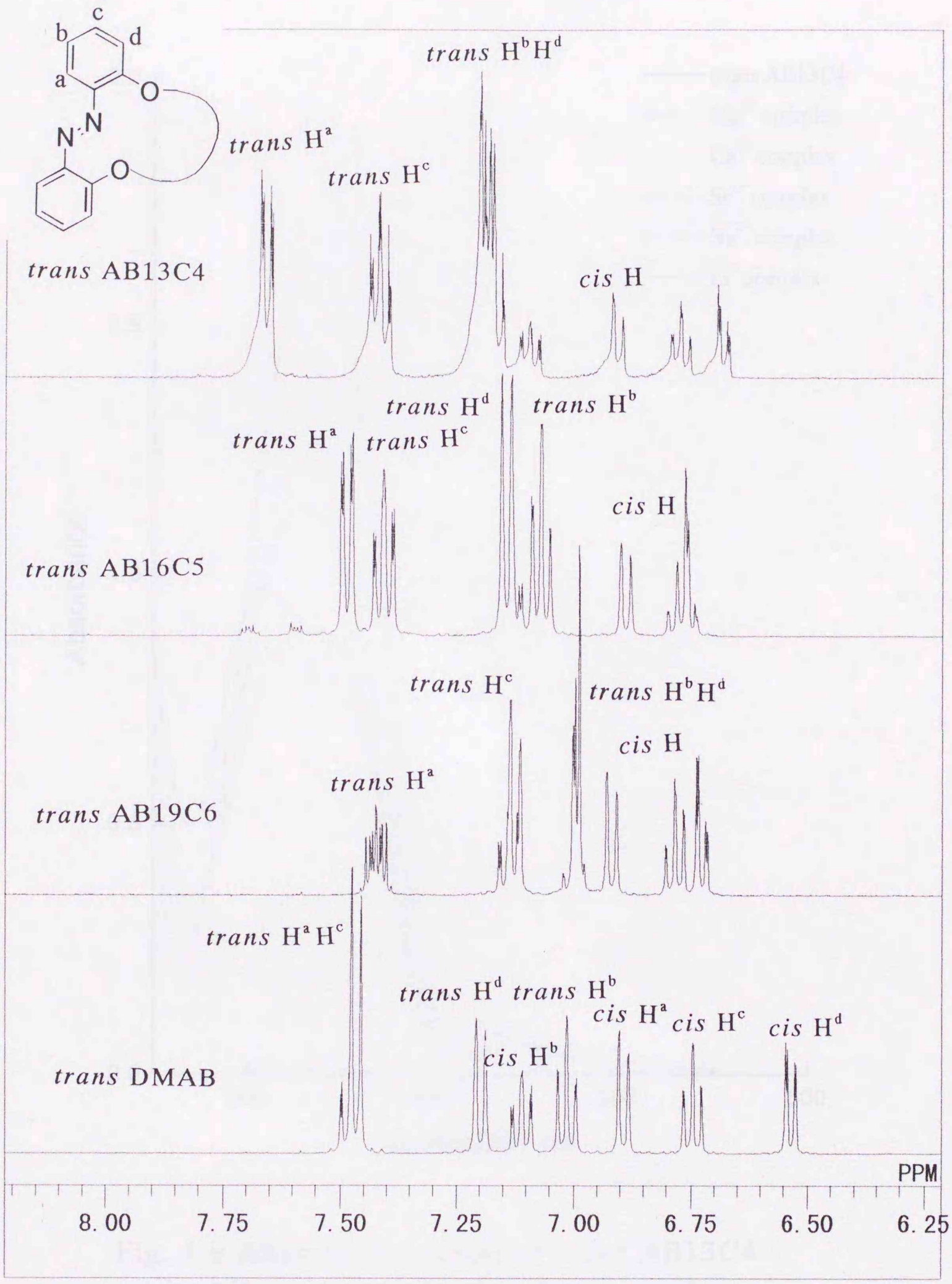

Fig. 4.8 ^{1}H NMR spectra of azobenzocrown ethers and DMAB
solvent acetonitrile-d_3 at 25°C

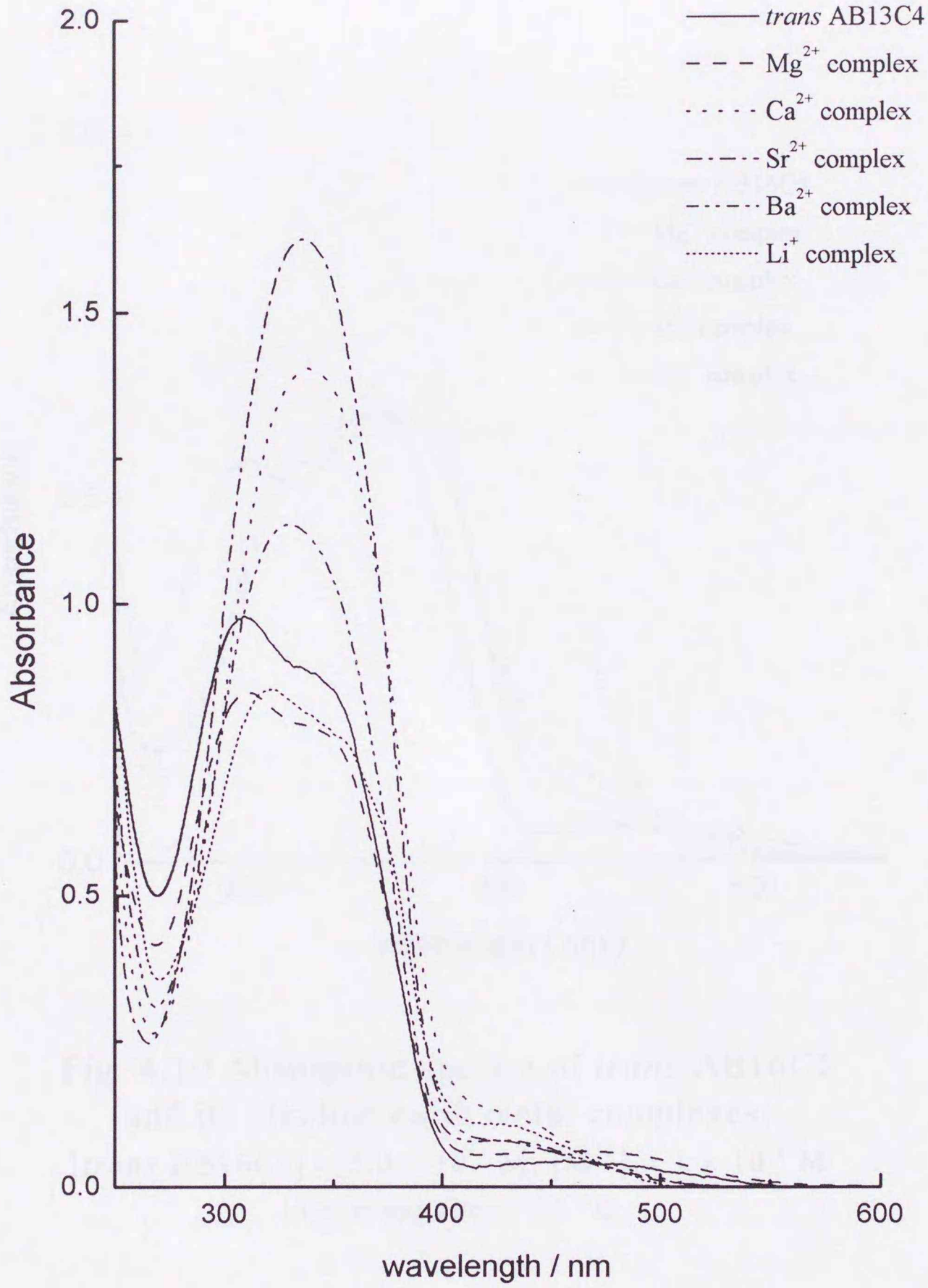

Fig. 4.9 Absorption spectra of *trans* AB13C4 and its Li^+ and alkaline earth metal complexes.
[*trans* AB13C4] = 1.0×10^{-4} M, $[M^{n+}] = 1 \times 10^{-1}$ M
in acetonitrile at 25 °C

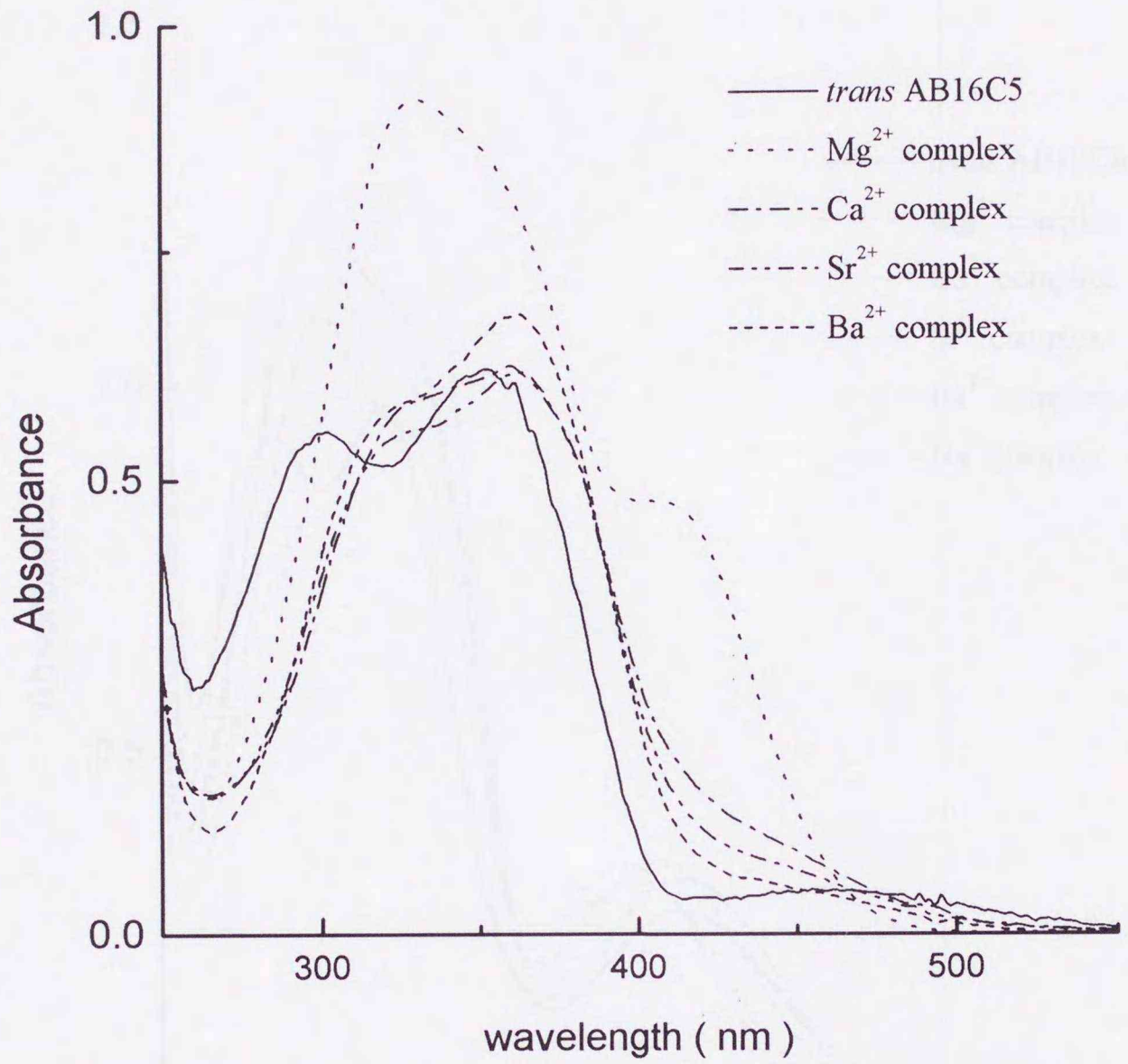

Fig. 4.10 Absorption spectra of *trans* AB16C5 and its alkaline earth metal complexes.
[*trans* AB16C5] = 5.0×10^{-5} M, $[M^{2+}] = 1 \times 10^{-1}$ M
in acetonitrile at 25 °C

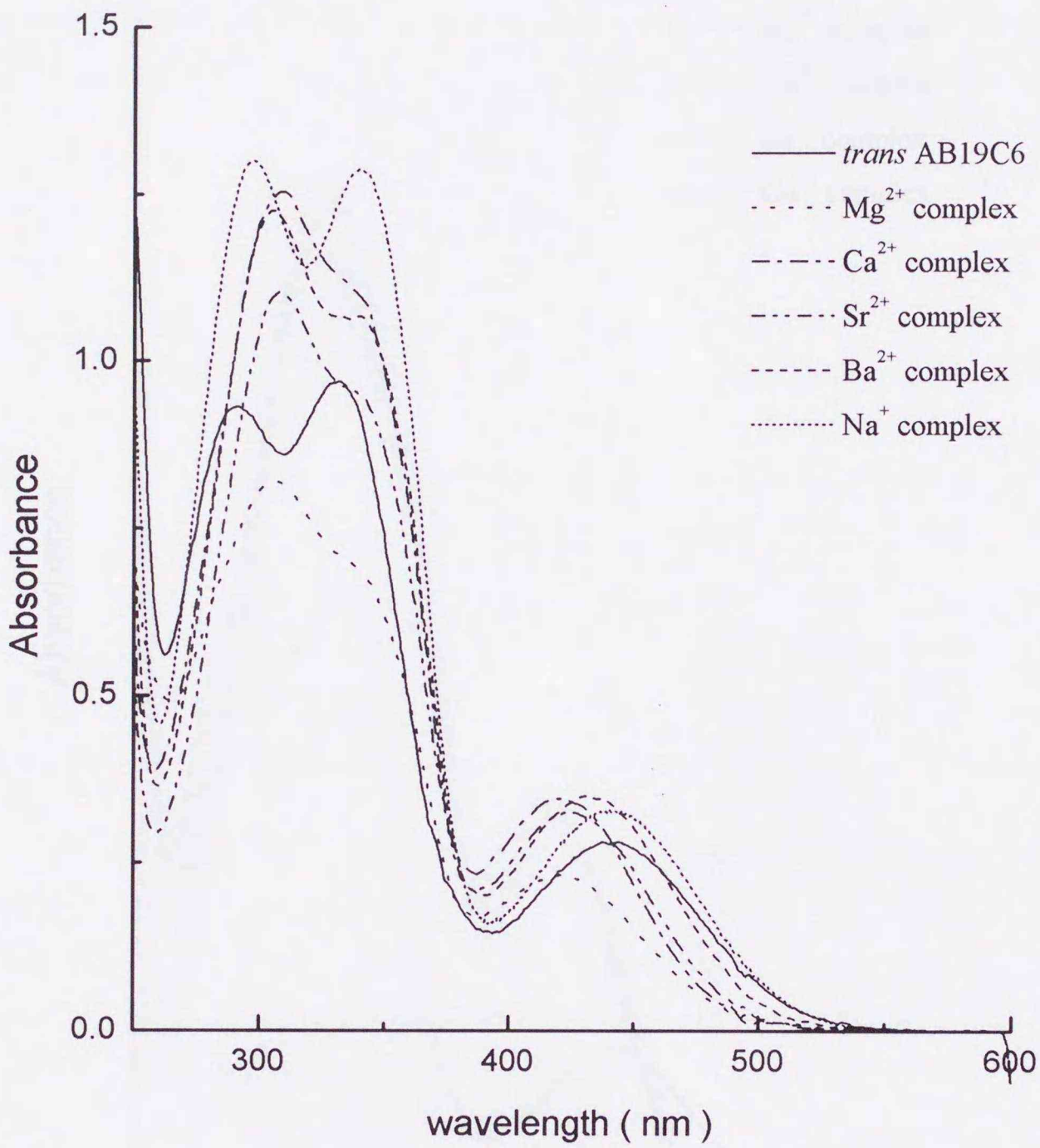

Fig. 4.11 Absorption spectra of *trans* AB19C6 and its Na^+ and alkaline earth metal complexes.
[*trans* AB19C6] = 1.0×10^{-4} M, $[M^{n+}] = 1 \times 10^{-1}$ M
in acetonitrile at 25 °C

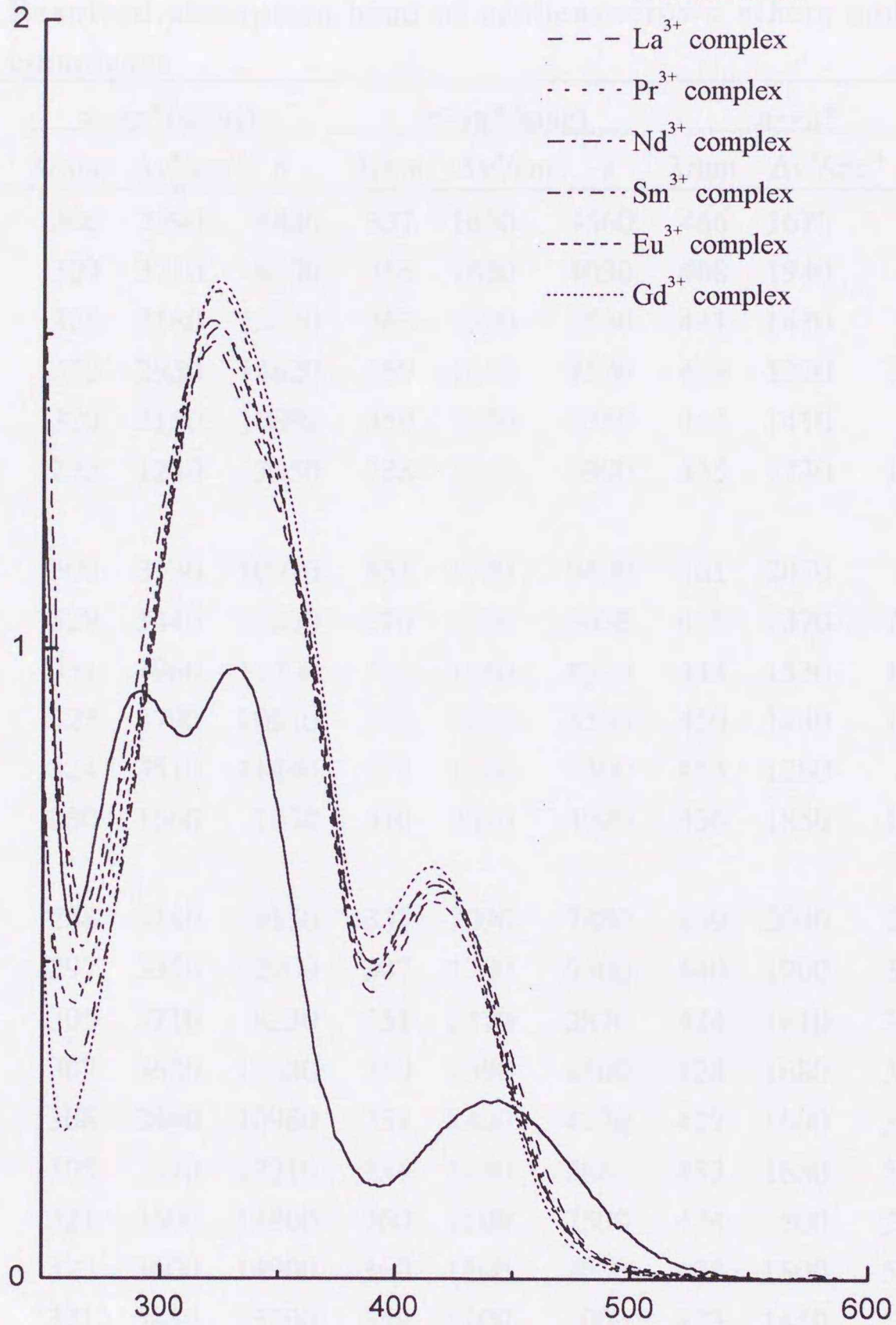

Fig. 4.12 Absorption spectra of *trans* AB19C6 and its rare earth metal complexes.
[*trans* AB19C6] = 1.0×10^{-4} M, $[M^{3+}] = 1 \times 10^{-1}$ M in acetonitrile at 25 °C

Table 4.1. Resolved absorption band of azobenzocrown ethers and their complexes

		π→π*(short)			π→π*(long)			n→π*		
	Cation	λ/nm	$\Delta\nu^a$/cm^{-1}	ε	λ/nm	$\Delta\nu^a$/cm^{-1}	ε	λ/nm	$\Delta\nu^a$/cm^{-1}	ε
AB13C4	--	308	3590	9830	357	1650	4660	466	1670	450
(*trans*)	Mg^{2+}	309	3710	8500	358	1680	4030	468	1940	640
	Ca^{2+}	326	3180	13120	363	1590	5540	441	1410	970
	Sr^{2+}	322	2950	14820	359	1640	7520	444	1320	680
	Ba^{2+}	320	3150	10890	359	1620	4550	444	1410	710
(*cis*)	--	252	1230	3350	288	3540	3990	435	1720	1220
AB16C5	--	300	3730	10970	351	1730	9400	461	2070	980
(*trans*)	Mg^{2+}	329	3440	18200	370	1500	5030	418	1370	7320
	Ca^{2+}	331	3960	11700	374	1560	4620	444	1530	1120
	Sr^{2+}	325	3790	10910	373	1680	6550	450	1440	1050
	Ba^{2+}	324	3510	11490	371	1700	8300	453	1280	830
(*cis*)	--	280	1560	1630	310	3680	4090	436	1850	1560
AB19C6	--	288	3140	9150	337	2090	7880	439	2040	2830
(*trans*)	Na^{+}	297	3350	12900	347	1700	9500	440	1900	3300
	Mg^{2+}	305	3710	8230	351	1470	2870	424	1810	2210
	Ca^{2+}	307	3620	12530	350	1390	4500	424	1680	3340
	Sr^{2+}	308	3440	10980	351	1400	4220	427	1800	3200
	Ba^{2+}	305	3370	12210	351	1490	5860	433	1880	3510
	La^{3+}	321	3600	14800	360	1100	2500	424	1500	5500
	Pr^{3+}	322	3600	14900	360	1100	2200	423	1500	5400
	Nd^{3+}	321	3850	15200	359	1100	2000	423	1450	5300
	Sm^{3+}	322	3500	15100	360	1150	2200	421	1500	5400
	Eu^{3+}	322	3500	15600	357	1200	1900	421	1550	5200
	Gd^{3+}	324	3650	15800	360	1000	1600	421	1400	5300
(*cis*)		276	1590	2670	308	3300	3750	433	1980	1610
DMAB(*trans*)		311	4040	6820	372	2000	7660	469	1390	990
DMAB(*cis*)		277	1820	2170	313	3090	3140	434	1860	1010

λ : peak center, Δν : half width of peak

Alkaline earth metal complexes. The band in visible light region around 460 nm due to $n \rightarrow \pi^*$ transition of azo group shifted to shorter wavelength by the complexation with alkaline earth metal ions. The magnitude of this shift reflects the interaction between azo group and metal ions, and indicates the stabilization of ground state of lone pair electron (n) of azo group and/or the destabilization of excited $n\pi^*$ level by the positive charge of the metal ions. Figs. 4.13-4.16 show the energy-level changes by the complexation, and indicate that the spectral shifts are attributed to both the destabilization of the excited states should caused by the decrease of the lone-pair electron density induced by $n \rightarrow \pi^*$ excitation and stabilization of ground state due to complexation. The magnitudes of these shifts (Table 4.1) were in the order of $Ca^{2+} \geq Ba^{2+} = Sr^{2+} >> Mg^{2+}$ for AB13C4, $Mg^{2+} > Ca^{2+} > Sr^{2+} > Ba^{2+}$ for AB16C5, and $Ca^{2+} \cong Mg^{2+} > Sr^{2+} > Ba^{2+}$ for AB19C6, indicating the order of interaction energies between these metal ions and azo group of azobenzocrown ethers. However, these orders are not in parallel to those of the complex formation constants (Table 3.1). Especially, Mg^{2+} does not have so strong complexation ability with AB16C5 and AB19C6, but exhibits quite a large blue shift for AB16C5 ($\Delta\lambda$ = 43 nm), being larger than that of Ca^{2+}, whereas a smaller blue shift for AB19C6 ($\Delta\lambda$ = 15 nm) as same as that of Ca^{2+}. In the case of AB13C4, Mg^{2+} has almost the same complex formation constant as Sr^{2+} and Ba^{2+}, but magnitude of the shift was very small. This result indicates that the order of complexation abilities with alkaline earth metal ions with AB13C4, AB16C5 and AB19C6 are mainly dominated by the oxygen atoms of the crown ether moiety. As mentioned above, shift of $n \rightarrow \pi^*$ transition by complexation with metal ion indicates the magnitude of interaction between azo group and metal ion. Table 4.2 lists the values of $n \rightarrow \pi^*$ shift by complexation. These values in listed in Table 4.2 were obtained by subtracting excitation energy to $n\pi^*$ state of free azobenzocrown ether

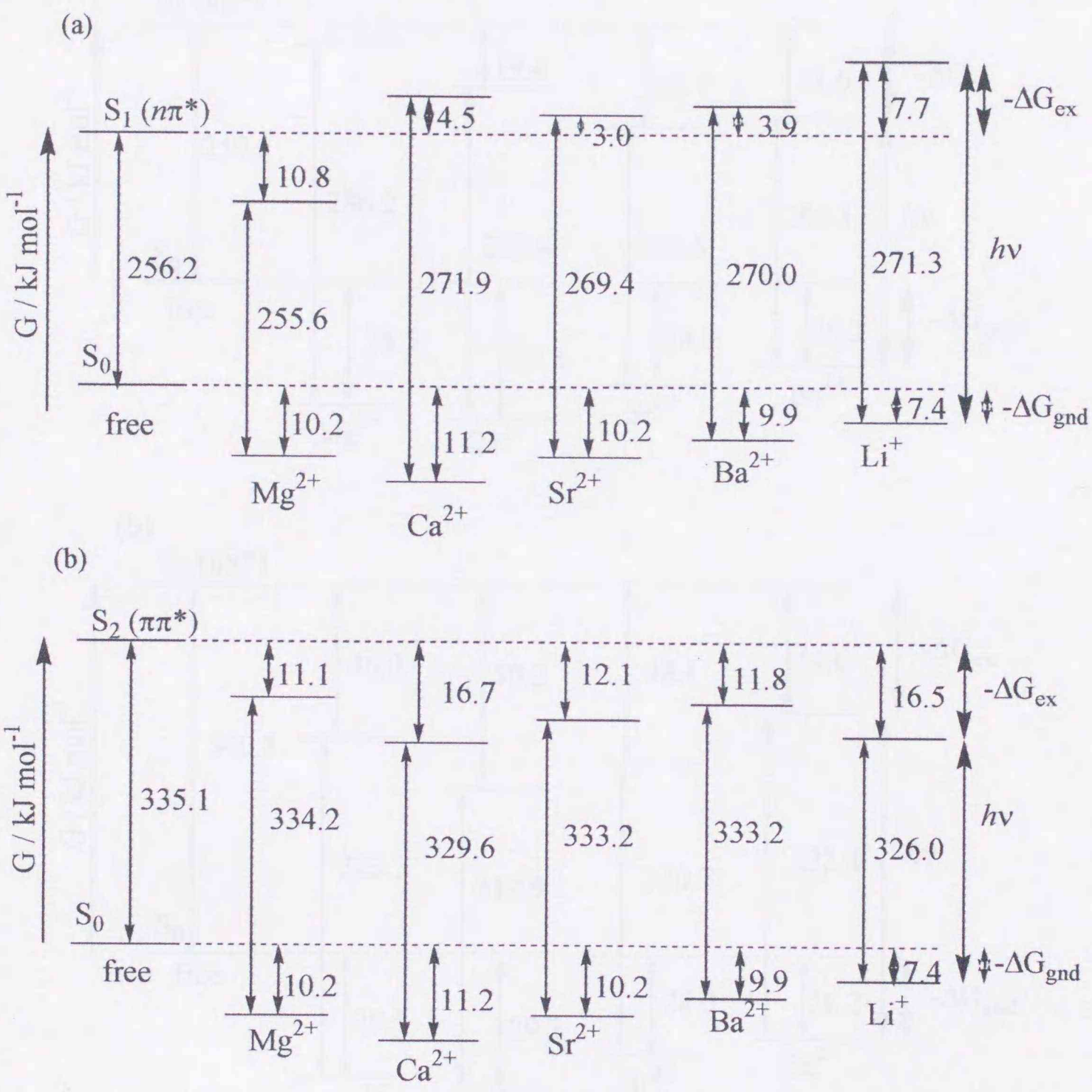

Fig. 4.13 Energy levels of ground and excited states
of *trans* AB13C4 and its metal complexes:
(a) n→π* and (b) π→π* (long wavelength)
The energy of free *trans* AB13C4 includes those of metal ions.

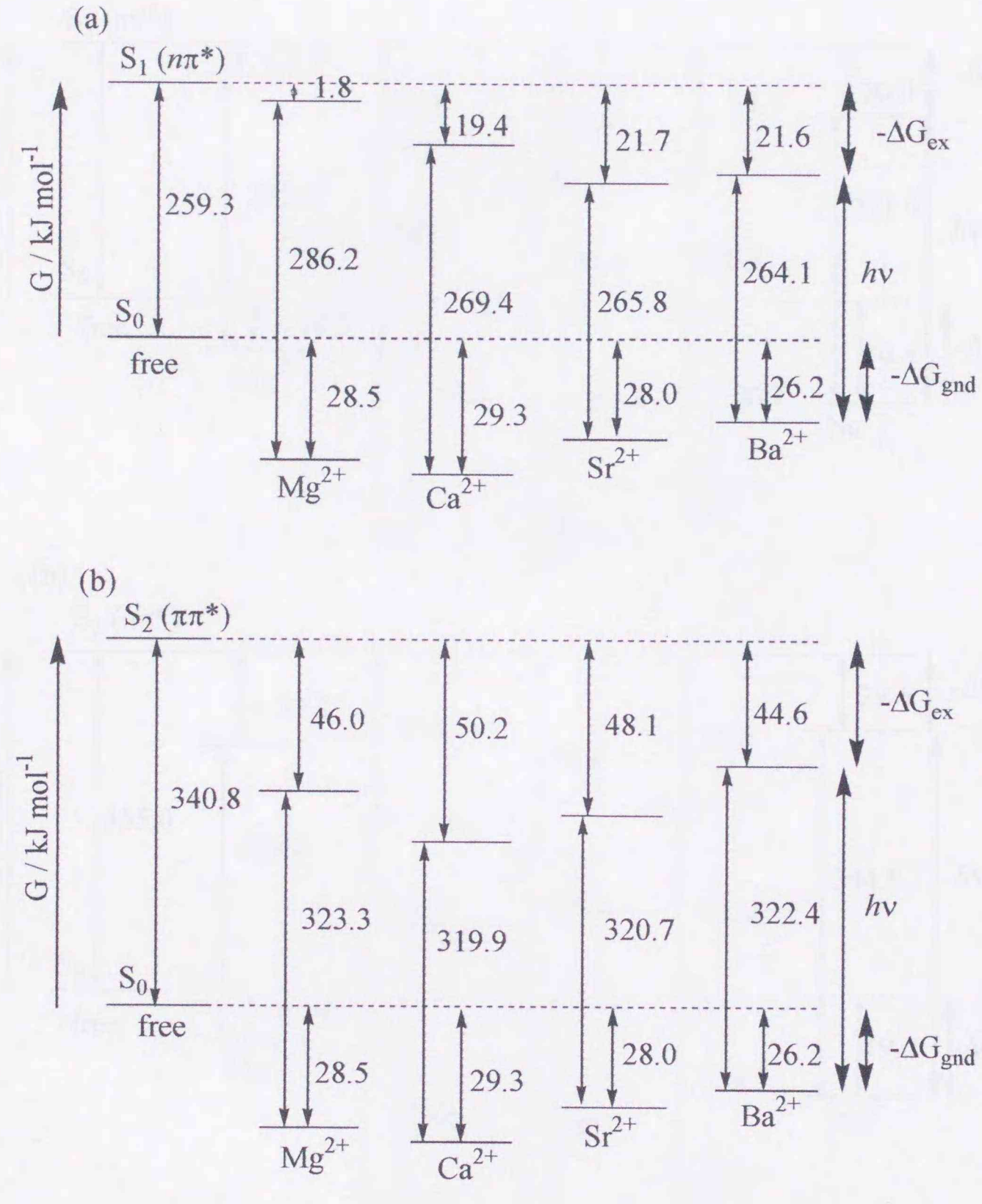

Fig. 4.14 Energy levels of ground and excited states
of *trans* AB16C5 and its metal complexes:
(a) n→π* and (b) π→π* (long wavelength)
The energy of free *trans* AB16C5 includes those of metal ions.

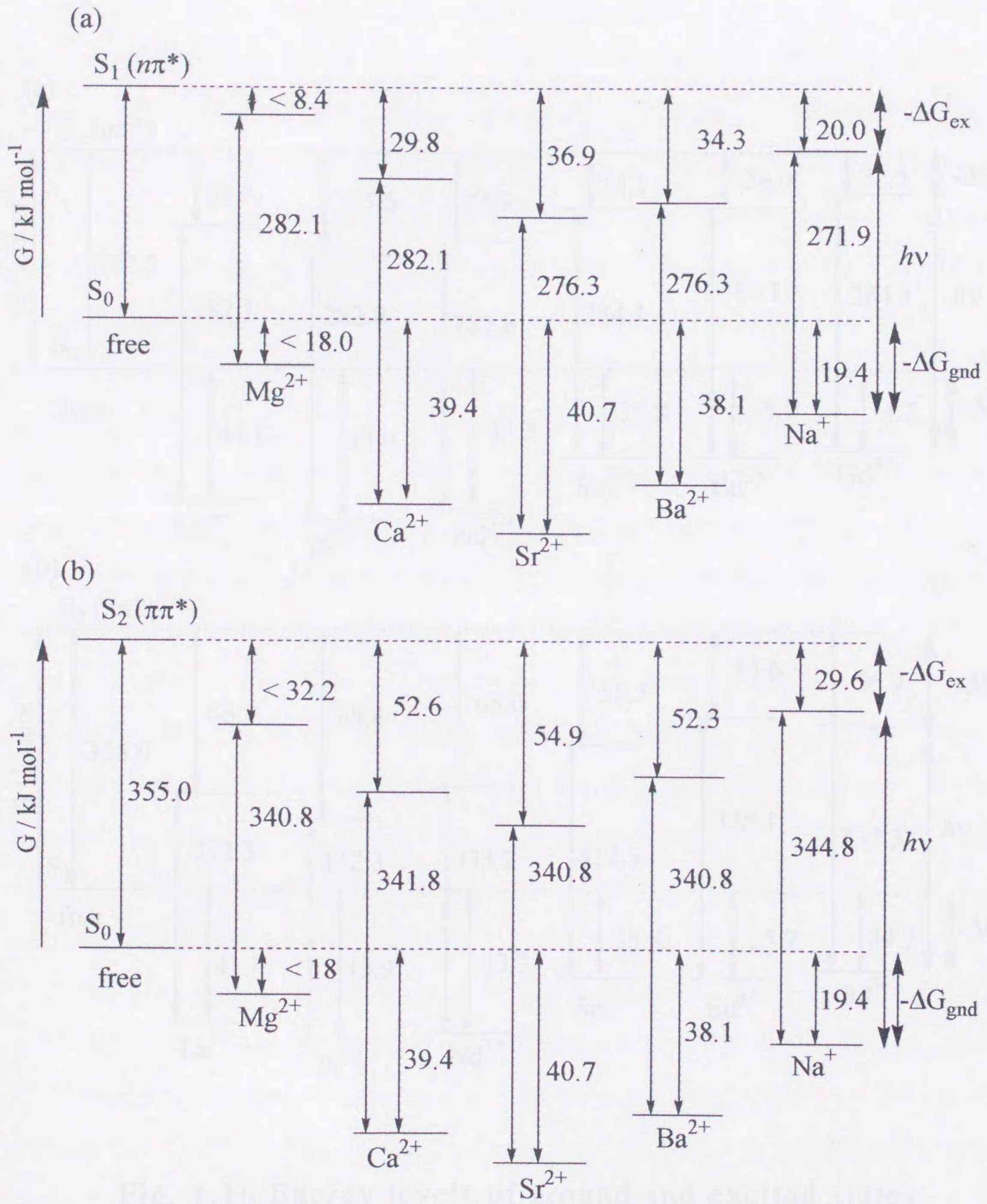

Fig. 4.15 Energy levels of ground and excited states of *trans* AB19C6 and its metal complexes: (a) n→π* and (b) π→π* (long wavelength)
The energy of free *trans* AB19C6 includes those of metal ions.

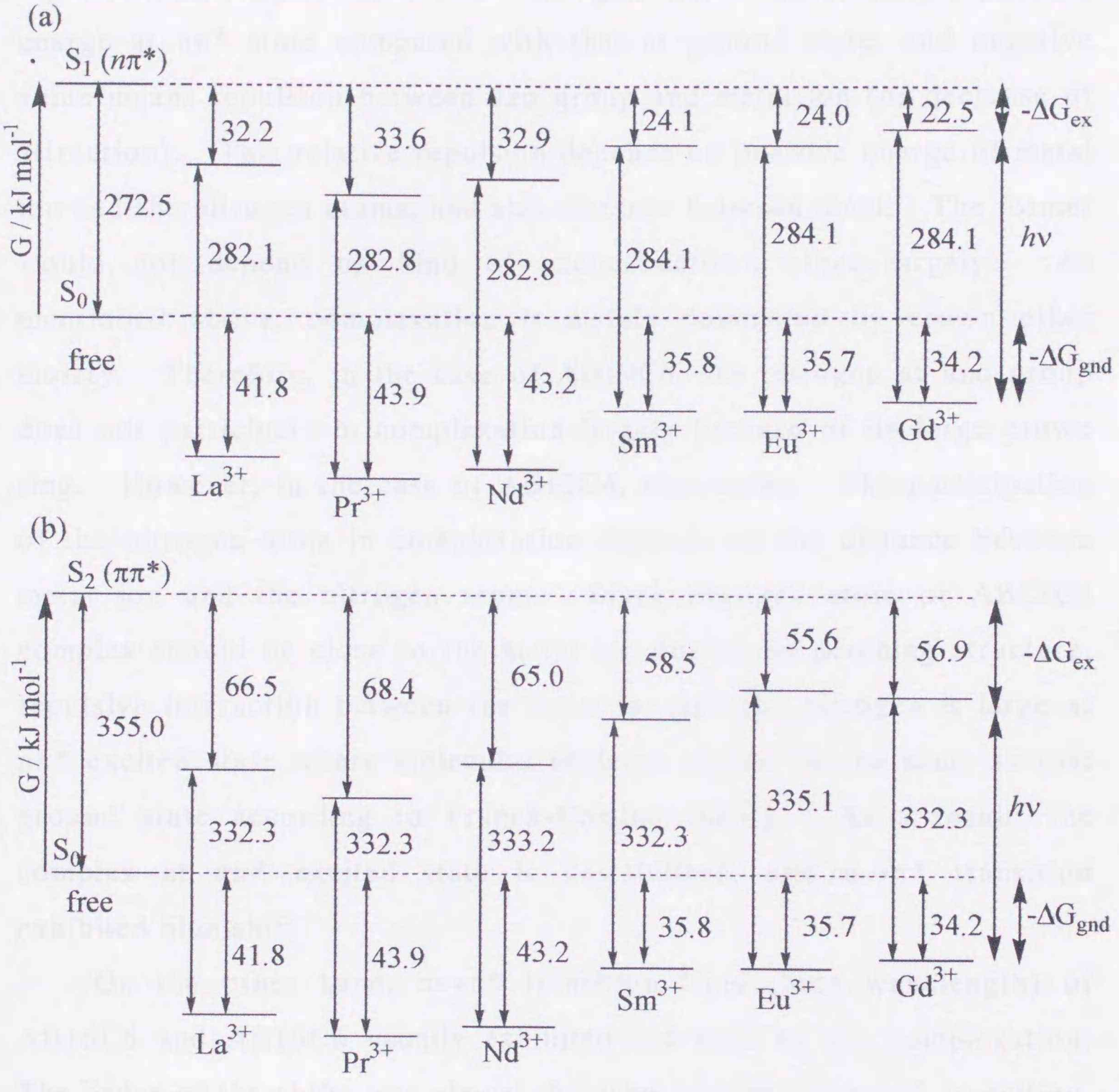

Fig. 4.16 Energy levels of ground and excited states of *trans* AB19C6 and its rare earth metal complexes: (a) n→π* and (b) π→π* (long wavelength) The energy of free *trans* AB19C6 includes those of metal ions.

from that of its complex. AB13C4, in many case, exhibits much larger $n\rightarrow\pi^*$ shift than AB16C5 and AB19C6. This is a result of relative repulsion between metal ion and nitrogen atom with relatively positive charge at $n\pi^*$ state compared with that at ground state, and negative value means repulsion between azo group and metal ion (or decrease of attraction). This relative repulsion depends on positive charge of metal ion and the nitrogen atoms, and also distance between them. The former would not depend on kind of azobenzocrown ether largely. As mentioned above, complexation is mainly dominated by crown ether moiety. Therefore, in the case of AB19C6, the nitrogen at azo group does not participate in complexation largely because of its large crown ring. However, in the case of AB13C4, *vice versa*. The participation of the nitrogen atom in complexation depends on the distance between metal ion and the nitrogen atom. Since nitrogen atom of AB13C4 complex should be close to the metal ion due to its perching structure, repulsive interaction between the metal ion and the nitrogen is large at $n\pi^*$ excited state where molecular skeleton should be the same as that ground state according to Franck-Condon theory. As a result, the complex at $n\pi^*$ excited state is destabilized, and $n\rightarrow\pi^*$ transition exhibited blue shift.

On the other hand, $\pi\rightarrow\pi^*$ transition band (long wavelength) of AB16C5 and AB19C6 usually exhibited red shift by the complexation. The order of the shifts was almost the same as that for $n\rightarrow\pi^*$ transition, except for Mg^{2+}. The dependence of magnitude of this red shift on the metal ions was smaller than that for $n\rightarrow\pi^*$ transition. Since the complexation of crown ethers brings stabilization of the ground state of the molecule, red shift of $\pi\rightarrow\pi^*$ transition by complexation means a larger stabilization of $\pi\pi^*$ excited level at the complexation compared with ground states from Figs. 4.13-4.16. The amounts of maximum stabilization of azobenzene moiety at the $\pi\pi^*$ excited state were ca. 20 kJ

mol^{-1} for AB16C5 for Ca^{2+}, ca. 14 kJ mol^{-1} for AB19C6 for Sr^{2+} and Ba^{2+} and 5.5 kJ mol^{-1} for AB13C4 for Ca^{2+}. This stabilization of azobenzene moiety shows that electron density on nitrogen atom at azo group is increased by $\pi \rightarrow \pi^*$ excitation, and this $\pi\pi^*$ excited state was more stabilized compared with ground state by positive charge of the cation in the complex. The reason for the difference between the amounts of the stabilization of AB16C5 and AB19C6 is not clear, because structures of these complexes in the excited states are hardly determined. However, in the case of AB13C4, longer $\pi \rightarrow \pi^*$ excitation bands of its complex showed small shift. Only Ca^{2+} complex exhibited red shift. The $\pi \rightarrow \pi^*$ excitation brings distribution of excited π electron to the nitrogen atoms at azo group through conjugate system within azobenzene moiety and increases of electron density in the nitrogen atoms.[1] Since electronic excitation would not change molecular skeleton according to Franck-Condon theory, and $\pi \rightarrow \pi^*$ excitation increase relative electron density of azo nitrogen atom. Then $\pi \rightarrow \pi^*$ excitation make attraction between nitrogen and metal ion stronger. This stabilization of $\pi\pi^*$ state depends on the distribution of excited π electron on nitrogen in addition to the distance between the nitrogen and metal ion. The shift of $\pi \rightarrow \pi^*$ was in the order of AB16C5 > AB19C6 > AB13C4. However, the electronic charge of oxygen at *o*-position which participate in the complexation and conjugate system is not clear at $\pi\pi^*$ excited state. Therefore, the detail can not be discussed.

Mg^{2+} complexes of azobenzocrown ethers. Mg^{2+} is much smaller than other alkaline earth metal ions and has covalent bonding character. A certain conformation should be required on complexation with Mg^{2+}. Therefore, Mg^{2+} complex exhibited different properties from other alkaline earth metal complexes which many not require such conformation. Azo group of AB13C4 hardly interacted with Mg^{2+}, considering a error of the results of the absorption spectral resolution due to much smaller

absorbance at n→π* excitation band as compared with larger π→π* excitation band. On the other hand, azo group of AB16C5 interacted with Mg^{2+} strongly (Table 4.2). The reason is that AB16C5 could take a conformation required by Mg^{2+} satisfactorily, and azo group could bind to Mg^{2+} as a result, although AB13C4 could not bind due to its rigidity. AB19C6 has large polyoxyethylene moiety, and the polyoxyethylene moiety is too large to take the requested conformation by Mg^{2+} for complexation according to "size-fitting" concept. Therefore, interaction between azo group of AB19C6 and Mg^{2+} was weak.

Rare earth metal complexes of AB19C6. Shapes of absorption spectra of AB19C6 complexes with rare earth metal ions did not depend on the kind of metal ions. The magnitude of the shift of n→π* transition band was more than that by complexation with Ca^{2+}. Since rare earth metal ions have almost the same ionic sizes as Ca^{2+}, and have a larger charge than Ca^{2+}, the larger ion-dipole interaction to the azobenzene moiety is expected. Complexation with these rare earth metal ions exhibited blue shift of n→π* transition and red shift of π→π* transition, and these shifts correspond to − 9.6 ~ − 11.6 kJ mol^{-1} and 19.9 ~ 21.7 kJ mol^{-1}, respectively. This indicates that rare earth metal ions interact with azobenzene moiety more strongly than alkaline earth metal ions. Structural change of azobenzene moiety by complexation with rare earth metal ions are expected to be larger than that by complexation with alkaline earth metal ions, because of absorption intensity of individual transition bands drastically changed by complexation with rare earth metal ions compared with alkaline earth metal ions. However detail is not clear. At nπ* excited state, rare earth metal ions are kept away from azo group charged less negatively, in other words, positively as well as alkaline earth metal ions. Since charge of rare earth metal ions is larger, this effect is also large. At ππ* excited state, as well as alkaline earth metal complexes, further large stabilization by complexation are

Table 4.2. Stabilization energy[a] of azo group by interaction with several metal ions

	Mg^{2+}	Ca^{2+}	Sr^{2+}	Ba^{2+}
AB13C4	-0.2	15.7	13.2	13.8
AB16C5	26.7	9.9	6.3	4.6
AB19C6	9.6	9.6	4.2	4.2

	La^{3+}	Pr^{3+}	Nd^{3+}	Sm^{3+}	Eu^{3+}	Gd^{3+}
AB19C6	9.6	10.3	10.3	11.6	11.6	11.6

[a]these unit is kJ mol^{-1}

obtained by large charge of metal ion in addition to by increase electron density of 2,2'-substituted oxygen and/or azo nitrogen atoms.

4.5 Conclusion.

Trans AB13C4, AB16C5, AB19C6 and DMAB exhibited unique properties in absorption spectra. The observed properties are those of azobenzene moieties of these compounds, since only azobenzene moieties have absorption bands in the visible and ultraviolet region within these compounds. These azobenzene moieties exhibited unique properties due to the repulsion between the etherial *o*-substituents and lone pairs of azo nitrogen atoms in *trans* isomers and also due to the distortion by polyoxyethylene moieties. Their spectral properties were changed by complexation with several metal ions. The degrees of change were depended on kind of metal ions. It is found that arrangement of positive charge near azobenzene moiety changes the spectral properties of azobenzene moiety.

CHAPTER 5
PHOTOISOMERIZATION OF AZOBENZOCROWN ETHER

5.1 Introduction.

Azobenzenes are well known compounds which undergo reversible isomerization reaction on the irradiation of ultraviolet or visible light, and their isomerization rates are usually fast.[33-43] Thus, numbers of their analogues of photofunctionalized compounds, such as a molecular switch controlled by light, have been investigated.[14,44,45] For example, an electrochemical approach has been proposed for actinometric measurements by using a difference between absorption wavelengths of these isomers.[46] A molecular switch for two functional groups of azobenzene and anthraquinone was reported to be controlled by light and electronic current.[47] Azobenzene moiety was impregnated into the crown ethers in order to control the complexation with alkali metal ions and extraction property of the ions by *trans-cis* isomerization.[48] However, these photoisomerization properties are mainly determined by substituents of the compounds. The substituent on the azobenzene group should be properly selected in order to change the isomerizing conditions, such as irradiation wavelength, isomerization rate, and thermal stability of the isomers.

Combinations of crown ether and photo functional molecule (*e.g.* spirobenzopyran,[49] malachite green,[50] spironaphtopyran,[51] and benzothiazolium styryl,[52]) allow controlling complexation ability for metal ions of crown ether moiety by photoisomerization and also thermal stability of unstable isomer of photo functional moiety by complexation with metal ions. However, the control of the photo isomerization by the external condition such as complexation has been seldom reported.

In this chapter, the control of photoisomerization reaction of azobenzocrown ethers by complexation with metal ions was investigated,

and detailed kinetics of the photoisomerization reactions and the reverse reactions of azobenzocrown ethers are discussed.

5.2 Experimental

5.2.1 Measurement of Photoisomerization Rate.

An acetonitrile solution of azobenzocrown ether (ca. 2×10^{-6} M) in a standard 1 cm quartz cell was irradiated by monochromated UV or visible light in the presence or absence of several metal perchlorates (1×10^{-2} M for AB13C4 and AB16C5, 1×10^{-4} M for AB19C6) and $Mg(ClO_4)_2$ (3×10^{-2} M). To prevent the inhomogeneity of the irradiation light strength, the absorbance of azobenzocrown ethers at the irradiation wavelength was made below 0.02. The absorption spectra were recorded at intervals of 1 min until 5 min, 2 min until 10 min, and 3 min in the rest. The ratio of the amount of *cis* and *trans* isomers at the photo stationary state was determined by the absorption spectra and/or peak areas of the ^{1}H NMR spectra. In the ^{1}H NMR method, the ratios were obtained from peak areas of the aromatic protons at the photo stationary state in the same conditions as the measurements of absorption spectra except for the azobenzocrown ether concentrations: [AB13C4], [AB16C5] and [AB19C6] = 1×10^{-4} M. The sample tube was rotated through out the measurement in order to keep a uniform light irradiation. In the case of absorption spectra, the ratio was obtained by spectrum fitting of the observed spectra at photo stationary state and numerically added spectra of *cis* and *trans* isomers. In the case of rare earth metal complexes, only absorption spectra were used to determine the ratio of the *cis*/*trans* isomers because measurement of ^{1}H NMR spectra could not be applicable due to paramagnetism of rare earth metal ions. Then, the photoisomerization rates and absolute quantum yields were calculated on the basis of a first order kinetics as described in the following section.

5.2.2 Evaluation of Efficiency of Photoisomerization

Since photo isomerization rates depend on the intensity of incident light and also on the absorption coefficient of the compound at a given irradiation wavelength, the rates should be normalized by the counts of

photon absorbed by the molecule. The normalized rate is identical to the absolute quantum yield of the isomerization. Although the method to obtain the quantum yields has been reported only briefly in several literatures,[33,34] no detail was described on the effects, for example, of the reverse reaction.

Several reaction mechanisms have been proposed for the photoisomerization. However, in the presence of metal salts the excited state of the *trans* isomer should be different from that of *cis* isomer, because *trans* isomer easily forms and *cis* isomer hardly forms complex. Thus, the present work assumed the essential scheme of Fig. 5.1 for the photoisomerization. According to Fig. 5.1, the absolute quantum yields for the respective isomerizations are evaluated as follows. When *cis* and *trans* isomers of the molecules (L_{cis} and L_{trans}, respectively) exist in a sample solution, the amounts of photons absorbed by *cis* and *trans* isomers (E_{cis} and E_{trans}) are given as follows,

$$E_{cis} = I_0 (1-T) \varepsilon_{cis} [L_{cis}] / \mathrm{Abs} \qquad (5.1)$$

$$E_{trans} = I_0 (1-T) \varepsilon_{trans} [L_{trans}] / \mathrm{Abs} \qquad (5.2)$$

where I_0 is intensity of light (count of photons per 1 s and per 1 cm^2), and ε_{cis} and ε_{trans} are molar absorption coefficients of *cis* and *trans* isomer, respectively. The T and Abs are transmittance and absorbance of the sample solution in the cell at a given irradiation wave length, respectively. At the condition of Abs <0.02, Abs can be approximated to $(1-T)/2.303$. Thus, the eqs. 5.1 and 5.2 are simplified, and the concentration of the isomers (C_{cis} and C_{trans}) excited to the S_1 or S_2 level per second are given as follows:

$$C_{cis} = 1000\, E_{cis} / N_A = 2.303 \times 10^3\, I_0\, \varepsilon_{cis}\, [L_{cis}] / N_A \qquad (5.3)$$

$$C_{trans} = 1000\, E_{trans} / N_A = 2.303 \times 10^3\, I_0\, \varepsilon_{trans}\, [L_{trans}] / N_A \qquad (5.4)$$

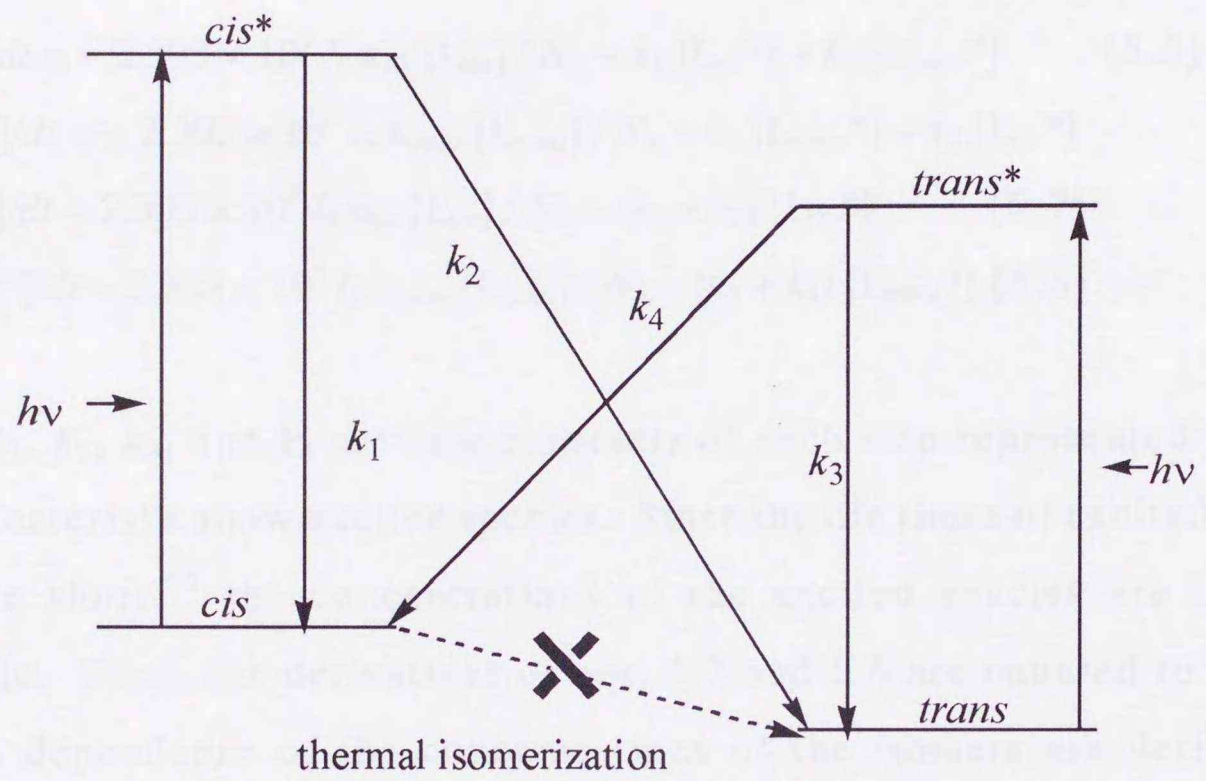

Fig. 5.1 Photoisomerization path of azobenzocrown ethers.

where, N_A is the Avogadro's Number, and the unit of concentration is expressed as M (mole dm^{-3}).

Differential equations for the isomerization kinetics are given as follows:

$$d[L_{cis}]/dt = -2.303 \times 10^3 I_0 \varepsilon_{cis} [L_{cis}] / N_A + k_1 [L_{cis}^*] + k_4 [L_{trans}^*] \quad (5.5)$$

$$d[L_{trans}]/dt = -2.303 \times 10^3 I_0 \varepsilon_{trans} [L_{trans}] / N_A + k_3 [L_{trans}^*] + k_2 [L_{cis}^*] \quad (5.6)$$

$$d[L_{cis}^*]/dt = 2.303 \times 10^3 I_0 \varepsilon_{cis} [L_{cis}] / N_A - (k_1 + k_2) [L_{cis}^*] \quad (5.7)$$

$$d[L_{trans}^*]/dt = 2.303 \times 10^3 I_0 \varepsilon_{trans} [L_{trans}] / N_A - (k_3 + k_4) [L_{trans}^*] \quad (5.8)$$

where, k_1, k_2, k_3, and k_4 are rate constants of each step represented in Fig. 5.1, and asterisks show excited species. Since the life times of excited states are quite short,[38] the concentrations of the excited species are usually negligible. Thus, the derivatives of eqs. 5.7 and 5.8 are equated to 0, and the time dependence of the concentrations of the isomers are derived as follows:

$$[L_{cis}] = \Phi_{t\text{-}c} \varepsilon_{trans} [L_t] / A + B \exp(-A\alpha t) \quad (5.9)$$

$$[L_{trans}] = \Phi_{c\text{-}t} \varepsilon_{cis} [L_t] / A + B' \exp(-A\alpha t) \quad (5.10)$$

where,

$$[L_t] = [L_{cis}] + [L_{trans}]$$

$$\Phi_{t\text{-}c} = k_4 / (k_3 + k_4)$$

$$\Phi_{c\text{-}t} = k_2 / (k_1 + k_2)$$

$$\alpha = 2.303 \times 10^3 I_0 / N_A$$

$$A = \Phi_{t\text{-}c} \varepsilon_{trans} + \Phi_{c\text{-}t} \varepsilon_{cis}$$

$$B = [L_{cis}]_{t=0} - [L_{cis}]_{t=\infty}$$

$$B' = [L_{trans}]_{t=0} - [L_{trans}]_{t=\infty} = -B$$

and

$$[L_{cis}]_{t=\infty} = \Phi_{t\text{-}c}\, \varepsilon_{trans}\, [L_t]\, /A$$

$$[L_{trans}]_{t=\infty} = \Phi_{c\text{-}t}\, \varepsilon_{cis}\, [L_t]\, /A$$

Here, $[L_{cis}]_{t=\infty}$ and $[L_{trans}]_{t=\infty}$ are the concentrations of respective isomers in photo stationary state.

From above equations, the time dependence of the absorbance of the sample solution at a monitoring wavelength, Abs^{obs}, are given as:

$$Abs^{obs} = (\varepsilon_{cis}{}^{obs}\, \varepsilon_{trans} \Phi_{t\text{-}c} + \varepsilon_{trans}{}^{obs}\, \varepsilon_{cis}\, \Phi_{c\text{-}t})[L_t] / A + (\varepsilon_{cis}{}^{obs} - \varepsilon_{trans}{}^{obs})\, B \exp(-A\alpha t) \quad (5.11)$$

Then, $A\alpha$ values are evaluated from the time dependence of the Abs^{obs}, experimentally, using non-linear least square curve fitting method (Marquardt method).[27] Since α is obtained from the light intensity for irradiation, the averaged quantum yield, A, can be obtained. Therefore, the absolute quantum yield of the photo isomerization of the both isomers is evaluated from following equations:

$$\Phi_{c\text{-}t} = A\, [L_{trans}]_{t=\infty} /(\varepsilon_{cis}\, [L_t]) \quad (5.12)$$

$$\Phi_{t\text{-}c} = A\, [L_{cis}]_{t=\infty} /(\varepsilon_{trans}\, [L_t]) \quad (5.13)$$

5.3 Results.

5.3.1 Photoisomerization of Azobenzocrown Ethers.

The UV and visible light irradiations of AB13C4, AB16C5, AB19C6, and DMAB caused both isomerization from *trans* to *cis* and *vice versa* (Fig. 5.2) depending on which was a starting compound. Since several (~ 10 times) repetition of the forward and reverse photo isomerizations did not give any degradations, these isomerization were reversible in this experiment. Both absolute quantum yields ($\Phi_{t\text{-}c}$ and $\Phi_{c\text{-}t}$) can be obtained as described in the previous section even in the cases where pure isomers are not used, and the present measurements were started with mixtures of *trans* and *cis* isomers in convenience (*cis* rich or *trans* rich solution).

The time dependence of the absorbance of AB16C5 solution (started with *cis* rich solution) at the $n\rightarrow\pi^*$ transition band irradiation is shown in Fig. 5.3, in which the time dependence in the presence of Ca^{2+} is also superimposed for comparison. Although $n\rightarrow\pi^*$ transition bands of *trans* and *cis* isomers were close to each other ($\Delta\lambda$ = 4-31 nm), the irradiation wavelengths were set to the absorption maxima of *trans* isomers. The molar ratios of *cis* and *trans* isomers in the photo stationary state under these light irradiations were determined from peak areas of ^1H NMR spectra except for rare earth metal ion complexes. From Fig. 5.3, both absolute quantum yields, $\Phi_{t\text{-}c}$ and $\Phi_{c\text{-}t}$, of AB16C5 were evaluated according to the method described in the previous section. The quantum yields for AB13C4, AB19C6 and DMAB were obtained similarly. Results are listed in Table 5.1.

Table 5.2 shows the quantum yields corresponding to irradiation at the $\pi\rightarrow\pi^*$ transition band. Here, *cis* isomer does not have $\pi\rightarrow\pi^*$ absorption bands at longer wave lengths around that of *trans* isomers (~ 350 nm). The irradiation wavelengths of Table 5.2 were set to the center of the longer wavelength band of $\pi\rightarrow\pi^*$ transitions which were obtained by spectral resolution described in previous section. Since these irradiation wavelengths were far from the $\pi\rightarrow\pi^*$ transition of the *cis* isomers, the molar

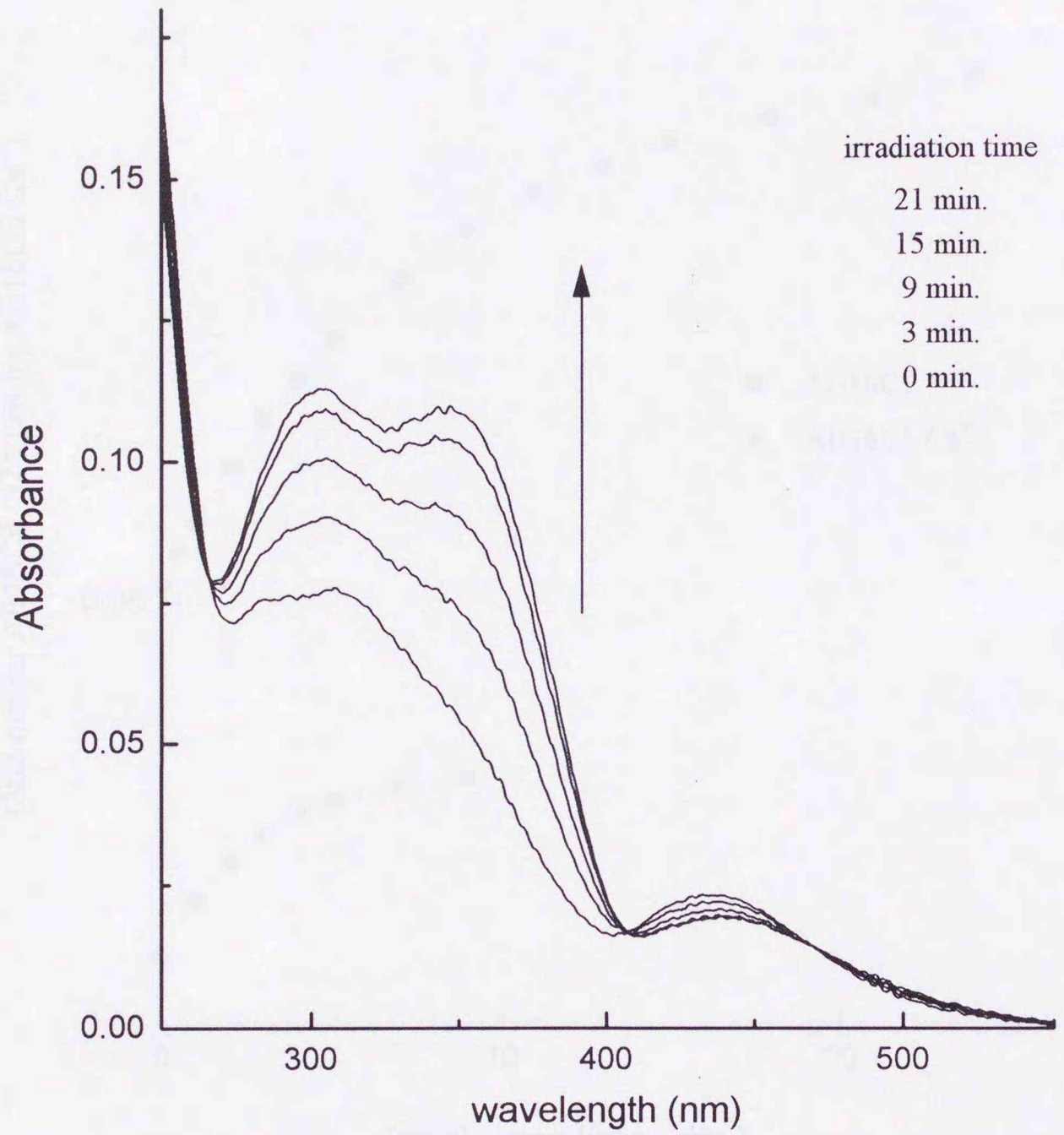

Fig 5.2 Photoisomerization of *cis* AB16C5
by irradiation at the n→π* absorption band (460 nm).
[AB16C5] = 1.4 ×10^{-6} M, 25 °C.

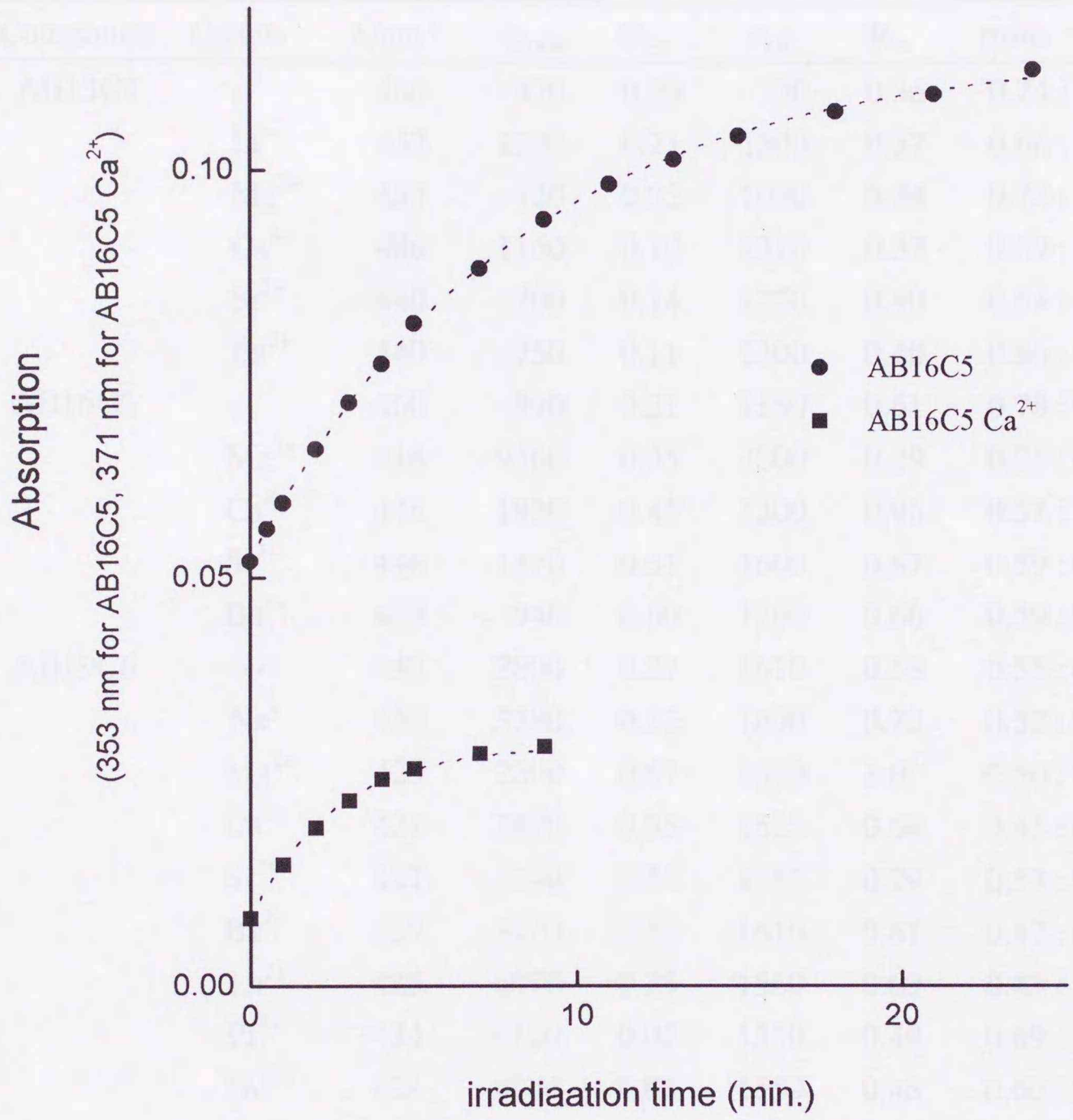

Fig. 5.3 Time dependence of absorbance of AB16C5 and its Ca^{2+} complex by the irradiation at the $n \rightarrow \pi^*$ absorption band.
460 nm and 446 nm for free AB16C5 and Ca^{2+} complex, respectively.

Table 5.1. Quantum yields of isomerization between *cis* and *trans* isomers of azobenzocrown ethers by irradiation at n→π* transition bands (25℃)

Compound	Cation	λ/nm [a]	ε_{trans}	$\Phi_{t\text{-}c}$	ε_{cis}	$\Phi_{c\text{-}t}$	*trans* : *cis* [b]
AB13C4	--	466	470	0.20	730	0.36	0.74 : 0.26
	Li^+	437	1200	0.21	1300	0.37	0.66 : 0.34
	Mg^{2+}	453	420	0.32	1030	0.34	0.72 : 0.28
	Ca^{2+}	436	1160	0.19	1310	0.37	0.69 : 0.31
	Sr^{2+}	440	700	0.14	1270	0.40	0.84 : 0.16
	Ba^{2+}	440	750	0.11	1300	0.40	0.86 : 0.14
AB16C5	--	460	940	0.21	1160	0.61	0.78 : 0.22
	Mg^{2+}	418	9560	0.35	3800	0.29	0.25 : 0.75
	Ca^{2+}	446	1920	0.45	1200	0.96	0.57 : 0.43
	Sr^{2+}	446	1470	0.51	1600	0.67	0.59 : 0.41
	Ba^{2+}	453	940	0.60	1200	0.68	0.59 : 0.41
AB19C6	--	440	2800	0.27	1610	0.58	0.55 : 0.45
	Na^+	439	3280	0.32	1600	0.70	0.52 : 0.48
	Mg^{2+}	423	2300	0.67	1540	1.0	0.50 : 0.50
	Ca^{2+}	421	3470	0.35	1525	0.64	0.45 : 0.55
	Sr^{2+}	427	3240	0.34	1565	0.79	0.53 : 0.47
	Ba^{2+}	439	3420	0.32	1610	0.61	0.47 : 0.53
	La^{3+}	425	6070	0.23	1560	0.69	0.43 : 0.57
	Pr^{3+}	424	6120	0.05	1550	0.49	0.69 : 0.31
	Nd^{3+}	424	6200	0.08	1550	0.48	0.60 : 0.40
	Sm^{3+}	423	5840	0.12	1540	0.56	0.55 : 0.45
	Eu^{3+}	423	5830	0.02	1540	0.51	0.85 : 0.15
	Gd^{3+}	421	6380	0.19	1520	0.43	0.35 : 0.65
DMAB	--	472	1000	0.60	600	0.65	0.44 : 0.56
azobenzene [c]		439	0.31		0.46		

Under this experimental condition ($[M^{2+}]= 1 \times 10^{-2}$ M for AB13C4, AB16C5, 1×10^{-4} M for AB19C6, $[Mg^{2+}] = 3 \times 10^{-2}$ M), more than 98 % of *trans* AB13C4, AB16C5 or AB19C6 existed as a metal complex.

[a] Irradiation wave length. [b] The *trans* : *cis* ratio at the photo stationary state. [c] ref. 38

Table 5.2. Quantum yields of isomerization between *cis* and *trans* isomers of azobenzocrown ethers by irradiation at $\pi \rightarrow \pi^*$ transition bands (25℃)

Compound	Cation	λ/nm [a]	ε_{trans}	$\Phi_{t\text{-}c}$	ε_{cis}	$\Phi_{c\text{-}t}$	*trans* : *cis* [b]
AB13C4	--	357	7770	0.087	1320	0.37	0.42 : 0.58
	Li^+	369	6380	0.34	930	0.43	0.16 : 0.84
	Mg^{2+}	365	4770	0.17	1080	0.27	0.27 : 0.76
	Ca^{2+}	365	11630	0.20	1080	0.51	0.20 : 0.80
	Sr^{2+}	362	13230	0.15	1190	0.30	0.15 : 0.85
	Ba^{2+}	362	8730	0.20	1190	0.39	0.21 : 0.79
AB16C5	--	353	12400	0.25	1870	0.18	0.10 : 0.90
	Mg^{2+}	369	14710	0.17	1050	0.13	0.05 : 0.95
	Ca^{2+}	374	11430	0.59	1260	0.05	0.01 : 0.99
	Sr^{2+}	373	11590	0.53	2890	0.11	0.05 : 0.95
	Ba^{2+}	370	13070	0.39	3560	0.13	0.08 : 0.92
AB19C6	--	339	9180	0.26	3260	0.19	0.20 : 0.80
	Na^+	347	12480	0.13	2570	0.55	0.35 : 0.65
	Mg^{2+}	335	7020	0.41	3510	0.50	0.38 : 0.62
	Ca^{2+}	349	9950	0.37	2500	0.33	0.18 : 0.82
	Sr^{2+}	351	8480	0.33	2380	0.46	0.28 : 0.72
	Ba^{2+}	351	6560	0.32	2380	0.46	0.32 : 0.68
	La^{3+}	360	10420	0.19	920	0.83	0.28 : 0.72
	Pr^{3+}	361	10520	0.07	1570	0.40	0.45 : 0.55
	Nd^{3+}	360	10760	0.07	920	0.56	0.40 : 0.60
	Sm^{3+}	360	10680	0.09	920	0.53	0.34 : 0.66
	Eu^{3+}	359	10710	0.02	1000	0.66	0.75 : 0.25
	Gd^{3+}	360	11280	0.20	920	0.61	0.20 : 0.80
DMAB	--	371	9700	0.46	420	0.52	0.05 : 0.95
azobenzene [c]		317		0.15		0.21	

Under this experimental condition ($[M^{2+}] = 1 \times 10^{-2}$ M for AB13C4, AB16C5, 1×10^{-4} M for AB19C6, $[Mg^{2+}] = 3 \times 10^{-2}$ M), more than 98 % of *trans* AB13C4, AB16C5 or AB19C6 existed as a metal complex.

[a] Irradiation wave length. [b] The *trans* : *cis* ratio at the photo stationary state. [c] ref. 38

coefficients of *cis* isomer was small, and the accuracy of the $\Phi_{c\text{-}t}$ values for these cases is not so good.

5.3.2 Effects of Metal Ions on Photoisomerization of Azobenzocrown Ethers.

Alkaline earth metal ions in the solution of *trans* AB13C4, AB16C5, or AB19C6 form stable complexes. When *trans* isomers of them existed as a complex more than 98 % under the presence of excess amount of alkaline earth metal ion ($[M^{2+}] = 10^{-2}$ M for AB13C4 and AB16C5, and 10^{-4} M for AB19C6), the observed $\Phi_{t\text{-}c}$s were those of the complexes of these azobenzene compounds. *Trans* AB19C6 also forms stable complexes with light rare earth metal ions in acetonitrile solution. In this case, $\Phi_{t\text{-}c}$s of these complexes were evaluated as well as those of alkaline earth metal complexes. At lower concentrations of the salts ($[M^{2+}] \leq 10^{-4}$ M), *cis* isomer hardly formed the complex. This is supported by ^{1}H NMR spectra of *cis* AB19C6 and those in the presence of alkaline earth metal ions whose concentration was 10^{-4} M. These ^{1}H NMR spectra had the same chemical shifts one another (Fig. 5.4). However, at relatively high concentrations of the salts ($[M^{2+}] \geq 10^{-2}$ M), a comparable amount of the complex of *cis* isomer of AB16C5 with alkaline earth metal ions was formed as shown from these ^{1}H NMR spectra (Fig. 5.5). Under this condition, *cis* AB16C5 exhibited different ^{1}H NMR spectra from that of *cis* AB16C5 in the absence of alkaline earth metal ions. Since the rate of the exchange of the complex and free species is fast, the chemical shifts of a complex and a free species are averaged. Dependence of ^{1}H NMR of *cis* AB16C5 on the concentration of alkaline earth metal ion (Table 5.3) showed that ca. 20 % of *cis* AB16C5 formed a complex with alkaline earth metal ion under this condition. The $\Phi_{c\text{-}t}$ values for AB16C5 in the presence of metal ions are average values of $\Phi_{c\text{-}t}$ of free and species forming complexes. In the case of AB13C4, ^{1}H NMR

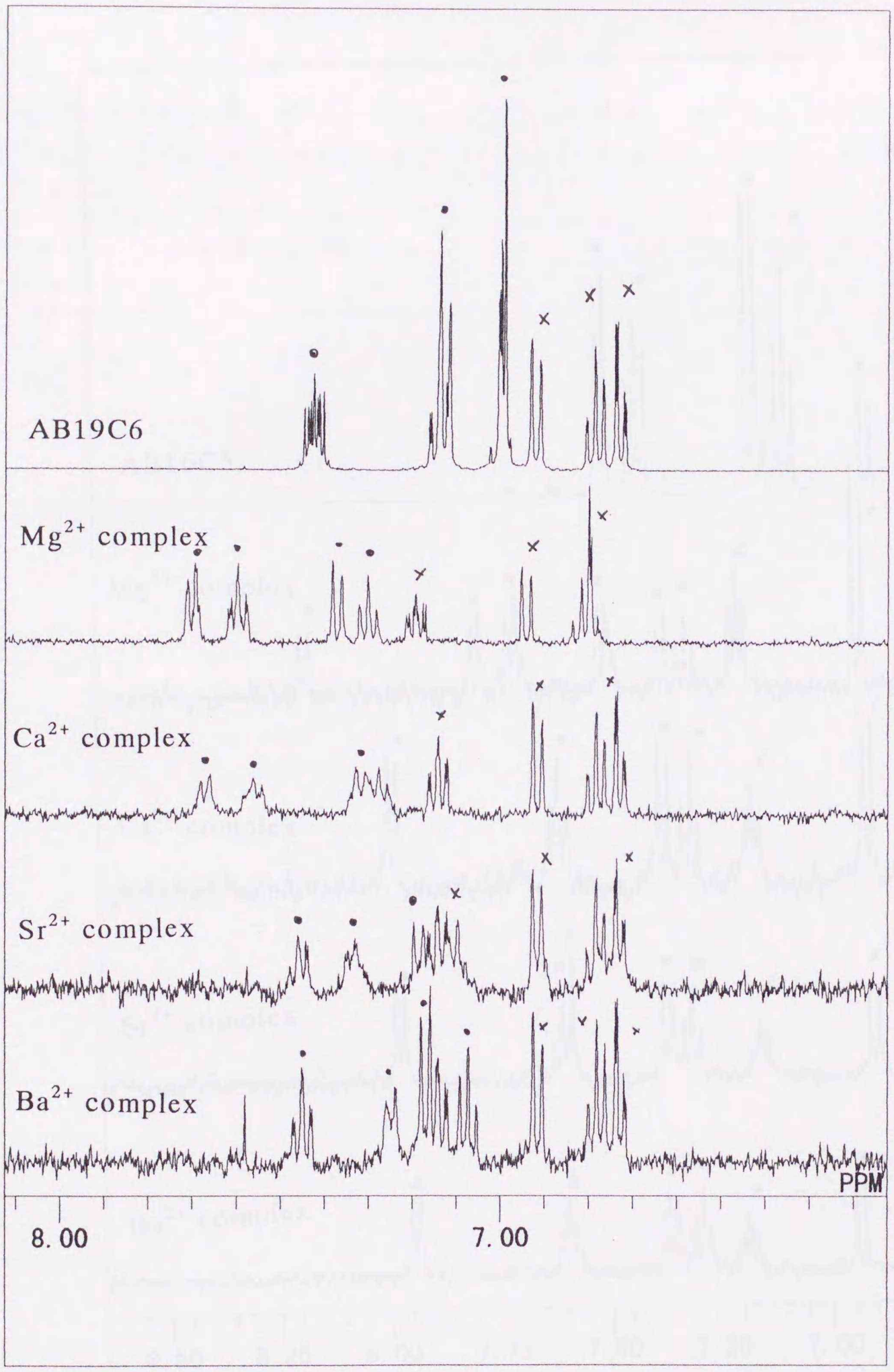

Fig. 5.4 ^{1}H NMR spectra of AB19C6 and its complexes.
[AB19C6] = 1×10^{-4} M, $[M^{2+}] = 1 \times 10^{-4}$ M in acetonitrile-d_3 at 25 °C.
The signs • and × mean *trans* isomer and *cis* isomer, respectively.

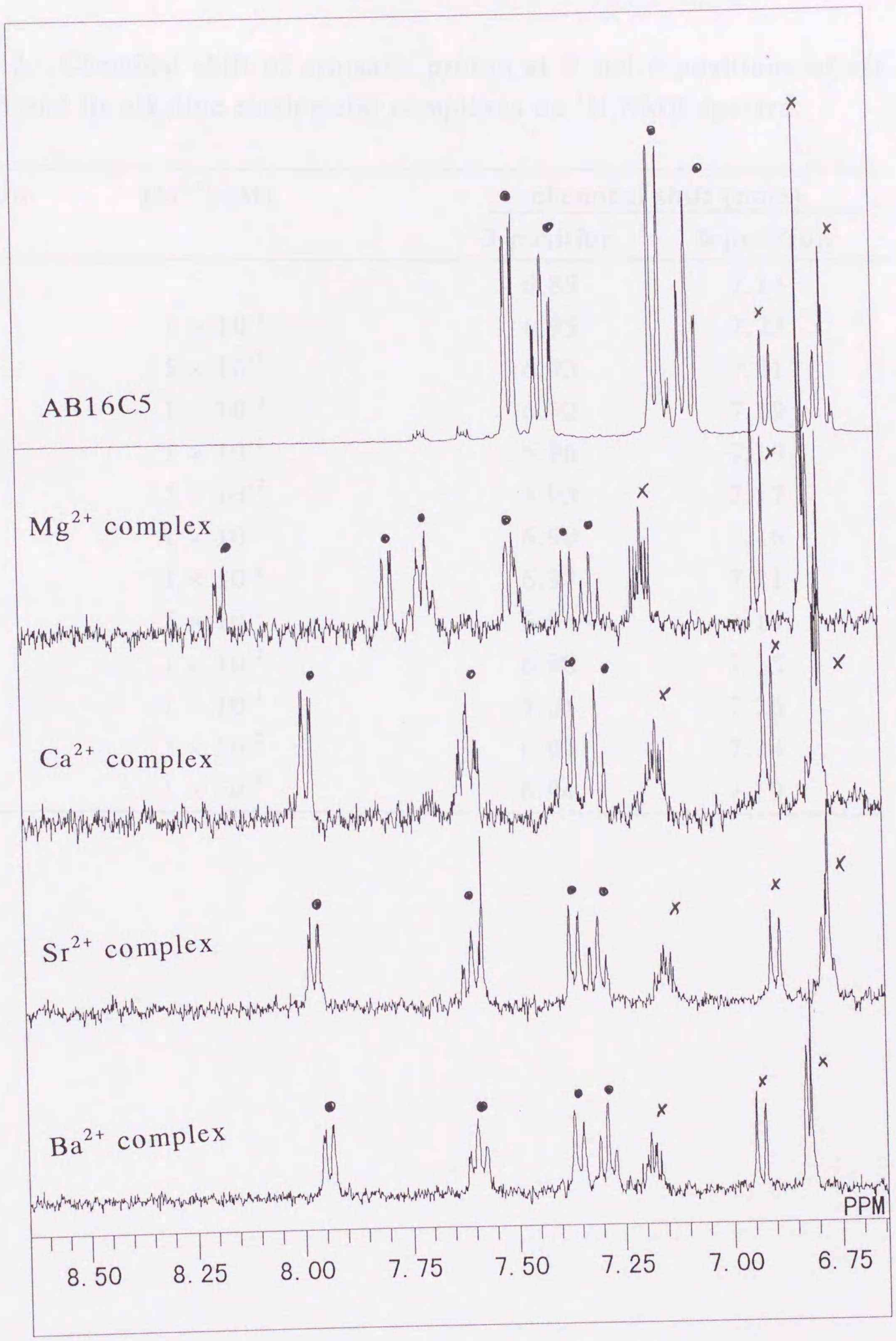

Fig. 5.5 ^{1}H NMR spectra of AB16C5 and its complexes.
[AB16C5] = 1×10^{-4} M, [M^{2+}] = 1×10^{-2} M in acetonitrile-d_3 at 25 °C.
The signs • and × mean *trans* isomer and *cis* isomer, respectively.

Table 5.3 Chemical shift of aromatic proton at 3 and 6 positions of *cis* AB16C5 and its alkaline earth metal complexes on ^{1}H NMR spectra.

Metal ion	$[M^{2+}]$ (M)	chemical shift (ppm)	
		3-position	6-position
–		6.89	7.14
Mg^{2+}	1×10^{-1}	6.95	7.23
	5×10^{-2}	6.93	7.21
	1×10^{-2}	6.92	7.19
Ca^{2+}	1×10^{-1}	6.96	7.19
	5×10^{-2}	6.93	7.17
	1×10^{-2}	6.90	7.16
Sr^{2+}	1×10^{-1}	6.97	7.21
	5×10^{-2}	6.95	7.19
	1×10^{-2}	6.90	7.15
Ba^{2+}	1×10^{-1}	7.01	7.26
	5×10^{-2}	6.99	7.24
	1×10^{-2}	6.94	7.19

spectra shown in Fig. 5.6 showed that *cis* AB13C4 did not form complex under this condition ($[M^{n+}] = 10^{-2}$ M).

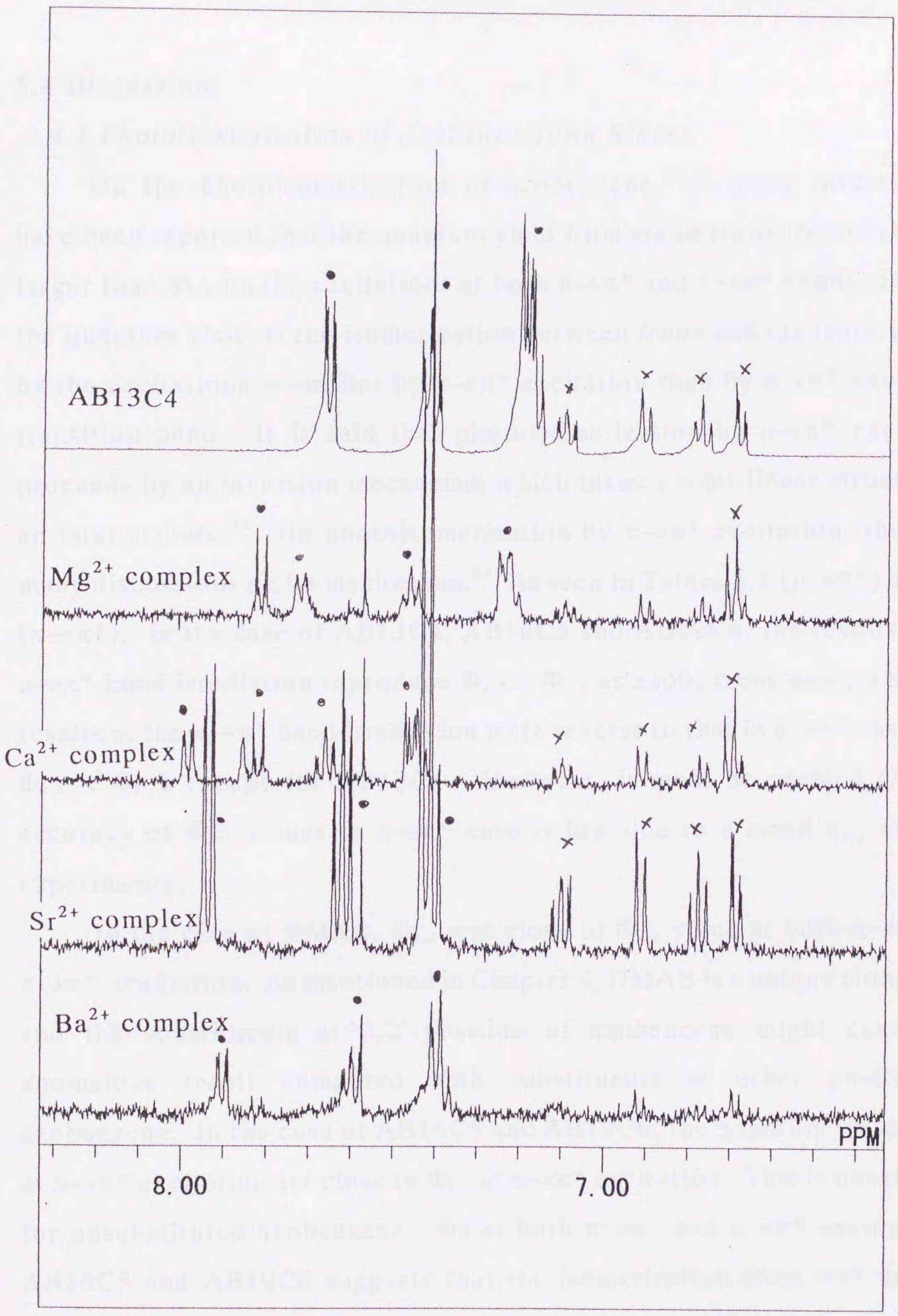

Fig. 5.6 ^{1}H NMR spectra of AB13C4 and its complexes.
[AB13C4] = 1×10^{-4} M, [M^{2+}] = 1×10^{-2} M in acetonitrile-d_3 at 25 °C.
The signs • and × mean *trans* isomer and *cis* isomer, respectively.

5.4 Discussion.

5.4.1 Photoisomerization of Azobenzocrown Ethers.

On the photoisomerization of azobenzene,[33,34] many investigators have been reported that the quantum yield from *cis* to *trans* isomer ($\Phi_{c\text{-}t}$) is larger than $\Phi_{t\text{-}c}$ on the excitations at both n→π* and π→π* bands, and that the quantum yield of the isomerization between *trans* and *cis* isomer ($\Phi_{t\text{-}c}$) by the excitations is smaller by π→π* excitation than by n→π* excitation transition band. It is said that photoisomerization by n→π* excitation proceeds by an inversion mechanism which takes a semi-linear structure as an intermediate.[35] On photoisomerization by π→π* excitation, there are many discussions on its mechanism.[35] As seen in Tables 5.1 (n→π*) and 5.2 (π→π*), in the case of AB13C4, AB16C5 and AB19C6, the results at the n→π* band irradiation reproduce $\Phi_{c\text{-}t} > \Phi_{t\text{-}c}$ as azobenzene case, while the results at the π→π* band irradiation were reverse to that in n→π* case (*i.e.*, $\Phi_{c\text{-}t} < \Phi_{t\text{-}c}$) except for AB13C4. However, it must be noticed that the accuracy of $\Phi_{c\text{-}t}$ values in π→π* case is low due to a small ε_{cis} at these experiments.

In the case of DMAB, $\Phi_{c\text{-}t}$ was close to $\Phi_{t\text{-}c}$ value at both n→π* and π→π* irradiation. As mentioned in Chapter 4, DMAB is a unique compound, and the substituents at 2,2'-position of azobenzene might cause this anomalous result compared with substituents at other position of azobenzene. In the case of AB16C5 and AB19C6, the quantum yields, $\Phi_{t\text{-}c}$, at π→π* excitation are close to $\Phi_{t\text{-}c}$ at n→π* excitation. This is not the case for unsubstituted azobenzene. Φs at both π→π* and n→π* excitation of AB16C5 and AB19C6 suggests that the isomerization from ππ* and nπ* excited states of *trans* isomer of azobenzocrown ethers takes place via a different pathway. Rotational and inversion processes can be likely ones for ππ* and nπ*, respectively, which were also proposed for azobenzene by calculation[38] and experiment[39,40]. However, a possibility of internal

conversion from ππ* to nπ* excited state with a high efficiency can not be excluded.

On the other hand, in the case of AB13C4, $\Phi_{t\text{-}c}$ was always smaller than $\Phi_{c\text{-}t}$. And $\Phi_{t\text{-}c}$ at π→π* irradiation of AB13C4 was not close to its $\Phi_{t\text{-}c}$ at n→π* irradiation differently from the cases of others. And, $\Phi_{t\text{-}c}$ at π→π* of AB13C4 was extremely small. As mentioned above, rotation process can be likely ones for π→π* on the photoisomerization of azobenzocrown ethers. If rotation process of usual azobenzene can be likely ones for π→π*, rotation process seldom proceeds on photoisomerization of AB13C4. Inversion process does not need large space for photoisomerization, while rotation process does need. Since AB13C4 can not have such a space because of its short polyoxyethylene moiety, photoisomerization of AB13C4 may proceed via inversion process. However, quantum yields of photoisomerization by n→π* and π→π* from *trans* to *cis* isomer of another azobenzocrown ether were the same values for which inversion is the only possible isomerization pathway due to intramolecular steric hindrance.[41] Therefore, in the case of AB13C4, a possibility that, photoisomerization proceeds differently from those in the case of AB16C5 and AB19C6 can be remained.

The quantum yields from *trans* to *cis* isomer were in the order of $\Phi_{t\text{-}c}$(DMAB) > $\Phi_{t\text{-}c}$(AB16C5, AB19C6) > $\Phi_{t\text{-}c}$(azobenzene) > $\Phi_{t\text{-}c}$(AB13C4) for π→π* excitation, whereas $\Phi_{t\text{-}c}$(DMAB) > $\Phi_{t\text{-}c}$(azobenzene) > $\Phi_{t\text{-}c}$(all azobenzocrown ethers) for n→π* excitation. If photoisomerization by π→π* excitation takes place via nπ* state, the quantum yield of photoisomerization by π→π* excitation must be smaller than that by n→π* excitation. These different substituent effects in two cases also suggest that the isomerization path from *trans* to *cis* isomer of AB16C5, AB19C6 and DMAB at π→π* excitation does not occur via nπ* excited state,[33,34] but via a direct isomerization path from ππ* excited state as mentioned above. Difference of properties between unsubstituted azobenzene and

azobenzocrown ethers are due to their non- plane structure. This result may be attributed to the non planer structures of AB16C5, AB19C6, or DMAB due to the substituents at 2,2'-position, as suggested from absorption spectra (*vide ante*) and ^{1}H NMR spectra (Fig. 4.1).

In these azobenzene series, AB13C4 has so small cavity due to short polyoxyethylene moiety, that motion of its azobenzene moiety should be extremely suppressed. Therefore, quantum yields of photoisomerization of AB13C4 were small.

5.4.2 Effects of Complexation with Alkaline Earth Metal Ions

The quantum yields from *trans* to *cis* isomerization at both n→π* and π→π* excitations increased when AB16C5 and AB19C6 were formed complexes with any alkaline earth metal ions except for Mg^{2+} complex of AB16C5. Since the complexation with metal ion usually stabilizes the structure of the ligand molecule by ion-dipole interaction, the thermal or photoisomerization rate is decreased.[45,46] However, the present results show the increases of the quantum yields by the complexation.

The quantum yields $\Phi_{t\text{-}c}$ by π→π* excitation of AB16C5 were in the order of $Ca^{2+} >> Sr^{2+} > Ba^{2+} > Mg^{2+}$ (Table 5.2). This order is parallel to the complex formation constants for these ions and also to the shifts of the π→π* absorption bands except for Mg^{2+}. Therefore, the increase of quantum yield should be caused by the formation of chelating bond between metal ion and oxygen and/or nitrogen atoms on the azobenzene moiety. However, the cavity size of *trans* AB16C5 (0.85-0.90 Å in radius) is smaller than those of the ions (radii of these metal ions are 1.14, 1.32, and 1.49 Å for Ca^{2+}, Sr^{2+} and Ba^{2+}, respectively),[28] and the ideal fitting in size is not expected. Therefore, large complex formation constants are hardly achieved. Even though, the relatively large formation constants (Table 3.1) reveal an existence of the strong chelating interactions between metal ion and the azobenzene moiety, which are strengthened by π→π* excitation (~

20 kJ mol^{-1}, see Fig. 4.14(b)). These chelating bonds will cause the molecular strain even in the transient or excited singlet state, and will promote the isomerization from *trans* to *cis*.

On the other hand, when the n→π* transition bands of AB16C5 were excited, the quantum yields $\Phi_{t\text{-}c}$ were in the order of Ca^{2+} < Sr^{2+} < Ba^{2+} (Table 5.1). The $\Phi_{t\text{-}c}$ values were still larger than that of free AB16C5. The order of $\Phi_{t\text{-}c}$ is just in the order of the stability energy of the excited state (Fig. 4.14(a)). The chelating bond also promotes the isomerization from *trans* to *cis* in the nπ* excited singlet state as in the above case.

The quantum yields of the isomerization from *cis* to *trans* ($\Phi_{c\text{-}t}$) of AB16C5 at n→π* irradiation were not so much affected by the addition of Sr^{2+} or Ba^{2+}. However, from dependence of chemical shift of *cis* isomers on ^1H NMR spectra on concentration of metal ion which are summarized in Table 5.3, the amount of shift of *cis* AB16C5 was the largest in presence of Ba^{2+} under this condition. In addition, there are few discussions on photoisomerization from *cis* to *trans* isomer and $\Phi_{c\text{-}t}$ was not so accurate because of stability constants not evaluated correctly of these complexes. Therefore, the discussion of these effects remains untreated in the present study.

The quantum yields of the isomerization from *trans* to *cis* of AB19C6 by excitation at π→π* transition bands were also increased by the presence of alkaline earth metal ions, and the difference among the metal ions were smaller than that in the case of AB16C5. Except for Mg^{2+}, the quantum yield was in the order of Ca^{2+} > Sr^{2+} > Ba^{2+}. Though the order was not the same as the stability of excited state, the difference was small. The reason for this increase of the quantum yield is probably the same as that in the case of AB16C5. The increase of quantum yield by complexation was also smaller than that in AB16C5 case, probably because of the smaller stability energy (14 kJ mol^{-1}) than that in AB16C5 case (Fig. 4.14(a)). These tendency were also observed for the quantum yields at n→π* excitation except for Mg^{2+}. In

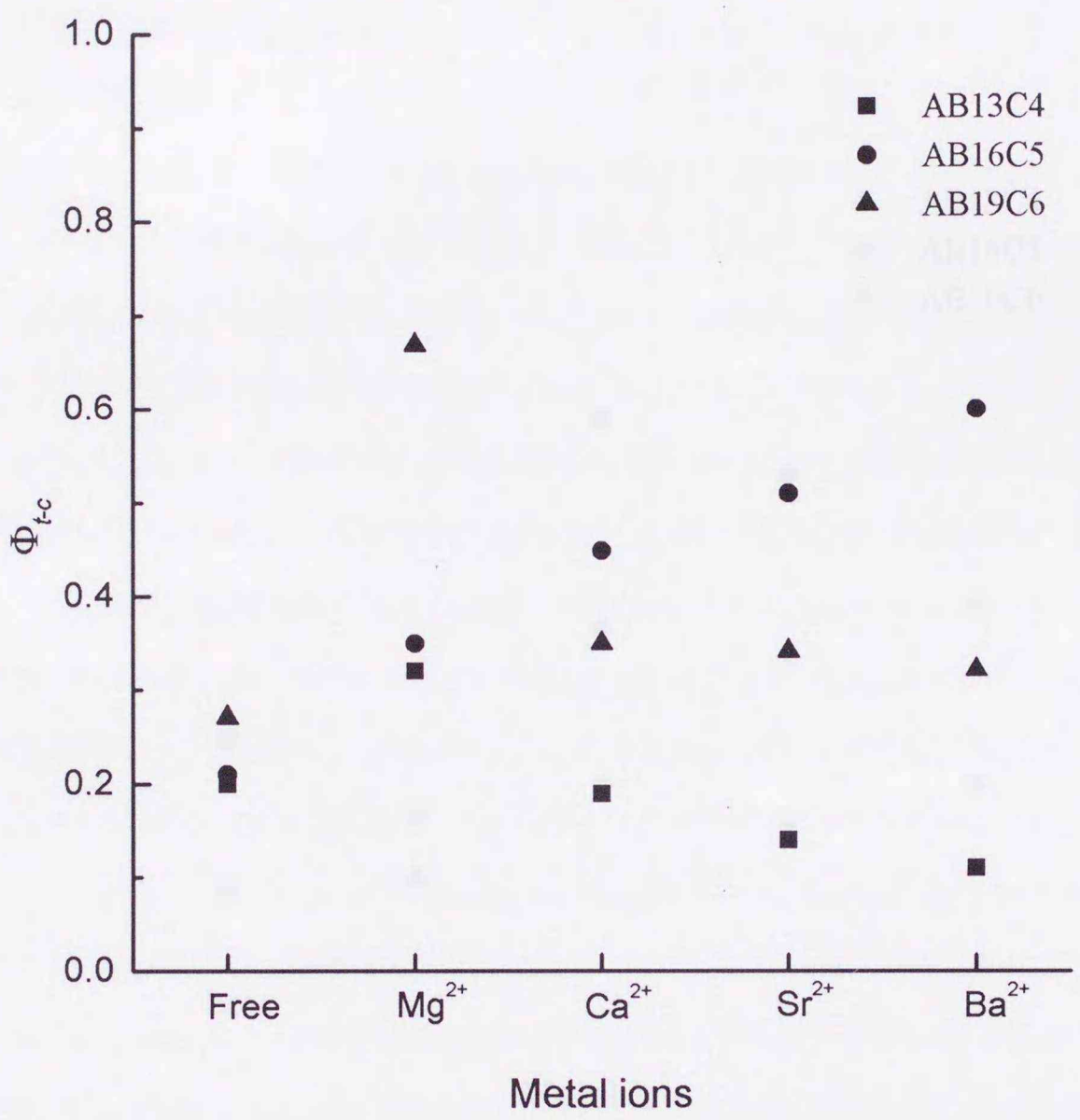

Fig. 5.7 Quantum yields of photoisomerization from *trans* to *cis* isomers of azobenzocrown ethers and their alkaline earth metal complexes by irradiation at $n\rightarrow\pi^*$ transition bands.

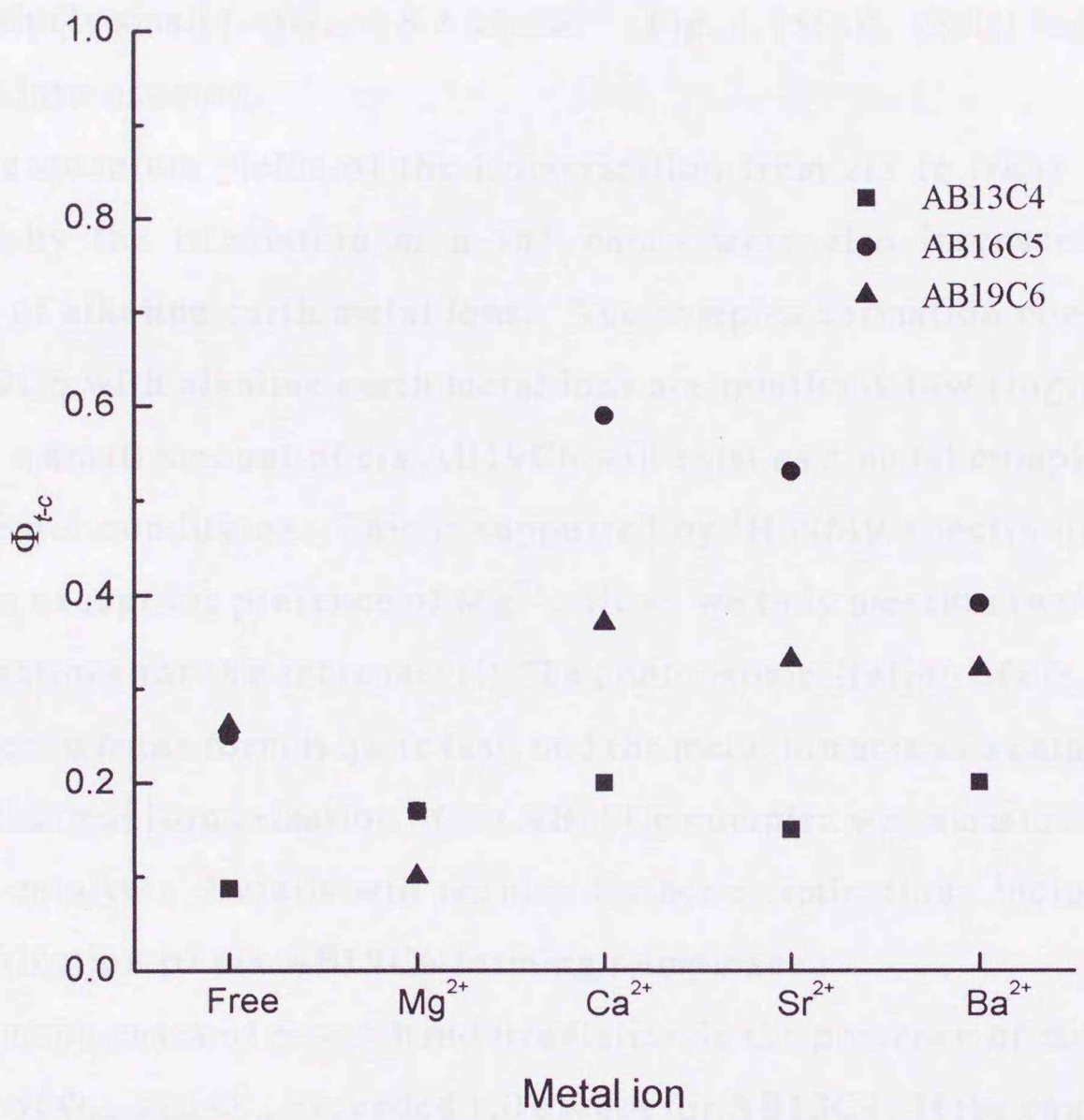

Fig. 5.8 Quantum yields of photoisomerization from *trans* to *cis* isomers of azobenzocrown ethers and their alkaline earth metal complexes by irradiation at $\pi \rightarrow \pi^*$ transition bands.

the Mg^{2+} case, the n→π* band irradiation gave higher quantum yield than the other metal ions, even though the stability at excited state of the complex was relatively small ($-\Delta G_{ex} < 8.4$ kJ mol^{-1} : Fig. 4.15(a)). Other factor must be taken into account.

The quantum yields of the isomerization from *cis* to *trans* ($\Phi_{c\text{-}t}$) of AB19C6 by the irradiation at n→π* bands were also increased by the addition of alkaline earth metal ions. The complex formation constants of *cis* AB19C6 with alkaline earth metal ions are relatively low ($\log_{10} K < 3$), and only a small amount of *cis* AB19C6 will exist as a metal complex at the experimental conditions. This is supported by ^{1}H NMR spectra under this condition except for presence of Mg^{2+}. Here, we only mention two possible of explanations for this increase: (i) The photo isomerization of *cis* AB19C6 complexes to *trans* form is quite fast, and the metal ion acts as a catalyst, and (ii) The thermal isomerization of *cis* AB19C6 complex was assisted by metal ion as a catalyst. Details will require further examinations including the characterization of *cis* AB19C6 forming complexes.

In many cases of n→π* band irradiation in the presence of metal ions, the sums of $\Phi_{t\text{-}c}$ and $\Phi_{c\text{-}t}$ exceeded 1.0 except for AB13C4. If the sum of them does not exceed 1.0, photoisomerization from *cis* to *trans* and *vice versa* take place via a common intermediate state, which has been suggested in unsubstituted azobenzene.[33,34,38] This suggests that the isomerization processes from *trans* to *cis* and from *cis* to *trans* isomers of the metal complexes do not proceed via the common intermediate state.

On the other hand, in the case of AB13C4, alkaline earth metal ions forming complexes affected the photoisomerization, and this effect was different from that in the case of AB16C5 and AB19C6. The quantum yields from *trans* to *cis* isomer at n→π* irradiations of AB13C4 were not increased by complexation with alkaline earth metal ions except for Mg^{2+}. At n→π* excitation, complexation with Ca^{2+} did not affect $\Phi_{t\text{-}c}$, and complexation with Sr^{2+} and Ba^{2+} suppressed photoisomerization from *trans* to *cis* isomer.

These results can be explained according to the energy diagrams shown in Fig. 4.13(a). Figure 4.13(a) shows that AB13C4 at nπ* excited state are destabilized by complexation with alkaline earth metal ions (ΔG_{ex} > 3.0 kJ mol^{-1}) except for Mg^{2+}. Destabilization by complexation at excited state means that there is not any chelating bond which prompts photoisomerization of alkaline earth metal complexes of AB16C5 and AB19C6, and may repulse metal ions. If metal ion in the complex is light, the metal ion will be released from the compound immediately. If metal ion in the complex is heavy, the metal ion will keep a form of the complex, and the metal ion should be steric hindrance for photoisomerization. Destabilization energy is in the order of Ca^{2+} > Ba^{2+} > Sr^{2+}. Since Ca^{2+} is relatively light ion and the destabilization energy was large, Ca^{2+} should be released from the compound at nπ* excited state due to destabilization energy. As the result, photoisomerization behavior of AB13C4 at n→π* transition would not be affected by complexation with Ca^{2+}. On the other hand, Sr^{2+} and Ba^{2+} are heavy ions compared with Ca^{2+}, and destabilization energy of these complexes is smaller than that of Ca^{2+} complex. Therefore, a part of these metal ions would keep a complex structure in the excited state. While repulsion of Ba^{2+} is larger than that of Sr^{2+}, suppression of photoisomerization at n→π* transition by complexation with Ba^{2+} was larger than that by complexation with Sr^{2+}. Since Ba^{2+} is a heavier ion than Sr^{2+}, most of Ba^{2+} could remain as a complex. Therefore, the quantum yields of the Ba^{2+} complex were smaller than those of the Sr^{2+} complex. On the other hand, Mg^{2+} may not be released from nπ* excited state. As described in Chapter 4, Mg^{2+} interacts weakly with azo group through charge-dipole interaction compared with other alkaline earth metal ions. Mg^{2+} would be seldom affected by rearrangement of electrons at azo group by n→π* excitation, because interaction between Mg^{2+} and azo group should be weak in its structure. Therefore, excited azo group differently from other alkaline earth metal ions would not repulse Mg^{2+}.

In the case of $\pi \rightarrow \pi^*$ irradiation of AB13C4, $\Phi_{t\text{-}c}$s of their complexes were larger than that of AB13C4 not forming complex. $\Phi_{t\text{-}c}$ via $\pi\pi^*$ excitation state was in the order of $Ca^{2+} = Ba^{2+} > Mg^{2+} > Sr^{2+}$, however these difference between values of them was a little. The order of stabilization energy at $\pi\pi^*$ excited state was $Ca^{2+} > Sr^{2+} > Ba^{2+} > Mg^{2+}$, and the differences between values of them were also small. These stabilization energies were smaller than that of AB16C5 or AB19C6, and values of $\Phi_{t\text{-}c}$s are smaller than that of AB16C5 or AB19C6. However, photoisomerization of AB13C4 at $\pi \rightarrow \pi^*$ transition was increased by complexation with alkaline earth metal ions as well as AB16C5 and AB19C6. From these results, complexation with alkaline earth metal ions gave different effects for photoisomerization of AB13C4 from those of AB16C5 and AB19C6. This could be attributed to the perching structure of AB13C4 complexes. The quantum yields of photoisomerization from *cis* to *trans* isomer at $n \rightarrow \pi^*$ transition of AB13C4 in the presence of alkaline earth metal ions were almost the same as that of free AB13C4. This also means that *cis* AB13C4 did not form a complex with these metal ions. However, it should be noted that these values at $\pi \rightarrow \pi^*$ transition have a large error because of no absorption band at this region.

From these results, effects of complexation with alkaline earth metal ions on photoisomerization of azobenzocrown ethers should mainly be attributed to the stabilization by complexation with these metal ions at the excited state.

5.4.3 Effect of Complexation with Rare Earth Metal Ions.

AB19C6 formed complexes with light rare earth metal ions. Complexation with the rare earth metal ion affected photoisomerization of AB19C6 in the case of complexation with alkaline earth metal ion. While complexation with alkaline earth metal ion accelerated photoisomerization from *trans* to *cis* isomer at both $n \rightarrow \pi^*$ and $\pi \rightarrow \pi^*$ transitions, complexation

with rare earth metal ion extremely suppressed photoisomerization from *trans* to *cis* isomer at these excited state. Especially, Eu^{3+} complex remarkably suppressed the photoisomerization. The order of quantum yield of photo isomerization from *trans* to *cis* isomer by $n\rightarrow\pi^*$ excitation was $La^{3+} > Gd^{3+} > Sm^{3+} > Nd^{3+} > Pr^{3+} > Eu^{3+}$, and that by $\pi\rightarrow\pi^*$ excitation was $Gd^{3+} = La^{3+} > Sm^{3+} = Pr^{3+} = Nd^{3+} > Eu^{3+}$. In the photoisomerization from *cis* to *trans* isomer, irradiation wavelengths were not those at the peak top. Particularly, at $\pi\rightarrow\pi^*$ excitation, *cis* isomer does not have an absorption band. Therefore, the quantum yields of photoisomerization from *cis* to *trans* isomer have a large error as complexes with alkaline earth metal ions. In the case of alkaline earth metal complex, the quantum yields increased with the stabilization energy of complexes at excited states. Different points between alkaline earth metal ions and rare earth metal ions are ionic charge and presence of paramagnetism. The effects carried by these two differences on photoisomerization behavior of azobenzocrown ethers are discussed.

5.4.4. Effects of Metal Ion's Charge on Photoisomerization of AB19C6.

Rare earth metal ions except for La^{3+} have paramagnetism. Comparison of quantum yields of photoisomerization among La^{3+} and Ca^{2+} and Na^+ complexes whose ionic sizes are almost the same as each other is suitable for the discussion on effect of ionic charge on photoisomerization, because paramagnetism brings an effect of intersystem crossing to photophysical process. The quantum yields of photoisomerization from *trans* to *cis* isomer of AB19C6 complexes were in the order of $Ca^{2+} > Na^+ >$ free $> La^{3+}$ by $n\rightarrow\pi^*$ excitation, and in the order of $Ca^{2+} >$ free $> La^{3+} > Na^+$ by $\pi\rightarrow\pi^*$ excitation. The effects of complexation with Ca^{2+} on photoisomerization have been discussed above already. Fig. 4.16 shows stabilization energies at both $n\pi^*$ and $\pi\pi^*$ excited state by complexation with individual rare earth metal ion. As shown in Fig. 4.16, complexation with La^{3+} brought larger stabilization energy to both $n\pi^*$ and $\pi\pi^*$ excited

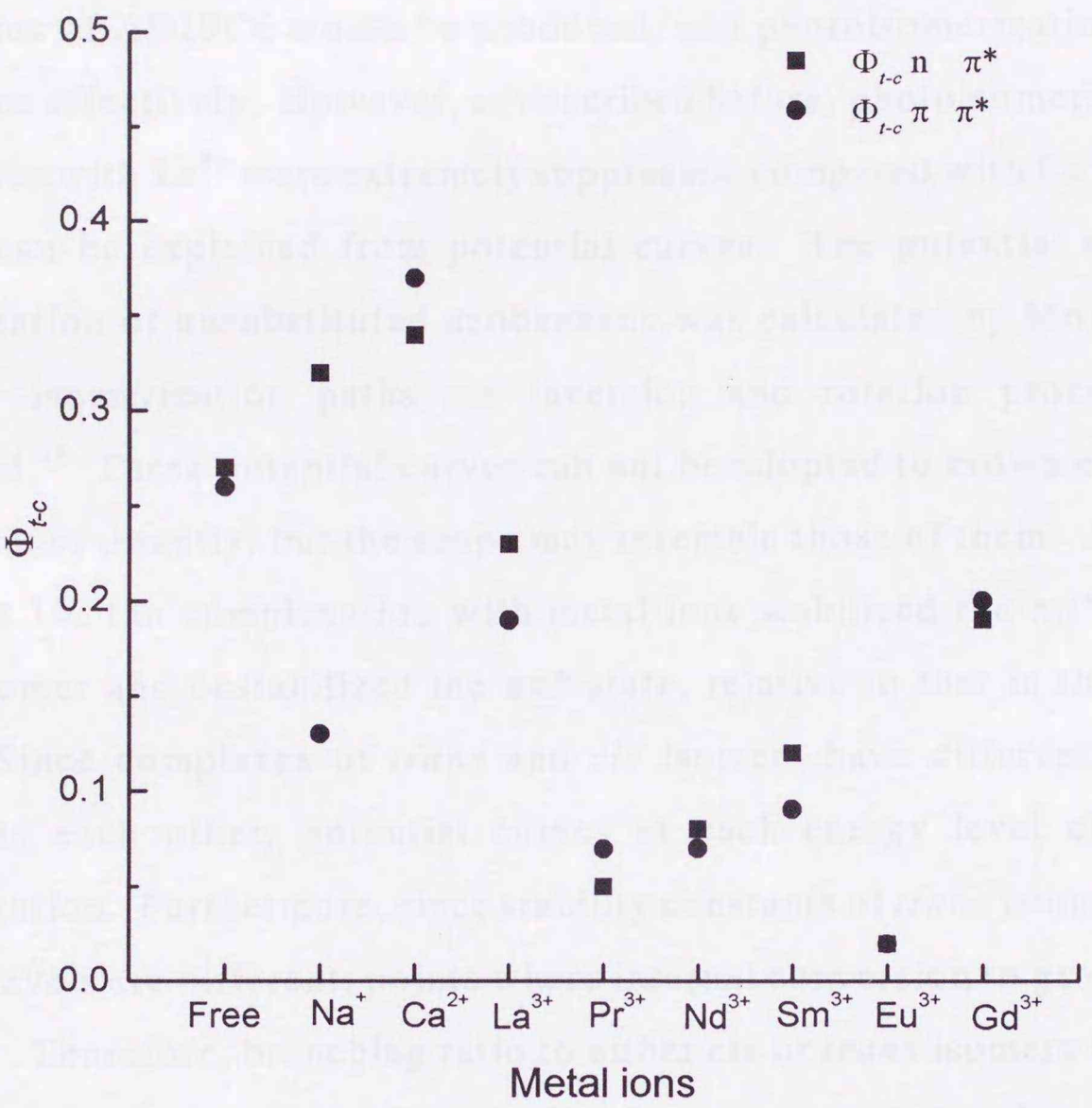

Fig. 5.9 Quantum yields of photoisomerization from *trans* to *cis* isomers of AB19C6 and its rare earth metal complexes.

state than complexation with Ca^{2+}. Therefore, chelating bond which promoted photoisomerization at excited state of alkaline earth metal complexes of AB19C6 would be produced, and photoisomerization should take place effectively. However, as described before, photoisomerization of complexes with La^{3+} were extremely suppressed compared with Ca^{2+}. These results can be explained from potential curves. The potential curve for isomerization of unsubstituted azobenzene was calculated by Monti et al., and the isomerization paths via inversion and rotation process were proposed.[38] These potential curves can not be adopted to crown ether type azobenzenes directly, but the shape may resemble those of them. As shown in Fig. 4.16, the complexation with metal ions stabilized the $\pi\pi^*$ state of *trans* isomer and destabilized the $n\pi^*$ state, relative to that in the ground state. Since complexes of *trans* and *cis* isomers have different stability constants each other, potential curves at each energy level change by complexation. Furthermore, since stability constants of *trans* isomer at each energy levels are different, points where internal conversion to ground state change. Therefore, branching ratio to either *cis* or *trans* isomers should be changed by complexation (Fig. 5.10). In the case of complexation with alkaline earth metal ions, this effect increased the branching ratio to *cis* isomer from both excited states, and $\Phi_{t\text{-}c}$ was increased. In the case of La^{3+} complex, excited *trans* isomer by $n\rightarrow\pi^*$ excitation is stabilized by complexation more largely than in the case of Ca^{2+} complex. La^{3+} interacts with crown ether moiety more strongly than Ca^{2+} because La^{3+} has larger charge than Ca^{2+}. And motion of crown ether moiety would be suppressed more strongly by complexation with La^{3+} than that by complexation with Ca^{2+}. Therefore activation energy of isomerization of La^{3+} complex at ground state would be higher than that of free AB19C6. In the case of alkaline earth metal complex, activated state at ground state was also stabilized by complexation. This is supported by thermal isomerization which was promoted by complexation. However, in the case of La^{3+}

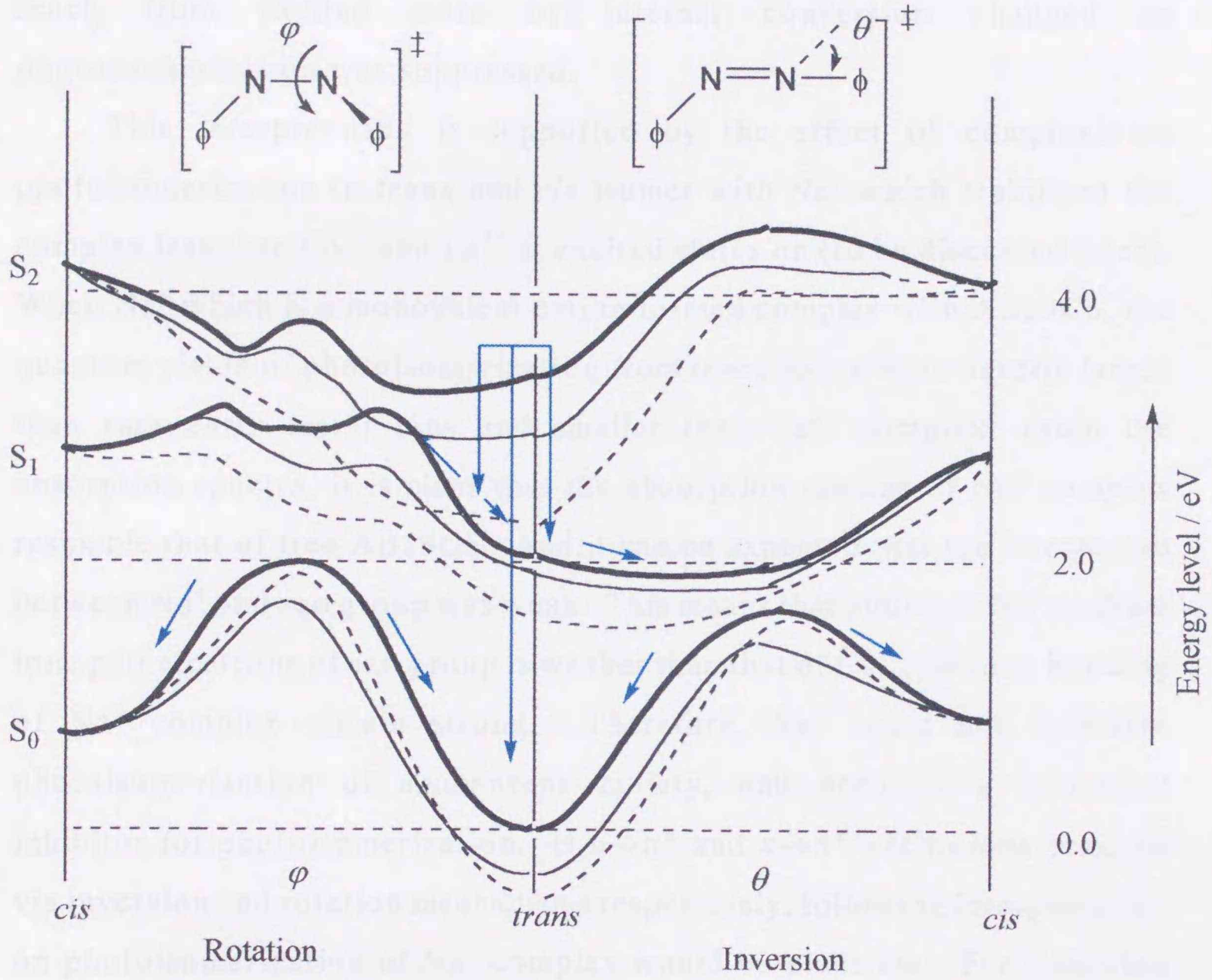

—— uncomplexed azobenzocrown ether
——— alkaline earth metal complexes
------ rare earth metal complexes

Fig. 5.10 Schematic representation of the S_0, S_1, and S_2 potential energy curves of free azobenzocrown ethers (——) adopted from the results of calculations reported in ref. 42, predicted curves of its alkaline earth metal complex (———), and that of rare earth metal complex (·····).

complex, the activated state at ground state was not stabilized by complexation. Therefore, the branching ratio at the point where molecule reach from excited state by internal conversion changed as photoisomerization was suppressed.

This interpretation is supported by the effect of complexation photoisomerization to *trans* and *cis* isomer with Na^+ which stabilized the complex less than Ca^{2+} and La^{3+} at excited states on (to be discussed later). When Na^+ which is a monovalent cation formed complex with AB19C6, the quantum yields of photoisomerization from *trans* to *cis* were usually larger than rare earth metal ions and smaller than Ca^{2+} complex. From the absorption spectra, it is clear that the absorption spectra of Na^+ complex resemble that of free AB19C6. And it can be expected that the interaction between Na^+ and azo group was weak. This means that ability of Na^+ to draw lone pair electrons of azo group is weaker than that of Ca^{2+}, and azo bonding of Na^+ complex remain strong. Therefore, Na^+ could not facilitate photoisomerization of azobenzene moiety, and becomes a structural inhibitor for photoisomerization. If $n\rightarrow\pi^*$ and $\pi\rightarrow\pi^*$ excitations proceed via inversion and rotation mechanisms respectively, following interpretation on photoisomerization of Na^+ complex would be plausible. For inversion mechanism, since large space is not needed for isomerization,[42] existence of Na^+ would not be steric inhibitor for isomerization. Therefore, quantum yield by $n\rightarrow\pi^*$ excitation increased in result of weak interaction between Na^+ and azobenzene moiety. On the other hand, rotation mechanism needs large space for isomerization.[42] Since Na^+ becomes steric inhibitor for rotation mechanism, quantum yield by $\pi\rightarrow\pi^*$ excitation decreased.

From these discussions, ionic charge affects the motion of crown ether moiety and stabilization at both excited state and ground state. In the case of complex with trivalent metal ion, excited complex is extremely stabilized, and thermal isomerization is suppressed. Complexation with trivalent metal ions leads quantum yields of photoisomerization to be low. These effects

facilitated photoisomerization. In the case of complexation with monovalent ion, the interaction between AB19C6 and metal ion is weak. Therefore, Na^+ exhibits different effects from divalent and trivalent metal ions on photoisomerization of AB19C6.

5.4.5 Effects of Paramagnetism on Photoisomerization.

Rare earth metal ions except for La^{3+} have paramagnetism. If paramagnetism does not affect photoisomerization of azobenzocrown ether complex, these rare earth metal complexes should exhibit almost the same photoisomerization behavior one another. Alkaline earth metal complexes also exhibited different photoisomerization behavior one another. In this case, sizes of each alkaline earth metal ions are different one another and the stabilization energies at excited state are also different. Azobenzocrown ethers which form complexes with different alkaline earth metal ions must take different geometry due to their different metal ionic sizes from their absorption spectra. And, those potential curves have different shapes in all energy levels. Therefore, ratios of amounts of *cis* and *trans* isomers were essentially different. In the case of rare earth metal complexes, absorption spectra of these complexes quite resembled to one another. Therefore, difference on photoisomerization behavior of these rare earth metal complexes can be attributed to this paramagnetism. Paramagnetism may increase intersystem crossing from excited singlet state to excited triplet state. In the case of photoisomerization of rare earth metal complexes with paramagnetism, the participation of triplet state into photoisomerization process should be taken into account. These complexes had the same quantum yields of photoisomerization from *trans* to *cis* isomer in both $n\rightarrow\pi^*$ and $\pi\rightarrow\pi^*$ excitation. Since rare earth metal complexes including La^{3+} complex stabilized $^1\pi\pi^*$ state, intersystem crossing from $^1\pi\pi^*$ to T_1 which is probably $^3n\pi^*$ state would take place as well as that from $^1n\pi^*$ to T_1 state. The lifetime of T_1 state is usually longer compared with those of excited

singlet states. Since long life time means small k_1 and k_3 shown in Fig. 5.1, increase of quantum yield of photoisomerization from *trans* to *cis* isomer is expected. And triplet state has a lower energy compared with singlet states. Since the stabilization of the excited state was carried by an ion-dipole interaction, the triplet state would be also stabilized by complexation as well as other states. Since measurement of absorption spectra due to $S_0 \rightarrow T_1$ can not be carried out, detail can not be discussed. However, if the absorption of $S_0 \rightarrow T_1$ were allowed, these rare earth metal complexes would exhibit the same $S_0 \rightarrow T_1$ absorption spectra one another. Therefore stabilization at the triplet state by complexation would be parallel to those at other states. Fig. 5.11 shows predicted potential curve at triplet state by Monti et al.[38] In the case of rare earth metal complexes with paramagnetism, the complex had smaller quantum yields of photoisomerization from *trans* to *cis* isomer, when its complex formation constant is larger except for Eu^{3+} complex. This result would be concluded as following. Complexation with Pr^{3+} or Nd^{3+} stabilized the triplet state largely. This large stabilization would causes non-adiabatic crossing point between potential surface of the triplet state and that of the ground state, and photoisomerization from *trans* to *cis* isomer would be suppressed extremely as shown in Fig. 5.11. Complexation with Gd^{3+} would not stabilize the triplet state largely compared with complexation with Pr^{3+} and Nd^{3+}. Therefore, the crossing point would not be present, and quantum yields from *trans* to *cis* isomer of Gd^{3+} complex would be larger than Pr^{3+} and Nd^{3+} complexes. $\Phi_{t\text{-}c}$s of Eu^{3+} complex were extremely small although complexation with Eu^{3+} does not stabilize the triplet state. In these rare earth metal ions, only Eu^{3+} is easily reduced to Eu^{2+} ($E_{redox}^{\circ} = -0.43$ V vs. NHE).[53] The azobenzene unit is reported to be reproduced *trans* isomer by the redox reaction.[46] Although the oxidation potential of azobenzenes have not been reported, the potential of the S_1 and T_1 state is estimated to be ca. + 2.0 V and + 1.5 V higher than that of the ground state from excitation energy and calculation,[38] respectively, and the

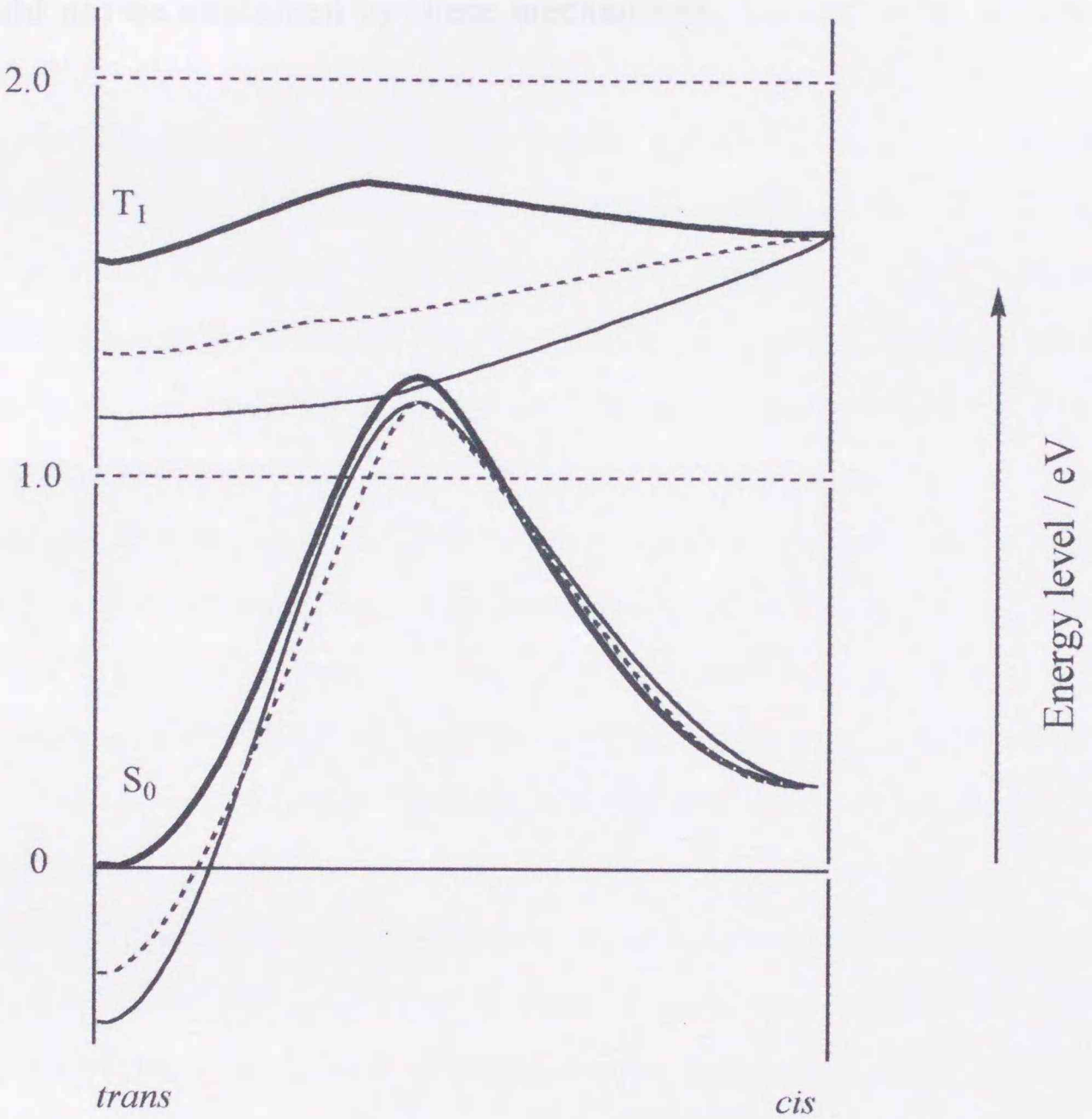

Fig 5.11 Schematic representation of S_0 and T_1 potential energy curves of AB19C6 and its rare earth metal complexes (——) adopted from the results of prediction reported in ref. 38, and predicted curves of its Pr^{3+} complex (——) and Gd^{3+} complex (·····).

possibility of the redox reaction could be expected. In this case, excited *trans* isomer is deactivated to ground state by an electron transfer quenching mechanism.

The energy level of excited *cis* isomer was unknown. The increase of $\Phi_{c\text{-}t}$ could not be explained by these mechanisms.

5.5 Conclusion.

The quantum yields of photo isomerization were examined on three azobenzene compounds with polyoxyethylene ring. It became clear that the photo isomerization behavior of these compounds is controlled by means of the complexation with metal ions and/or the change of the irradiation band. And as mentioned above, the probability that photoisomerization of azobenzocrown ethers proceeds via triplet state by complexation with paramagnetic rare earth metal ions is suggested. Stabilization at the triplet state by complexation with these metal ions was found to affect efficiency of photoisomerization because larger stabilization which brought smaller quantum yield. And redox property of metal ion forming complex suppressed photoisomerization.

The factors which affect photoisomerization between *trans* and *cis* isomer by complexation with metal ion are found to be (1) surface charge of metal ion, (2) suitability between metal ion size and size of polyoxyethylene unit, (3) electron densities of coordination atoms of azobenzene unit, (4) redox potential of metal ion in the complex, (5) paramagnetism of metal ions on photoisomerization.

Photoisomerization of azobenzocrown ethers was controlled by these factors. This controlling method is easy, simple, and reversible. When molecular switch is constructed using these compounds, this molecular switch can obtain suitable property for its purposes by reversible complexation with metal ions. This concept as new method which controls functional molecule is expected applied to several fields.

CHAPTER 6
Conclusion

Recently, many studies on functional organic compounds with regard to photoisomerization have been reported. The most familiar method to verify the functionality of organic compounds is by introducing and/or varying its functional group. Introducing and/or varying the functional group means a new compound is but synthesized, hence varying the function of the new compound further. However, it would be impossible to get back the original function of that compound. If a complexation unit exists within a molecule, the function could be varied easily and reversibly by the changing complexed metal ion. In the present work, the compounds used here consist of crown ether moiety having complexation ability with metal ions and azobenzene moiety, thus, it exhibits reversible photoisomerization behavior. The photoisomerization behavior of azobenzene moiety could be controlled by complexed metal ions. The knowledge obtained in the present work is described as follows.

In Chapter 3, only *trans* isomers of crown ether type azobenzenes form complexes with alkali and alkaline earth metal ions due to polyoxyethylene moiety. Usually, complexes of these azobenzenes with alkaline earth metal ions are more stable than those with alkali metal ions. Azobenzene compound with larger polyoxyethylene moiety has larger complexation ability, while smaller azobenzene compound is excellent in term of selectivity. Furthermore, AB19C6 having the largest polyoxyethylene moiety was found to form stable complexes with light rare earth metal ions. These complexes with the rare earth metal ions are more stable than complexes with the alkaline earth metal ions.

In Chapter 4, conformation of these azobenzene compounds and interaction between complexed metal ion and azo group were discussed in accordance with their absorption spectra. Azobenzene compounds used in

this work found to have unique electron structures as compared with the usual azobenzene due to the presence of oxygen atoms at 2,2'-positions. Interaction between lone pair electrons at azo group and complexed metal ion seems not to reflect on complexation behavior. Furthermore, effects of the length of polyoxyethylene moiety on electron system of azobenzene moiety were clarified.

In Chapter 5, photoisomerization behavior of azobenzenes used in the previous chapter was discussed. Photoisomerization, from *trans* to *cis* isomers of azobenzenes used in this work, was usually accelerated by complexation with alkaline earth metal ions. Photoisomerization of AB19C6 became slower by complexation with rare earth metal ions. In the both cases of $n\rightarrow\pi^*$ and $\pi\rightarrow\pi^*$ excitations, stabilization by complexation at individual excited states(*i.e.* $n\pi^*$ and $\pi\pi^*$ excited states) affected photoisomerization behavior of these complexes.

The present work suggested one typical method to vary a function of organic compound easily and reversibly by complexation with metal ions. And, in this work, basic properties were studied for that particular purpose. Thus, from the viewpoints of easiness and recovery of the materials, the method suggested in the present work is obviously different from familiar methods. These azobenzene compounds used in this work are expected not only to be applied in functionalized material but also to give a strategy to development of functional devices.

REFERENCES

1. Christian, G. D. In *Analytical Chemistry* (4 Ed.); John Wiley & Sons: New York, 1986, Chapter 13.
2. Cotton, F. A.; Wilkinson, G. In *Basic Inorganic Chemistry* (4 Ed., in Japanese); Baifukan: Tokyo, 1979, p 368, p 378.
3. Pedersen, C. J. *J. Am. Chem. Soc.*, **1967**, *98*, 2495.
4. Pedersen, C. J.; Frensdroff, H. K. *Angew. Chem. Int. Ed. Engl.*, **1972**, *11*, 16.
5. (a) Kimura, K.; Hayata, E.; Shono, T. *J. Chem. Soc., Chem. Commun.*, **1984**, 271. (b) Wong, K. H.; Ng, H. L. *Tetrahedron Lett.*, **1979**, *20*, 4295.
6. Gruenwald,T. I. *J. Am. Chem. Soc.*, **1974**, *96*, 2879.
7. (a) Takagi, M.; Nakamura, H.; Ueno, K. *Anal. Lett.*, **1977**, *10*, 1115. (b) Nakamura, H.; Takagi, M.; Ueno, K. *Talanta*, **1979**, *26*, 921.
8. Kitazawa, S.; Kimura, K.; Shono, T. *Bull. Chem. Soc. Jpn.*, **1983**, *56*, 3253.
9. Nakamura, H.; Sakka, H.; Takagi, M.; Ueno, K. *Chem. Lett.*, **1981**, 1305.
10. Nishida, H.; Katayama, Y.; Katsuki, H.; Nakamura, H.; Takagi, M.; Ueno, K. *Chem. Lett.*, **1982**, 1853.
11. Bourson, J.; Pouget, J.; Valeur, B. *J. Phys. Chem.*, **1993**, *97*, 4552. and literature there in.
12. Nishi, H. In *Shikiso no Kagaku*; Taniguchi, M.; Seo, M. Eds.; Kyoritsu Shuppan: Tokyo, 1985, p27.
13. Horie, K.; Ushiki, H. In *Hikari Kinou Bunshi no Kagaku*; Kodansha: Tokyo, 1992, p103, p105.
14. Sasaki, T.; Ikeda, T.; Ichimura, K. *Macromolecules*, **1993**, *26*, 151.
15. Liu, Z. F.; Hashimoto, K.; Fujishima, A. *Nature*, **1990**, *347*, 658.
16. Shiga, M.; Nakamura, H.; Takagi, M.; Ueno, K. *Bull. Chem. Soc. Jpn.*,

1984, *57*, 412.

17. Takagi, M.; Nakamura, H. *J. Coord. Chem.*, **1986**, *15*, 53.
18. Ketekke, B. H.; Boyd, G. E. *J. Am. Chem. Soc.*, **1947**, *69*, 2800
19. Harris, D. H.; Tompkins, E. R. *J. Am. Chem. Soc.*, **1947**, *69*, 2792.
20. Nair, S. G. K.; Smutz, M. *J. Inorg. Nucl. Chem.*, **1967**, *29*, 1787.
21. Bünzli, J. C. G.; Wessner, D. *Coord. Chem. Rev.*, **1984**, *60*, 191
22. Liu, Y.; Han, B.; Li, Y.; Chen, R.; Puchi, M.; Inoue, Y. *J. Phys. Chem.*, **1996**, *100*, 17361.
23. Kolthoff, I. M. *Anal. Chem.*, **1979**, *51*, 1.
24. Meguro, Y.; Muto, H.; Yoshida, Z. *Anal. Sci.*, **1991**, *7*, 51.
25. Sasaki, T.; Umetani, S.; Le, Q. T. H.; Matsui, M.; Tsurubou, S. *Analyst*, **1996**, *121*, 1051.
26. Alexander, V. *Chem. Rev.* **1995**, *95*, 273
27. Marquardt, D. W. *J. Soc. Ind. Appl. Math.*, **1963**, *11*, 431.
28. Shannon, R. D.; Prewitt, C. T. *Acta Crystallor. Sect. B,* **1969**, *25*, 925.
29. Schwarzenbach, G.; Gut, R.; Anderregg, G. *Helv. Chim. Acta*, **1954**, *37*, 937.
30. Liu, Y.; Lu, T.-B.; Tan, M.-Y.; Hakushi, T.; Inoue, Y. *J. Phys. Chem.*, **1993**, *97*, 4548.
31. Rau, H. *Angew. Chem. Int. Ed. Engl.*, **1973**, *12*, 224.
32. Sugimori, A. In *Yuuki Hikari Kagaku*; Shokabo: Tokyo, 1991, p 32.
33. Zimmerman, G.; Chow, L. Y.; Pail, U. J. *J. Am. Chem. Soc.*, **1958**, *80*, 3258.
34. Yamashita, S.; Ono, H.; Toyama, O. *Bull. Chem. Soc. Jpn.*, **1962**, *35*, 1849.
35. Rau, H. In *Photochromism. Molecules and Systems*; Darr, H., Bouas-Laurent, H., Eds.; Elsevier: Amsterdam, 1990: Chapter 4, and literature therein.
36. Ronayette, J.; Arnaud, R.; Lebourgeous, P.; Lemaire, J. *Can. J.*

Chem., **1974**, *52*, 1848.

37. Morgante, C. G.; Struve, W. S. *Chem. Phys. Lett.*, **1979**, *68*, 267
38. (a) Monti, S.; Gardini, E.; Bortolus, P.; Amouyal, E. *Chem. Phys. Lett.*, **1981**, *77*, 115. (b) Monti, S.; Gardini, E.; Palmieri, P. *Chem. Phys.* **1982**, *71*, 87. (c) Bortolus, P.; Monti, S. *J. Phys. Chem.*, **1979**, *83*, 648.
39. Rau, H.; Lüddecke, E. *J. Am. Chem. Soc.*, **1982**, *104*, 1616.
40. Shen, Y-Q.; Rau, H. *Makromol. Chem.*, **1991**, *192*, 945.
41. Rau, H. *J. Photochem.*, **1984**, *26*, 221.
42. Lednev, I. K.; Ye, T.; Hester, R. E.; Moore, J. N. *J. Phys. Chem.*, **1996**, *100*, 13338.
43. Victor, J. G.; Torkelson, J. M. *Macromolecules*, **1987**, *20*, 2241.
44. Tamaoki, N.; Yoshimura, S.; Yamaoka, T. *Thin Solid Films*, **1992**, *221*, 132.
45. Anzai, J.; Sakasegawa, S.; Takemura, T.; Osa, T. *Mater. Sci. Eng. C*, **1994**, *2*, 102.
46. Liu, Z.; Morigaki, K.; Hashimoto, K.; Fujishima, A. *Anal. Chem.*, **1992**, *64*, 134.
47. Shaika, T.; Iyoda, T.; Honda, K.; Shimidzu, T. *J. Chem. Soc., Perkin Trans II*, **1993**, 1181.
48. (a) Shinkai, S.; Minami, T.; Kusano, Y.; Manabe, O. *J. Am. Chem. Soc.*, **1983**, *105*, 1851. (b) Shinkai, S.; Nakaji, T.; Ogawa, T.; Shigematsu, K.; Manabe, O. *J. Am. Chem. Soc.*, **1981**, *103*, 111. (c) Shinkai, S.; Ogawa, T.; Kusano, Y.; Manabe, O.; Kunikawa, K.; Goto, T.; Matsuda, T. *J. Am. Chem. Soc.*, **1982**, *104*, 1960.
49. (a) Kimura, K.; Yamashita, T.; Yokoyama, M. *J. Chem. Soc., Perkin Trans II*, **1992**, 613. (b) Inoue, M.; Noguchi, Y.; Isagawa, K. *Angew. Chem. Int. Ed. Engl.*, **1994**, *33*, 1163.
50. (a) Kimura, K.; Mizutani, R.; Yokoyama, M.; Arakawa, R.; Matsubayashi, G.; Okamoto, M.; Doe, H. *J. Am. Chem. Soc.*, **1997**,

119, 2062. (b) Kimura, K.; Kaneshige, M.; Yokoyama, M. *J. Chem. Soc., Chem. Commun.*, **1994**, 1103.

51. Inoue, M.; Ueno, M.; Tsuchiya, K.; Nakamura, K.; Konishi, K.; Kitao, T. *J. Org. Chem.*, **1992**, *57*, 5377.
52. (a) Lednev, I. K.; Hester, R. E.; Moore, J. N. *J. Am. Chem. Soc.*, **1997**, *119*, 3456. (b) Lednev, I. K.; Ye, T. Q.; Hester, R. E.; Moore, J. N. *J. Phys. Chem. A*, **1997**, *101*, 3456.
53. Cotton, F. A.; Wilkinson, G.; Gaus, P. L. In *Basic Inorganic Chemistry* (2 Ed.); John Wiley & Sons: New York, 1987, p 551.

Acknowledgment

I gratefully acknowledge the contribution of Prof. Hiroshi Nakamura of Division of Material Science, Graduate School of Environmental Earth Science, Hokkaido University, who has provided continuous guidance, continuing interest, valuable suggestions and critical reading of the manuscript in this study.

I feel grateful to Prof. Masatsugu Shimomura, Research Institute for Electronic Science, Hokkaido University, for his valuable suggestions and encouragement throughout the present study and helpful advice for the preparation of the present manuscript.

I express the gratitude to Prof. Takayoshi Nakamura, Research Institute for Electronic Science, Hokkaido University, and Prof. Ken-ichi Hirao, Kazuhiko Ichikawa, Division of Material Science, Graduate School of Environmental Earth Science, Hokkaido University, for their useful suggestions throughout the present study and helpful advice for the preparation of the present manuscript.

I thank Prof. Kiyoshi Hasebe, Division of Material Science, Graduate School of Environmental Earth Science, Hokkaido University, and the honorary Prof. Mitsuhiko Taga, Faculty of Science, Hokkaido University, who introduced me into this area of chemistry.

I am also grateful to the honorary Prof. Hideaki Kita, Graduate School of Environmental Earth Science, Hokkaido University, for his kind guidance for the preparation of English manuscripts, and Prof. Makoto Takagi, Department of Chemical Science and Technology, Faculty of Engineering, Kyushu University, for providing azobenzocrown ethers used in the present study.

I am very thankful to Dr. Shunitz Tanaka, Division of Material Science, Graduate School of Environmental Earth Science, Hokkaido University, Dr. Tatsuya Morozumi, Department of Chemistry, Faculty of

Science, Hokkaido University, Dr. Olaf Karthaus, Research Institute for Electronic Science, Hokkaido University, for their useful comments, discussions and encouragement, and Mr. Teiichiro Nomura for experimental assistance.

It remains for me to thank Dr. Masami Fukushima, Dr. Satoshi Hikima, Mr. Mikio Kawasaki, and many people whom I am very much for their kindness.

inches 1 2 3 4 5 6 7 8

cm 1 2 3 4 5 6 7 8 9 10 11 12 13 14 15 16 17 18 19

Kodak Color Control Patches

Blue Cyan Green Yellow Red Magenta White 3/Color Black

Kodak Gray Scale

C Y M

A 1 2 3 4 5 6 **M** 8 9 10 11 12 13 14 15 **B** 17 18 19